

Aus dem Zentralinstitut für Seelische Gesundheit
der Medizinischen Fakultät Mannheim
(Direktor: Prof. Dr. med. Andreas Meyer-Lindenberg)

Exploration of the biological mechanisms in neuropsychiatric disorders using multimodal imaging

Inauguraldissertation
zur Erlangung des Doctor scientiarum humanarum (Dr. sc. hum.)
der
Medizinischen Fakultät Mannheim
der Ruprecht-Karls-Universität
zu
Heidelberg

vorgelegt von
Guo-Ying Wang

aus
Shanxi
2017

Dekan: Herr Prof. Dr. rer. nat. Dr. med. Sergij Goerd
Referentin: Frau apl. Prof. Dr. Gabriele Ende

Table of contents

| | |
|---|-----------|
| ABBREVIATIONS | III |
| CHAPTER I. GENERAL INTRODUCTION | 1 |
| 1 OUTLINE..... | 2 |
| 2 STUDY BACKGROUND AND IMAGING IMPLICATION..... | 4 |
| 2.1 Alcohol addiction | 4 |
| 2.1.1 Alcohol dependence, abstinence, withdrawal..... | 4 |
| 2.1.2 Underlying neurochemical mechanisms..... | 6 |
| 2.1.3 MRS neurometabolite level changes in withdrawal and abstinence | 7 |
| 2.1.4 Partial recovery of brain volumes with abstinence..... | 8 |
| 2.1.5 The potential link between neurometabolites and brain volume recovery | 9 |
| 2.2 Borderline Personality Disorder | 9 |
| 2.2.1 Clinical picture..... | 9 |
| 2.2.2 Impulsivity and its measurement | 10 |
| 2.2.3 Neurochemical basis of impulsivity | 11 |
| 2.2.4 Neural correlates of impulsivity | 11 |
| 2.2.5 Associations of regional GABA with BOLD | 13 |
| 3 NEUROIMAGING TECHNICAL BACKGROUND | 14 |
| 3.1 Structural MRI (sMRI)..... | 14 |
| 3.1.1 The physical basis of sMRI | 14 |
| 3.1.2 Voxel-based analysis | 15 |
| 3.1.3 Surface-based analysis..... | 17 |
| 3.2 ¹H MRS..... | 19 |
| 3.2.1 The physical basis of ¹ H MRS..... | 20 |
| 3.2.2 ¹ H MRS of Glu, Gln, GABA | 22 |
| 3.2.3 Quantification of metabolites | 23 |
| 3.3 Functional MRI..... | 25 |
| 3.3.1 The physical basis of functional MRI..... | 25 |
| 3.3.2 The physiological basis of fMRI | 26 |
| 3.3.3 The neural signalling basis of fMRI | 27 |
| 3.3.4 Data analysis | 28 |
| 4 AIMS OF THE THESIS | 30 |

| | |
|--|------------|
| CHAPTER II. EMPIRICAL STUDIES | 33 |
| 5 Longitudinal mapping of gyral and sulcal patterns of cortical thickness and brain volume regain during early alcohol abstinence | 34 |
| 6 Negative association between MR-spectroscopic glutamate markers and grey matter volume after alcohol withdrawal in the hippocampus: a translational study in humans and rats | 58 |
| 7 ACC GABA levels are associated with functional activation and connectivity in the fronto-striatal network during interference inhibition in patients with borderline personality disorder..... | 91 |
| CHAPTER III. GENERAL DISCUSSION | 126 |
| 8 GENERAL DISCUSSION..... | 127 |
| 8.1 Brain recovery during early alcohol abstinence | 127 |
| 8.1.1 Summary of the findings | 127 |
| 8.1.2 Limitation | 129 |
| 8.1.3 Outlook | 130 |
| 8.2 Biological mechanisms underlying impulsivity in BPD | 130 |
| 8.2.1 Summary of the findings | 130 |
| 8.2.2 Limitations | 132 |
| 8.2.3 Future directions | 133 |
| 9 SUMMARY | 134 |
| 10 REFERENCE | 136 |
| CURRICULUM VITAE | 146 |
| PUBLICATIONS | 147 |
| ACKNOWLEDGEMENT..... | 148 |

Abbreviations

| | |
|-------------------------|---|
| ADS | Alcohol Dependence Scale |
| ADP | Alcohol Dependent Patients |
| ADHD | Attention-Deficit/Hyperactivity Disorder |
| BIS | Barratt Impulsiveness Scale |
| CMRO₂ | Blood Oxygen Consumption |
| BOLD | Blood Oxygen Level Dependent |
| BPD | Borderline Personality Disorder |
| CBF | Cerebral Blood Flow |
| CSF | Cerebrospinal Fluid |
| CIE | Chronic Intermittent Exposure |
| CTh | Cortical Thickness |
| Cr | Creatine |
| DTI | Diffusion Tensor Imaging |
| EPI | Echo Planar Imaging |
| FDR | False Discovery Rate |
| FWE | Family Wise Error Rates |
| FISP | Fast Imaging with Steady Precession |
| FWHM | Full Width at Half Maximum |
| fMRI | Functional Magnetic Resonance Imaging |
| GABA | γ -aminobutyric acid |
| GCA | Gaussian Classifier Array |
| GLM | General Linear Model |
| Glu | Glutamate |
| Gln | Glutamine |
| GM | Gray Matter |
| HCS | Healthy Controls |
| HRF | Hemodynamic Response Function |
| IFC | Inferior Frontal Cortex |
| MRSI | Magnetic Resonance Spectroscopic Imaging |
| MRS | Magnetic Resonance Spectroscopy |
| MEGA-PRESS | MEscher-GARwood Point REsolved Spectroscopy |
| MNI | Montreal Neurological Institute |
| MANCOVA | Multivariate Analysis with Covariates |
| NAA | N-acetylaspartate Acid |
| NMDA | N-methyl-D-aspartate |
| OCDS | Obsessive Compulsive Drinking Scale |
| PRESS | Point-RESolved Spectroscopy |
| PFC | Prefrontal Cortex |
| RF | Radio Frequency |
| ROIs | Regions of Interest |
| sMRI | Structural Magnetic Resonance Imaging |
| SMA | Supplementary Motor Area |
| SA | Surface Area |
| SBM | Surface-based morphometry |
| eTIV | Estimated Total Intracranial Volume |
| VBM | Voxel-based morphometry |

TP
WM

Time Point
White Matter

CHAPTER I.
GENERAL INTRODUCTION

1 Outline

It has been increasingly recognized that combining multimodal brain imaging data promotes a more comprehensive understanding of biological processes in the brain and pathologies in mental disorders, which can also uncover hidden features in unimodal imaging (Calhoun & Sui, 2016). Moreover, the joint information across these modalities reveals crucial information, such as the impact of brain neurochemistry on brain structures and functions, the effect of psychopathology, and the relationship between those alterations and cognitive deficits.

Thus, the present doctoral thesis focused on the multimodal imaging investigation of brain mechanisms in alcohol addiction (project I) and borderline personality disorder (BPD) (project II). In brief, the emphasis of thesis was on the association of brain neurochemistry with: 1) the brain volume recovery within the first two weeks of abstinence in alcohol dependent patients (ADP) and the rat model. 2) brain functions related to impulsivity in patients with BPD.

Three imaging measures of particular interest were applied in the frame of the thesis: Magnetic Resonance Spectroscopy (MRS) to measure the neurochemical levels in the brain tissues; structural Magnetic Resonance Imaging (sMRI) to estimate brain volumes and cortical thickness; functional Magnetic Resonance Imaging (fMRI) to examine hemodynamic response related to neural activity and functional connectivity during impulse control.

The general introduction part (chapter I) consists of the following points: 1) the clinical background knowledge and literature review of imaging findings related to those two disorders 2) a brief technical overview of the three imaging modalities described from three aspects: the biophysical basis of the corresponding MRI signal; methods for data processing; and the assumptions made to interpret the results.

In the main experiment part (chapter II), for each brain imaging project, we first infer the unimodal information by separately visualizing results from unimodal analyses. This offers the different results provided by each modality in a qualitative manner. Afterwards, a multimodal data integration analysis is presented to capitalize the relationship between MRS-

GENERAL INTRODUCTION

derived neurochemistry and the other two modalities: sMRI-derived morphometry (project I), and fMRI-derived function measures (project II).

In the general discussion (chapter III), the power of the studies is estimated, limitations, and outlook are outlined.

2 Study background and imaging implication

2.1 Alcohol addiction

2.1.1 Alcohol dependence, abstinence, withdrawal

Alcohol dependence and abstinence

Alcohol dependence is a highly prevalent neuropsychiatric disorder in which an individual is physically or psychologically dependent on alcohol, causing great personal, familial and social harm. Moreover, alcohol dependence has been shown to be one of the fifth leading causes of death worldwide (Rehm et al., 2009), with approximately 25% of the deaths in the age group of 20-39 years¹. In Germany, every fifth bed in hospital has been occupied by alcohol-related disorders, and related societal costs are around 30 billion euros per year (Laramée et al., 2013).

Extensive research efforts have focused on the mechanism of alcohol dependence. It is shown to be a progressive chronic brain disease, associated with changes in brain morphology, function, gene expression, neurometabolism, psychology, and behavior (Cui et al., 2015; Schulte et al., 2012). Those changes, in turn, may contribute to the progression of alcohol dependence.

Despite the high relapse rate of alcohol use, about 18.2% of ADP can maintain abstinence after detoxification, indicating a potential of recovery from alcohol dependence. Studies have suggested that brain function, structure, and neurochemical levels show variable recovery during sustained alcohol abstinence (Cui et al., 2015; Demirakca et al., 2011a; Ulrich

¹ Based on the Global status report on alcohol and health 2014

GENERAL INTRODUCTION

Frischknecht et al., 2017; Hermann, Weber-Fahr, Sartorius, Hoerst, Frischknecht, Tunc-Skarka, Perreau-Lenz, Hansson, Krumm, Kiefer, Spanagel, Mann, Ende, & Sommer, 2012; van Eijk et al., 2013). Moreover, those biological changes are associated with different stages of abstinence, suggesting recovery from alcohol dependence to be a dynamic process (Brousse et al., 2012; Crews et al., 2005; Demirakca et al., 2011b; Heilig, Egli, Crabbe, & Becker, 2010a; Hermann, Weber-Fahr, Sartorius, Hoerst, Frischknecht, Tunc-Skarka, Perreau-Lenz, Hansson, Krumm, Kiefer, Spanagel, Mann, Ende, & Sommer, 2012; O'Neill, Cardenas, & Meyerhoff, 2001). However, the evidence is still limited. The extent and spatial preference of early brain recovery attributed to abstinence and its associations with other indicators (e.g. withdrawal induced hyperglutamatergic state) are not well established.

Overview of alcohol withdrawal

Alcohol withdrawal refers to a set of symptoms provoked once drinking is terminated in alcohol dependent individuals. It usually occurs when the blood alcohol concentrations drops under the tolerance threshold, normally below 1g/L. The severity of withdrawal during abstinence can vary from mild symptoms such as tremor, sweating, nausea, hypertension, vomiting, to severe and life-threatening symptoms such as auditory hallucinations, illusions, seizures, and delirium. These symptoms and signs usually start at six hours after the last drink, peaks at 24 to 72 hours, and last five to seven days (Simpson, Wilson, & Nordstrom, 2016). However, aside from those somatic symptoms of alcohol withdrawal that typically recover within a few days, those withdrawal symptoms which lead to psychological discomfort and negative affect, such as craving for alcohol and anhedonia, may linger for a protracted period of time (Martinotti et al., 2008). The persistence of these symptoms may serve as a powerful motivational force for alcohol relapse after periods of abstinence. Therefore, the fear of withdrawal symptoms emerging plays a prominent role in triggering relapse and sustained heavy drinking in alcohol dependent individuals after periods of abstinence. Moreover, the alcohol withdrawal may not only contribute to alcohol-related brain impairment, but also may affect brain recovery during abstinence.

GENERAL INTRODUCTION

2.1.2 Underlying neurochemical mechanisms

At the neurochemical level, the brain is in a homeostatic state before alcohol exposure (see Figure 2-1). When a person consumes alcohol, its acute effect is expressed as neurochemical imbalance in the brain. For example, high amounts of acute alcohol intake result in an increase in γ -aminobutyric acid (GABA) neurotransmission, and further induce a decrease in glutamate due to GABA inhibition, which produce acute alcohol effects (e.g. sedation, ataxia) (Brousse et al., 2012). With continued alcohol consumption, the brain induces an opposing neurochemical adaptation that tends to diminish the GABAergic function and elevate glutamatergic function to counterbalance the alcohol effects. In other words, the brain develops tolerance for alcohol. However, at this stage (chronic alcohol consumption), the brain is in a state of hyperexcitability and physiologically dependent on alcohol. Once alcohol consumption is stopped, the new neuroadaptation unbalances the neurochemistry. Like the seesaw tilting to opposite side, this unbalanced adaptation produces the withdrawal syndromes (hyperexcitability of the brain), which is opposite to the original sedative effects of alcohol. These disturbances last until these adaptations can be reversed in the brain to restore equilibrium.

Moreover, the extent of the neurochemical imbalances (e.g. Glutamate (Glu)/GABA) has been suggested to be exacerbated in repeated withdrawal, resulting in increased severity symptoms of future withdrawal episodes. This may contribute to an incremental psychological component of withdrawal to affect relapse risk. The studies of the 'kindling' phenomenon also suggest that exacerbated changes in neurochemical systems following repeated withdrawal may make the brain more vulnerable to this neurochemical perturbation, resulting in increasingly severe brain atrophy, functional and cognitive impairment (for review see (Becker, 1998)).

GENERAL INTRODUCTION

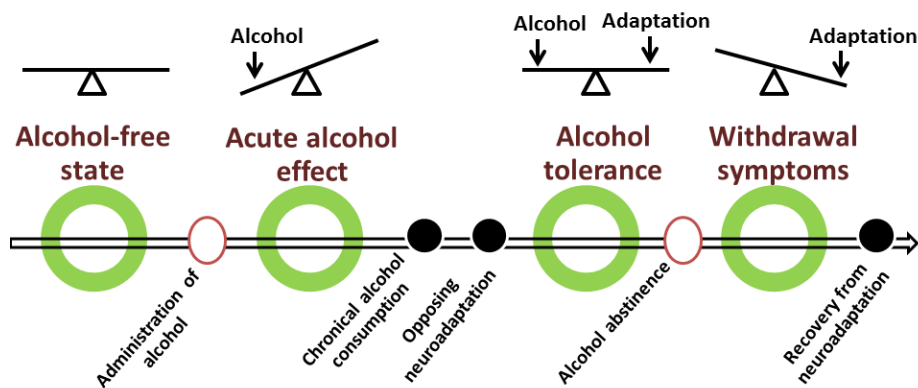


Figure 2-1 The brain neurochemistry adaptations in alcohol dependence, withdrawal.

The following sections will give an overview of previous imaging findings, in order to provide a theoretical basis of the current project.

2.1.3 MRS neurometabolite level changes in withdrawal and abstinence

As mentioned, hyperglutamatergic metabolism in alcohol withdrawal is a consequence of neurochemical adaptation initially triggered to compensate for continued presence of alcohol in the brain. Consistent with that, a translational MRS study (Hermann, Weber-Fahr, Sartorius, Hoerst, Frischknecht, Tunc-Skarka, Perreau-Lenz, Hansson, Krumm, Kiefer, Spanagel, Mann, Ende, & H., 2012) found an increase in prefrontal Glu levels during acute alcohol withdrawal in ADP and the rat model. These elevated Glu levels return to normal within a few weeks of abstinence in both species.

Additionally, regarding to non-specific metabolite, MRS studies have repeatedly found that lower N-acetylaspartate Acid (NAA) levels (a marker of neuronal variability and integrity) in alcohol dependent individuals can be normalized after weeks of abstinence (Hermann, Weber-Fahr, Sartorius, Hoerst, Frischknecht, Tunc-Skarka, Perreau-Lenz, Hansson, Krumm, Kiefer, Spanagel, Mann, Ende, & H., 2012; Mon, Durazzo, & Meyerhoff, 2012). For example, Mon and his colleagues (Mon et al., 2012) found NAA levels in the anterior cingulate cortex (ACC) significantly increased during four weeks of abstinence. The effect of lower NAA levels at one week of abstinence in ADP relative to healthy controls (HCs) cannot be observed at five weeks of abstinence. In line with that, a translational MRS study (Hermann et al.,

GENERAL INTRODUCTION

2012a) reported such NAA recovery effects could be observed within initial two weeks of abstinence.

2.1.4 Partial recovery of brain volumes with abstinence

Neuroimaging studies in alcohol dependence show widespread volume shrinkage in gray matter (GM) and white matter (WM). Specific regions have been consistently reported to be affected by alcohol dependence, including prefrontal areas, hippocampus, amygdala, caudate nucleus, putamen, and cerebellum (Bauer et al., 2013; Durazzo et al., 2011; Kuceyeski et al., 2013; Makris et al., 2008; Segobin et al., 2014).

Abstinence can result in recovery of GM and WM volume. Several imaging studies found a partial recovery of brain volume with abstinence, even during early abstinence (Demirakca et al., 2011a; Pfefferbaum et al., 1995; van Eijk et al., 2013). Moreover, in those studies with distinct abstinence time points, the recovery regions were not fully overlapping and even the extent of recovery within the same region differed, highlighting a dynamic nature of brain recovery.

Most of the previous studies obtained baseline measurements several weeks after abstinence (Durazzo et al., 2010; Fein et al., 2006; Shear et al., 1994; Sullivan et al., 2005a; Wrase et al., 2008), thus missing a potential recovery effect in early abstinence. Therefore, in our previous study, the ADP group was scanned within the first 24 hours after cessation of alcohol consumption, and then again after two weeks of supervised abstinence. Our preliminary analysis using the VBM approach found widespread cortical volume recovery within the initial two weeks of abstinence, despite of different recovery extents in distinct regions (van Eijk et al., 2013). However, no subcortical recovery was observed, although these changes (e.g. hippocampus, striatum) had been reported in other long-term abstinence studies (Makris et al., 2008; Sameti et al., 2011). It is possible that VBM analysis is not sensitive enough to detect the disease-induced subcortical changes, as e.g. reported by Bergouignan et al. for hippocampus (Bergouignan et al., 2009b). FreeSurfer has been shown to be more accurate in subcortical segmentation (Fischl et al., 2002). Therefore, the first goal of this thesis was to reanalyze the same sample with a different approach and to confirm that our observation in subcortical regions was purely due to the nature of abstinence rather than the method.

GENERAL INTRODUCTION

Important to note, FreeSurfer also offers the possibility to investigate the unknown nature of abstinence-induced volume changes in terms of gyral and sulcal pattern of cortical thickness and surface area, which could be differentially affected by alcohol dependence and early abstinence.

2.1.5 The potential link between neurometabolites and brain volume recovery

The hippocampus was a region of particular interest in this thesis. First, this is a region that often shows plasticity due to alcohol dependence and abstinence, which has been closely associated with neurogenesis and its functioning (Gazdzinski et al.; Kühn et al., 2014). Second, it has been shown that the hippocampus plays a prominent role in alcohol craving and relapse via modulating the rewarding / pleasant memory of alcohol consumption. More precisely, stimulation of the hippocampal glutamatergic neurons can induce dopamine release in the striatum resulting in craving and relapse behavior (Grace et al., 2007). Finally, the hippocampus is rich in glutamatergic innervation and vulnerable to excessive Glu during alcohol withdrawal which can induce excitotoxicity and neuronal cell death (Cippitelli et al., 2010; Hoffman, 1995; Prendergast et al., 2004; Spanagel, 2009; Tsai et al., 1998). Thus, the potential recovery capacity of the hippocampal volume during abstinence might be influenced by Glu levels. However, no imaging study has addressed this issue yet.

2.2 Borderline Personality Disorder

2.2.1 Clinical picture

BPD is a serious mental illness that affects approximately 2% of adults. It is characterized by behavioural impulsivity, affective dysregulation, instability in interpersonal relationships, self-image, aggression, and suicidal behaviour (Mauchnik and Schmahl, 2010). These dysregulations often disrupt an individual's sense of identity, long-term planning, and life quality.

BPD is diagnosed and defined according to DSM-5. BPD often co-occurs with other axis-I disorder, and it is uncommon to see an individual diagnosed solely with BPD (Fyer et al., 1988). The course of BPD is very variable, and most people show symptoms in early adult life. The prognosis is favorable, if treated adequately, i.e. about 86% of patients remit and

GENERAL INTRODUCTION

only about 10% of the patients relapse afterwards. However, although the social functioning improves after treatment, disability in social functioning of BPD is more severe than depression and other personality disorders (Gunderson et al., 2011).

2.2.2 Impulsivity and its measurement

Impulsivity is a core feature of BPD. According to the DSM-5, impulsivity is one of nine diagnostic criteria, and often interacts with some factor contributing to severity of the disorder, such as an increased risk factor of substance abuse and suicide.

Impulsivity has been assessed using a variety of measures from different theoretical frameworks. As personality traits, impulsivity is measured by self-report questionnaires based on the subject's self-perception of his/her behavior in daily life. On the other hand, researchers in cognitive neuroscience often assess impulsivity by measuring inhibitory control at behavioral level, which is based on the assumption that impulsive behavior is driven, at least partly, by the lack of behavior inhibition (Jacob et al., 2010).

Impulsivity traits were often measured by the Barratt Impulsiveness Scale (BIS), Eysenck's Impulsivity Questionnaire, and UPPS scale, where BPD patients consistently reported higher scores than healthy subjects. Among those questionnaires, the UPPS scales have been suggested to account for 64% BPD features (Peters et al., 2013; Sebastian et al., 2014a) and no such clear information was reported for the others. Accordingly, the UPPS scales possibly have more potential to clarify BPD-related impulsivity.

For the behavioral inhibition test, motor response inhibition (Go/nogo-, Stopsignal tasks) and interference inhibition task (Stroop-, Flank task) are typically used. Contrasting the self-report results, studies on inhibition control tasks in BPD patients have rendered mixed results (Jacob et al., 2010; Sebastian et al., 2014a). The divergent results may be due to the difference in applied tasks. But, BPD patients have not shown behavioral performance deficits in most studies. Furthermore, the studied BPD patients had always comorbid other psychological disorders, such as Attention-deficit/hyperactivity disorder (ADHD).

2.2.3 Neurochemical basis of impulsivity

Impulsivity is modulated by multiple neurotransmitters, including dopamine, serotonin, Glu and GABA (Dalley et al., 2008b; Ende et al., 2015a; Hoerst et al.). Multiple lines of evidence indicate that impulsive behaviour in impulse control disorders involves aberrant dopaminergic and glutamatergic functioning (see review (Naaijen et al., 2015)). The role of GABA in impulsivity, especially in BPD, is less frequently studied, despite the fact that GABAergic cells forming the key projections in fronto-striatal neurocircuitry. In the thesis we focused on the neurochemical role of GABA in impulsivity.

In healthy subjects, MRS studies indicate that GABA levels, especially in the fronto-striatal regions, play an important role in the regulation of inhibitory control and impulsivity (Dharmadhikari et al., 2015; Hayes et al., 2014; Kuhn et al., 2016; Quetscher et al., 2015). Silveri et al. (2013) reported that a lower ACC GABA/creatine(Cr) ratio in healthy adolescents was associated with worse go/nogo task performance. Boy et al. (2011) found that in healthy men higher prefrontal GABA levels were associated with lower rash impulsivity. One recent investigation by Ende et al., (2016) is supportive of these findings suggesting that lower ACC GABA levels in BPD patients and HCs are associated with higher impulsivity ratings. Therefore, the ACC has been selected as a primary target region to explore how abnormalities in ACC GABA levels may contribute to impulsive behaviour in BPD in this thesis.

2.2.4 Neural correlates of impulsivity

Neural correlates of impulsive behavior

In the past years, the neural substrates of impulsive behaviour have been mainly investigated in the context of inhibitory control task (including motor response inhibition, interference inhibition) in human as well as animal studies. The fronto-striatal network has been suggested to play a prominent role in the regulation of these processes (review see (Dalley et al., 2011a)). Those studies have shown that frontal regions, such as prefrontal cortex (PFC), ACC, supplementary motor area (SMA), pre-SMA, inferior frontal cortex (IFC) are important elements of this network. The striatum is also an important subcortical region involved in this

GENERAL INTRODUCTION

network, which receives the commands from cortical regions to withhold or promote a response (Dalley et al.; Quetscher et al., 2015).

A large number of fMRI studies have used behavioral inhibition tasks to assess neural correlates of inhibitory control in BPD. These studies suggest that the processes of inhibitory control consistently involve activation of the fronto-striatal network (Aron et al., 2007; Sebastian et al., 2014b; van Eijk et al., 2015b). In particular, several frontal regions of this network have been found to be less activated in BPD patients. For example, the ACC is associated with conflict detection and monitoring as well as emotion regulation (Botvinick et al., 2004; Kerns et al., 2004), and BPD patients demonstrated lower activation in the ACC compared to HCs during emotional interference inhibition tasks. In addition to ACC, (Wingenfeld et al., 2009) also found that medial frontal regions were less activated in BPD patients compared to HCs during the emotional Stroop task. This raises the possibility that impulsive behavior in BPD results from dysfunction in frontal areas. However, one must note that these patterns of hypoactivity in BPD might resemble rather dysfunctional processing of emotional regulation than disturbances associated with interference inhibition *per se*. In the study of (van Eijk et al., 2015a), whole brain analysis suggested that BPD patients did not show altered BOLD activation in any region for all three response inhibition tasks (Simon- , go/nogo- stop/go task) under emotionally neutral condition. Hence, the interpretation of these preliminary findings should be cautious.

On the other hand, although evidence has been found that the successful inhibitory control also relies on the efficient fronto-striatal communication, no imaging evidence could be found in regard to functional connectivity during inhibitory control in BPD patients.

Neural correlates of impulsive personality

It has been suggested that impulsivity traits greatly rely on individual variances in BOLD signal changes ((Brown et al., 2015); review see (Dalley et al., 2008a)). Moreover, several studies suggest that heightened impulsivity traits in clinical patients are associated with aberrant BOLD activation in the fronto-striatal network during inhibitory control (DeVito et al., 2013; Ding et al., 2014; Horn et al., 2003; Kaladjian et al., 2011), such as in patients with

GENERAL INTRODUCTION

schizophrenia, alcoholism, gambling addiction, highlighting that the fronto-striatal system is crucial in the regulation of impulsivity.

2.2.5 Associations of regional GABA with BOLD

The GABAergic signalling contributes dramatically to neural firing rates and hemodynamic response, which supposedly correlate with BOLD signal changes (Attwell and Iadecola, 2002; Logothetis, 2002; Logothetis et al., 2001). Multimodal imaging studies suggest that GABA levels in key regions (e.g. ACC) can predict task-modulated BOLD response (Donahue et al., 2010; Northoff et al., 2007) and functional connectivity (Sampaio-Baptista et al., 2015). Therefore, examinations of associations between MRS-derived metabolites and fMRI-derived functional measures provide us an opportunity to understand the role of ACC GABA in inhibition-related BOLD response in BPD.

3 Neuroimaging technical background

Magnetic resonance imaging is a powerful non-invasive technique capturing certain properties of the human brain *in vivo*. It utilizes strong magnetic fields, radio frequency pulses, and spatially varying magnetic gradient fields to create images of the brain. MRI methods are capable of generating pictures of the anatomy, neurochemical concentrations, as well as physiological processes. The following sections will give an introduction to the physical basis and concepts of the three applications of MRI (sMRI, MRS, fMRI). All of them will be described from three aspects: the biophysical basis of the MRI signal for each MRI modality, methods for data processing and the assumptions made to interpret the results.

3.1 Structural MRI (sMRI)

sMRI measures brain morphometry based on 3D high-resolution MR images. Several morphometry metrics can be derived from a sMRI scan, such as: GM volume, WM volume, cortical thickness (CTh), surface areas (SA), and cortical curvature. In this thesis two techniques for analyzing brain morphometry are used: surface-based morphometry (SBM) and voxel-based morphometry (VBM).

3.1.1 The physical basis of sMRI

The human body consists of ~70% water and the sMRI principles make use of the hydrogen atoms in the water molecule. The hydrogen nucleus consists of one proton with a nonzero spin and has an intrinsic magnetic moment. The strong magnetic field of the scanner (B_0) aligns the spins of hydrogen protons either parallel or anti-parallel to B_0 . The total difference between the number of protons in each alignment increases with greater magnetic field strength, which is referred as a net magnetization (M_0) in the tissue. The resonance frequency (Larmor frequency) of the protons' spin at a given B_0 is determined by an intrinsic property called gyromagnetic ratio which is the ratio of the protons' magnetic moment to its angular momentum. When a radio frequency (RF) pulse is applied at this Larmor frequency, protons absorb the energy of the RF pulse and are consequently excited into a higher energy level. When switching off the RF pulse, the excited protons return to a state of thermal equilibrium by emitting energy in the form of a weak RF signal. The mechanisms in which this signal is

GENERAL INTRODUCTION

dissipating are described by three tissue specific relaxation time constants: The longitudinal relaxation (T1) describes the process of nuclei losing energy to the molecular grid and returning to the thermodynamic state. The transverse relaxation (T2) is governed by the interaction of spins with each other thus falling out of alignment and stop producing a signal. Additionally considering small local field inhomogeneities to this dephasing process finally leads to the T2* relaxation which describes the actually observed exponential decay of the signal.

These three tissue specific properties create the contrast of different tissue types in MR images and are widely exploited to create high-resolution images of body and brain structure.

3.1.2 Voxel-based analysis

VBM is a one of most widely used automated techniques for the analysis of structural brain images by a voxel-wise comparison of the local volume or concentration of GM and WM between groups of subjects (Ashburner and Friston, 2000, 2001). Up to date, there are several VBM approaches implemented by different software packages. Here, the standard VBM protocols used in these two freely available software packages: (SPM, <http://www.fil.ion.ucl.ac.uk/spm/>), and FreeSurfer (subcortical regions) (<https://surfer.nmr.mgh.harvard.edu/>) are described.

Voxel-based analysis in SPM

The VBM analysis in SPM is straightforward. As illustrated in Figure 3-1, first high-resolution images of an individual are spatially normalized into the same stereotactic space (often called ‘template’ which is usually in standard space) in order to create voxel-wise correspondence across subjects. This is done by a non-linear registration which expands or contracts local brain areas to the template. A deformation field is created during this process, which is represented by a map of distances of how far each voxel in the input image needs move to the matching point in the template image. Then a “normalized” image is created by applying this deformation to the input image, which includes the voxel-to-voxel registration information. Afterwards, this deformed image is segmented into three tissue classes (GM, WM, and cerebrospinal fluid (CSF)). The segmented images have values indicating the probability of a given class, and the value at each voxel represents the ‘concentration or

GENERAL INTRODUCTION

density' (unmodulated data) or 'volume' (modulated data, the interpretations of modulation see below). For the modulated data each voxel is also multiplied by the factor of how much the local volume was shrunk or expanded during the nonlinear normalization process so that the total amount of GM, WM and CSF in the modulated images would remain the same as in the original image. This is done by calculating the Jacobian of the deformation field. Therefore, the voxel value in the modulated image represents the 'volume' at that location, while value in unmodulated images represents the 'concentration / or density'(Ashburner, 2009).

Finally the segmented tissue class images are spatially smoothed and combined in a voxel-wise parametric statistical test.

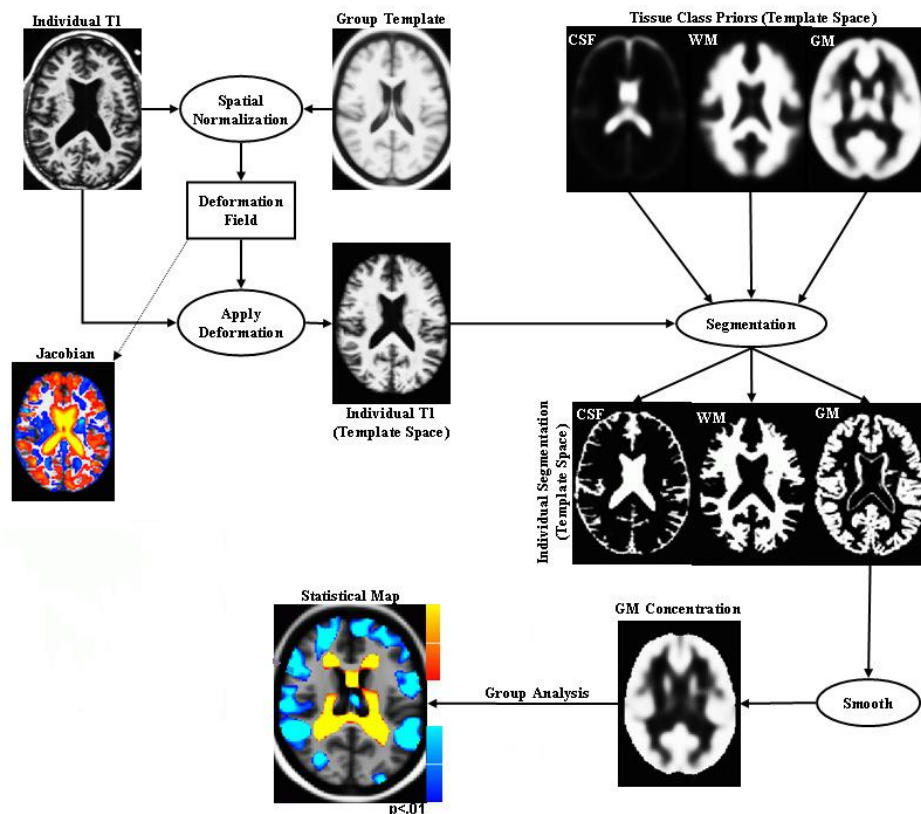


Figure 3-1 The pipeline of the VBM analysis in SPM. The figure is adopted and modified (Greve DN, Proc. Intl. Soc. Mag. Reson. Med. 19 (2011) with permission.

GENERAL INTRODUCTION

FreeSurfer's voxel-based (subcortical) segmentation stream

The difference of FreeSurfer from VBM is that brain voxels are only labelled to three tissue classes (GM, WM, CSF) based on the concentration value at that location. The subcortical segmentation procedures of FreeSurfer directly assigns each brain voxel in the normalized brain volume to one of about 40 labels, including: cerebral WM, cerebral cortex, lateral ventricle, inferior lateral ventricle, cerebellum WM, cerebellum cortex, thalamus, caudate, putamen, pallidum, hippocampus, amygdala, lesion, accumbens, vessel, third ventricle, fourth ventricle, brain stem, CSF (Fischl et al., 2002; Fischl et al., 2004).

There are several preprocessing steps before the segmentation step in FreeSurfer. First, the T1-weighted images are converted from DICOM to a ZLib compressed MGH (Massachusetts General Hospital) format and resampled to a 256 x 256 x 256 matrix. The intensity normalization is then applied to correct for intensity non-uniformity of the imaging data. This is followed by an affine registration to the MNI305 template (Collins et al., 1994), as well as the non-brain tissues removal using a hybrid watershed/surface deformation procedure (Segonne et al., 2004). Next, linear volumetric registration is performed to the FreeSurfer's default Gaussian classifier array (GCA) atlas where the encoding information is estimated from a manually labelling training set. Afterwards, a high dimensional nonlinear transformation and its inverse transformation to align with GCA atlas are computed. Finally, the automated volumetric labeling is performed, which is based upon both the subject-specific values (i.e. intensity) and the probabilistic atlas built from a training set. More detailed information of the stream applied by the subcortical volume-based analysis in FreeSurfer can be seen in FreeSurferWiki (<https://surfer.nmr.mgh.harvard.edu/fswiki>).

3.1.3 Surface-based analysis

Surface-based morphometry (SBM) means that morphometric parameters are driven from geometric models of the cortical surface. There are several implementations of SBM. In this thesis, the FreeSurfer's SBM stream will be described.

Surface-based methods in FreeSurfer construct the cortex as a triangulated mesh model based on the pial boundary and the WM boundary. The corner of each triangle is defined as a vertex, where the coordinates (X, Y, and Z) of the surface model are located. Once the coordinates of

GENERAL INTRODUCTION

each vertex are known, these triangles in 2D structure can be rendered as a 3D surface view. Moreover, knowledge of the coordinates enables computation of morphometric parameters. For example, the cortical thickness can be computed by the distance between the pial and WM surface. The sum of the areas of the triangles provides a measure of the surface area. The curvature is a direct measure of the folding pattern of the cortex, which is computed by sharpness of the cortical folding at that point.

The SBM processing stream in FreeSurfer includes several steps. As illustrated in Figure 3-2, after motion correction and removal of non-brain tissues (Segonne et al., 2004), the brain is segmented into the cortical GM and WM volumes based on the signal intensity and geometric structure of the grey-white interface (Fischl et al., 2004). Afterwards, the surface of the WM volume is tessellated, followed by the automated topology correction (Segonne et al., 2007) as well as surface deformation to obtain a smooth and accurate WM and pial boundary (Dale et al., 1999; Fischl and Dale, 2000). This 2D surface structure is then rendered as a 3D surface model, and can be inflated (unfolded) where the whole cortical surface (sulcal and gyral) is visible. During these processes, morphometric metrics for each subject can be computed, such as curvature, surface area, and cortical thickness. To enable inter-subject and intra-subject comparison, the data for each subject is normalized to a standard surface template in a 2D spherical surface-based coordinate system in order to match the structure features (e.g. curvature) across subjects. Similar to VBM, the SBM spatial normalization is also non-linear, meaning that the local surface may be constrained or enlarged to match the curvature better. After the spatial normalization, the images consisting of morphometric data (e.g. thickness) of each subject is mapped into a standard Talairach space for later group comparisons. Finally, this image is smoothed to improve the signal-to-noise ratio and to reduce local variations in the measurements for further analysis (Du et al., 2007). The quantitative surface estimates of local regions in FreeSurfer are driven in a set of spatially distinct ROIs obtained using the sulcogyral-based atlas (68 ROI parcellations) (Desikan et al., 2006) or a more refined atlas with 148 ROI parcellations (Destrieux et al., 2010). Figure 3-2 depicts the processing pipeline of the analysis in FreeSurfer.

GENERAL INTRODUCTION

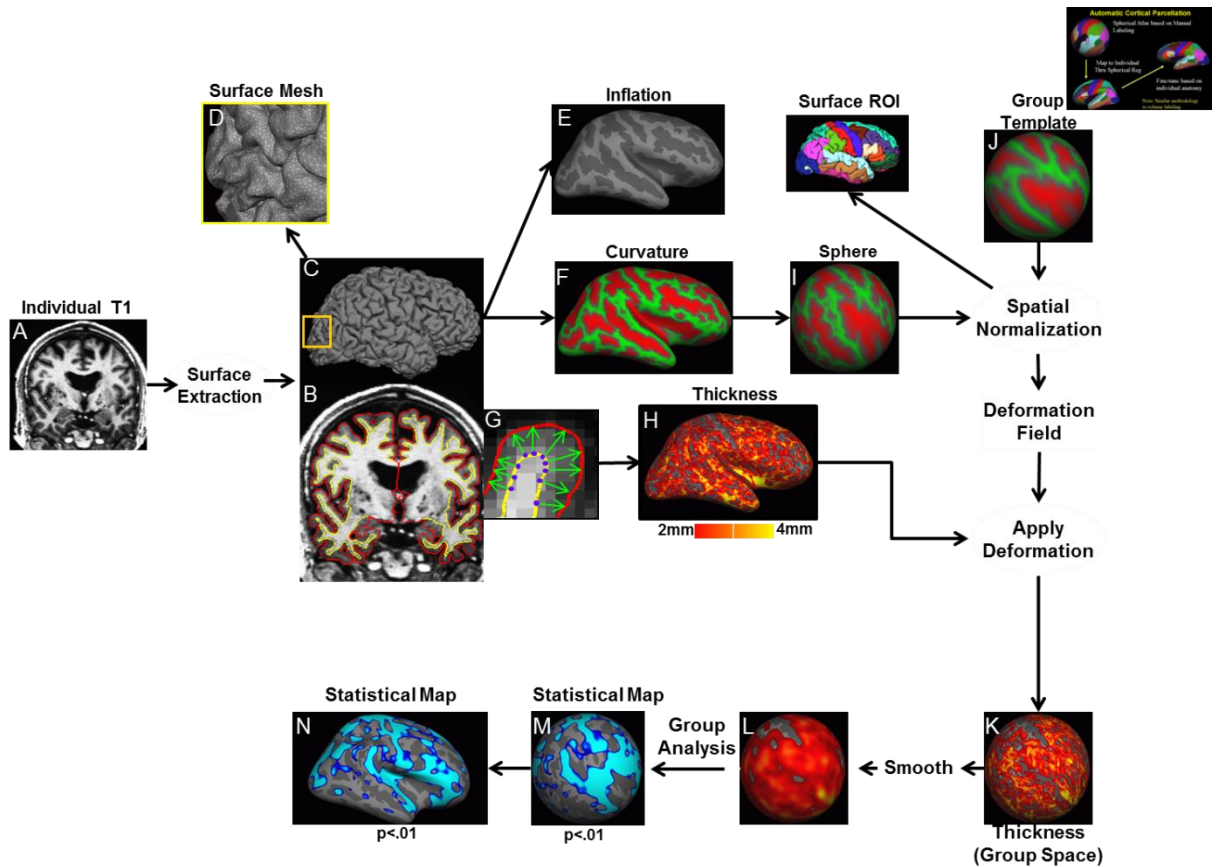


Figure 3-2 The pipeline of the surface-based analysis in FreeSurfer. The figure is adopted and modified (Greve DN, Proc. Intl. Soc. Mag. Reson. Med. 19 (2011)) with permission.

3.2 ^1H MRS

^1H MRS is a non-invasive method that allows investigating brain metabolite concentrations in vivo. It is widely used to trace disease-related metabolic changes, e.g. in mental disorders, and in this thesis addiction and impulsivity disorders were explored.

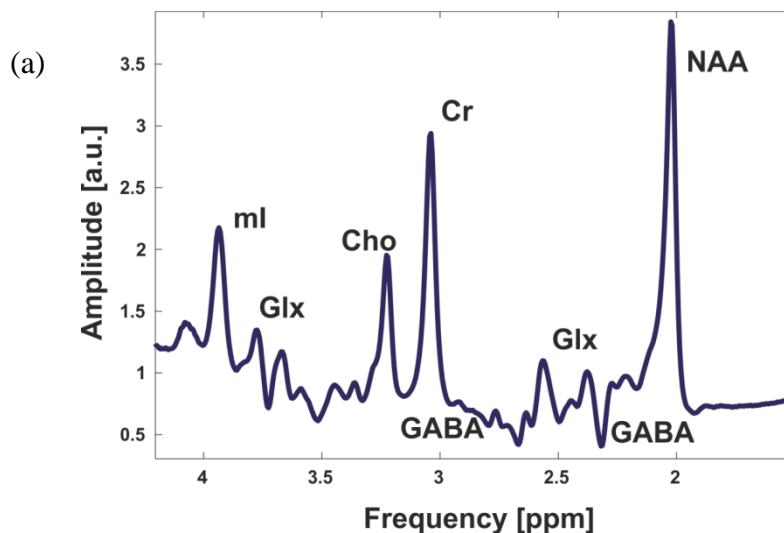
MR spectra can either be acquired from a single volume of interest (VOI) (often called voxel), known as single-voxel MRS or from an array of multiple voxels in 2D or 3D by performing a hybrid MRS and imaging experiment, referred to multi-voxel MRS or Magnetic Resonance Spectroscopic Imaging (MRSI). We focused on the single-voxel MRS in this thesis.

3.2.1 The physical basis of ^1H MRS

In contrast to sMRI, MRS is able to detect signals not only from hydrogens' spins in water molecules, but also from other molecules, such as NAA, Glu, glutamine (Gln), and GABA.

In brief, the structure of a molecule induces subtle changes to the local magnetic field that gives rise to the MR signal of each of the molecules protons. This slight change of the Larmor frequency causes MR signals from different metabolites, and thus different chemical environments, to be separated in the MRS spectrum along a frequency range, a phenomenon called chemical shift.

The individual chemical shift of the resonances gives information about the molecular group carrying hydrogen. Chemical shift is often reported in field-independent units (ppm, parts per million of the proton frequency). The scalar couplings of hydrogen nuclei in a metabolite are reflected by the peak pattern of the MR signals. The area under the peak is directly proportional to the concentration of the metabolite to which the nuclei belong. An example of a ^1H MRS spectrum is shown in Figure 3-3a.



GENERAL INTRODUCTION

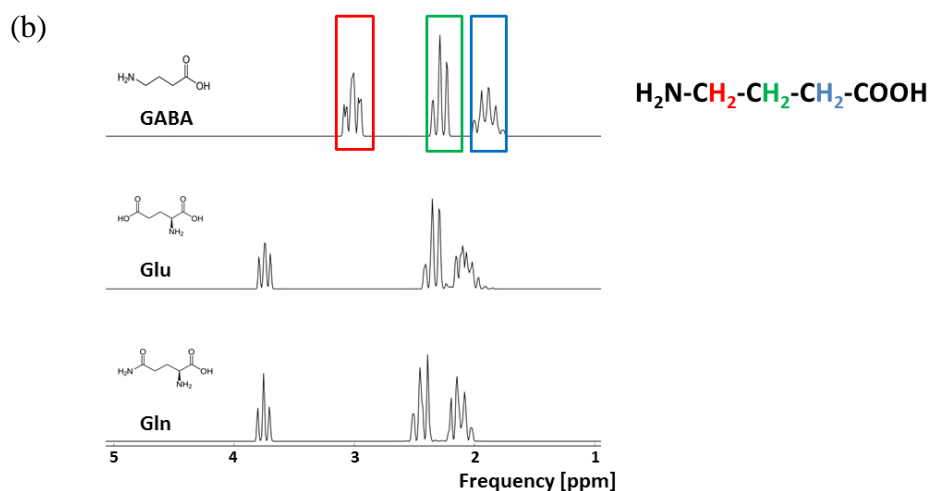


Figure 3-3 MR Spectrum (a) An example of an in vivo MR spectrum acquired by PRESS. The x axis corresponds to the metabolite frequency in ppm according to the chemical shift, and the y axis that corresponds to the peak amplitude (signal intensity, proportional to metabolite concentrations). The abbreviations shown in the figure correspond to: NAA (N-acetyl aspartate); Cho (choline); creatine (Cr); Glx [glutamate (Glu) and glutamine (Gln)]; mI(myo-inositol), GABA (γ -aminobutyric acid). (b) Simulated MR spectra of GABA, Glu and Gln at 3T and their corresponding chemical structures, as well as the assignments of the CH₂ spins of GABA.

As seen in Figure 3-3a, one common feature of the ^1H MRS is that the dispersion of the signals from different metabolites along the chemical shift axis is limited compared to the linewidth of signals. Thus MR signals from different metabolites overlap, and signals from less abundant or complex metabolites, such as Glu and GABA are obscured by the signals of more abundant metabolites (e.g. NAA, Cr). Another characteristic of the ^1H MR signal of many metabolites is the splitting of the metabolite signal into multiplets (see Figure 3-3b, the peaks representing a single hydrogen environment that are split into sub-peaks based on the protons surrounding the environment). This phenomenon is caused by *spin-spin coupling* or *J-coupling*, defined as an interaction between different hydrogen nuclei within a molecule induced by the MR external field, which changes the appearance of the spectrum (RA., 2007). The J-coupling-induced splitting of the signals results in lower peak amplitude along the chemical shift axis, both of which impede detection and quantification of the coupled metabolites, such as Glu and GABA.

3.2.2 ^1H MRS of Glu, Gln, GABA

Glu and GABA are the main excitatory and inhibitory neurotransmitters in the brain. Up to now, a wide variety of methods can be used for investigating glutamatergic and GABAergic processes, but MRS is still the only technique that allows the direct, non-invasive detection of endogenous Glu and GABA in the brain in vivo.

MRS of Glu, Gln

As illustrated in Figure 3-3b, Glu has several MRS-detectable peaks. Although in vivo the brain Glu concentration (6-12.5 mmol) is higher than the Cr concentration (4.5-10.5 mmol), the multiplets of Glu are spread across the chemical shift axis resulting in relatively small multiplet peaks compared to the prominent Cr peak at 3.1 ppm (see Figure 3-3 a).

Noteworthy, the chemical structure of Gln is very similar to Glu, which elicit similar effects of chemical shift and J-coupling. Therefore, Gln signals are largely overlapped with Glu signals in ^1H spectra. Since the chemical shift is increasing at higher field strength, the resonance signals of Glu and Gln become separable only at 7T or higher. Therefore, at 3T scanners used in most of research and clinical facilities, the separation of Glu and Gln resonance signals are usually seen as not reliable, when acquired with standard methods like Point-RESolved Spectroscopy (PRESS). Thus, the Glx concentration, indicating the sum of Glu and Gln, is often reported in clinical studies.

MRS of GABA

Similar to Glu, GABA also has three MRS-visible peaks in the spectrum, but its quantification is very difficult when using standard ^1H MRS techniques (such as PRESS). On the one hand, this is due to the spectral overlapping of the GABA peaks with other metabolites. On the other hand, the very low in vivo concentration of about 1mM in the normal brain makes a reliable quantification challenging.

However, the MEGA-PRESS (MEscher-GARwood Point RESolved Spectroscopy) sequence can successfully separate GABA signals from the rest of the spectrum. Thus, it is widely applied in MRS GABA measurements and currently serves as standard approach at typical

GENERAL INTRODUCTION

clinical field strengths. In short, as illustrated in Figure 3-3b, the MEGA-PRESS sequence is capable of separating the GABA signal at 3 ppm from the rest of the spectrum by applying editing pulses in two consecutive measurements and later subtraction of these datasets.

In more detail, MEGA-PRESS involves a *J-difference editing* technique, by collecting two datasets and using frequency-selective RF pulses and the molecules scalar coupling to manipulate one of the resonance lines by exciting only parts of the coupled system. In one data set (often referred as ‘edit-on’), a frequency-selective editing pulse is applied to GABA signals at 1.9 ppm in order to selectively invert the GABA signals at 3ppm (mediated by J-coupling). This pulse has no effect on other signals at 3 ppm (like choline or Cr), because they are not coupled to signals close to 1.9 ppm. In the other dataset (often referred as ‘edit-off’), the same editing pulse is applied at another chemical shift position with no metabolite frequencies of interest so that the J-coupling evolves freely. Thus, the subtraction of the ‘edit-on’ from the ‘edit-off’ spectrum removes the majority of peaks in the spectrum and only retains the signals which are affected by the editing pulses (review see (Mullins et al., 2014; Puts and Edden, 2012)).

It should be noted that there are mainly two different editing pulse schemes. In both schemes the first editing pulse in the ‘edit-on’ dataset is applied at 1.9 ppm. The difference is in the ‘edit-off’ dataset. Originally, the frequency of this second editing pulse was mirrored at the water resonance (4.7 ppm) resulting in an ‘edit-off’ pulse at 7.5 ppm. But since the resulting GABA peaks at 3 ppm also include signals originated from macro-molecules (MM), mirroring the editing pulse at 1.7 ppm (resulting in a pulse at 1.5 ppm) was suggested to effectively suppress any MM contribution to the GABA signal. To distinguish the two different methods the MM-unsuppressed GABA signal is often referred to ‘GABA+’, while the other is referred to MM-suppressed GABA or simply GABA.

3.2.3 Quantification of metabolites

The quantification process of metabolites in ^1H MRS consists of two steps. First, the accurate peak areas for the relevant metabolites are determined (total area under the metabolite signals proportional to the metabolite concentration). Second, careful calibration is applied for converting areas under the peak to metabolite concentrations.

GENERAL INTRODUCTION

There are two quantification strategies using an internal reference method for in vivo ^1H MR spectra: relative and absolute quantification.

Relative quantification

Relative quantification is one of the simplest approaches to quantify metabolites when one of the measured peaks (an endogenous metabolite) in the spectrum is chosen as a concentration standard (reference). The evaluated metabolites concentrations are expressed as ratios to this reference metabolite, which is supposed to be invariant or stable in all subjects. In the literature total Cr is the most commonly used reference metabolite. The great advantage of using signal ratios is its easy implementation: the acquisition of an extra water unsuppressed spectrum and tissue compartment correction can be avoided. Additionally, in some cases, it is more sensitive than the absolute quantification, e.g. reporting the Glu-Gln cycling status or GABA-Glu balance because the numerator and denominator of the fraction might change in opposite directions. However, tCr concentration is shown to be unstable not only in disease status (Aoki et al., 2012; Wang et al., 2015), but can also vary across regions in healthy brain and during aging (King et al., 2008). Therefore, although this method allows direct comparison with different conditions or samples, it remains uncertain with which metabolite the observed change in the ratio is associated.

Absolute quantification

Absolute quantification means that metabolites' concentrations are expressed in millimols per liter [mM] or institutional units ([i.u.]) or arbitrary units ([a.u.]) as in semi-quantitative methods. Commonly, the water signal of the same VOI is used as an internal reference. For that, in addition to the water suppressed in vivo MRS measurement a spectrum without water suppression in the same VOI is recorded, which serves as an endogenous concentration reference. Given that the water concentration in different brain tissues are well known and stable (40mol/L in WM; 46mol/L in GM; 55mol/L in CSF), the semi-quantification can be calculated. Furthermore, for absolute quantification the T1 and T2 relaxation time of water and the metabolite of interest have to be taken into account. Additionally, different brain tissues (CSF, GM, and WM) contain different concentrations of metabolites. For example, the concentration of metabolites in CSF is very low (Lynch et al., 1993) and is neglected, thus the

GENERAL INTRODUCTION

metabolites concentration has to be corrected for the CSF compartment to avoid an underestimation effect. For this calibration, an anatomical and segmented MR image is necessary to calculate the brain tissue compartment within the VOI.

3.3 Functional MRI

Functional MRI is a robust approach for measuring dynamic patterns of activity in the human brain. This method is capable to detect changes in brain activity and is based on two aspects: on a physical basis – magnetic properties of deoxyhemoglobin and on a physiological basis – an increase of blood flow at a greater rate than oxygen metabolism when the local neural activity increase. All these effects give rise to an increase in MR signal, called blood oxygen level dependent (BOLD) effect, when local neural activity increases during a cognitive task or the brain state changes. MR sequences using echo planar imaging (EPI) are able to obtain the whole brain BOLD activation pattern with a temporal resolution of approximately 2 seconds and a spatial resolution of about 2-3mm³.

Moreover, in recent years an increasing number of studies have used fMRI to explore functional connectivity between distinct brain areas with and without external stimuli or tasks. Several methods have been developed (Bullmore and Bassett, 2011; McLaren et al., 2012; Rissman et al., 2004) and a number of networks have been identified containing brain regions with synchronous BOLD fluctuations.

3.3.1 The physical basis of functional MRI

In contrast to sMRI signals, the fMRI signals arise from the recovery of transverse magnetization, T2* relaxation, which is mainly caused by local magnetic field inhomogeneity. In more detail, deoxyhemoglobin is paramagnetic and can induces local field inhomogeneity to surrounding microvasculature which leads to T2* reduction, while oxyhemoglobin is diamagnetic and therefore does not produce the same effect.

Cognitive processing is associated with an increase in neuronal firing rates of related brain regions. The increase in neural activity causes increased local blood flow in order to meet the greater demand for oxygen. Cerebral blood flow in the activated region exceeds the oxygen utilization, so that the local blood is more oxygenated with a relative decrease in

GENERAL INTRODUCTION

deoxyhemoglobin. The result of having lower levels of deoxyhemoglobin leads to an increase in $T2^*$ and an increase of the MRI signal, since the brain tissue becomes more magnetically uniform (see Figure 3-4). This phenomenon is called the BOLD effect.

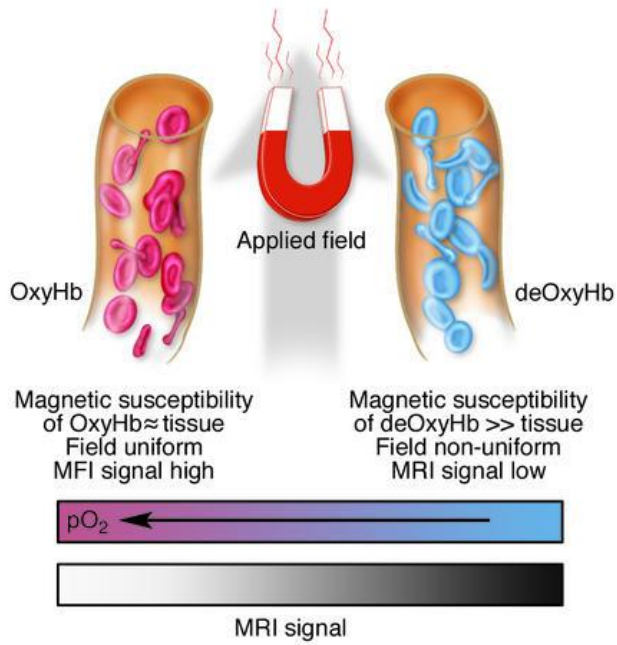


Figure 3-4 Schematic illustration of the origins of the BOLD effect in fMRI. While arterial blood is similar in its magnetic properties to tissue, deoxygenated blood is paramagnetic and so induces inhomogeneities within the magnetic field in tissue. These cause the MRI signal to decay faster. Signals from activated regions of cortex increase as the tissue becomes more magnetically uniform. The figure is adopted from (Gore, 2003) with permission.

3.3.2 The physiological basis of fMRI

As described in section 3.3.1, the magnitude of the BOLD signal reflects the ratio of oxy-/deoxyhaemoglobin. The neural activity changes have an effect on this ratio, which is modulated by several physiological factors, including the cerebral blood flow (CBF), and the cerebral metabolic rate of blood oxygen consumption ($CMRO_2$) (Buxton, 2013; Logothetis, 2008; Logothetis and Pfeuffer, 2004).

Furthermore, as neurons become more active, a time delay occurs before the CBF increases to meet the raised oxygen demand, so-called hemodynamic response. Therefore, the BOLD signal is a temporarily delayed profile of neural activity. A typical BOLD response to a signal stimulus is shown in Figure 3-5. The BOLD response peaks around 5 s after stimulation, and is followed by an undershoot that lasts as long as 10 s, until the signal returns to baseline level (at high magnetic fields, an initial undershoot around 1s after stimulation can sometimes be observed). Thus, the design of early event-related studies used a long time between events to

GENERAL INTRODUCTION

allow the response to return to baseline between stimulations. However, with improving knowledge about the hemodynamic response function (HRF), more complex designs with shorter inter-stimulus intervals were approached.

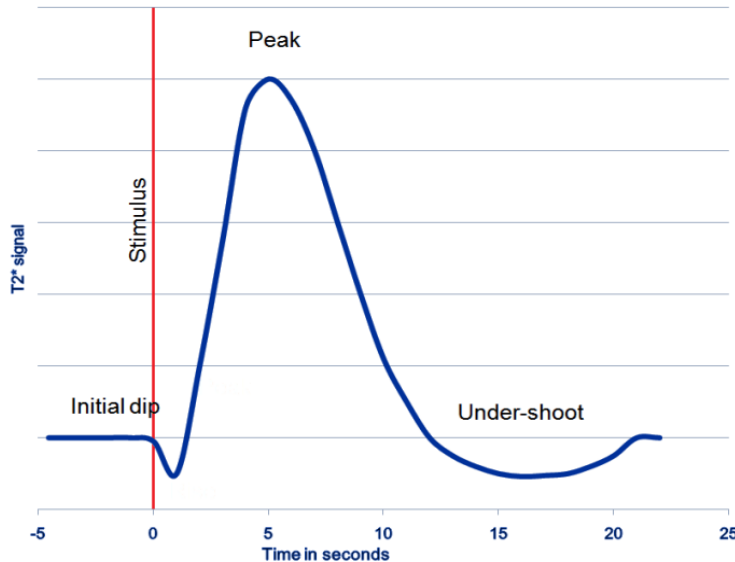


Figure 3-5 A typical (canonical) BOLD response.

3.3.3 The neural signalling basis of fMRI

In contrast to the traditional theory that the increase of blood flow is derived from the oxygen consumption or energy usage of the activated brain as outlined in previous section, recent work has suggested that the local blood flow is directly controlled by neurotransmitters (e.g. Glu, GABA) rather than oxygen usage. For example, exogenous Glu or NMDA (a Glu receptor agonist) dilates pial arterioles and microvessels in the neocortex and hippocampus (Fergus and Lee, 1997b; Lovick et al.). Likewise, another study suggests that exogenous GABA dilates microvessels via activating GABA_A receptor in the hippocampus and neocortex, and blockage of GABA_A receptors produces a microvessels constriction (Fergus and Lee, 1997a). Moreover, a change of neural processing with no change to the signalling systems by controlling CBF could fail to generate BOLD signals, but a change of processing with no net change of oxygen utilization could give rise to BOLD signals (Attwell and Iadecola, 2002).

GENERAL INTRODUCTION

To sum up, haemodynamic response to neural activity seems to be driven by neurotransmitter-related signalling and not directly arising from energy lack of brain tissue (for review see (Attwell and Iadecola, 2002)).

3.3.4 Data analysis

There are several software packages available for processing fMRI data. In the current thesis SPM8 was used for the pre-processing and statistical analysis of the fMRI data. This section describes the analysis pipelines required to create a statistical map of BOLD activation and task-dependent functional connectivity to an external stimulus.

Preprocessing pipeline of fMRI data

The preprocessing of the fMRI data before statistical analysis consists of several steps. First, 3D functional images were corrected for timing differences between slices. Images were then motion-corrected and realigned to the reference image of each scanning run, which aims to calculate the movement parameters and corrects for the movement between volumes. The spatial realignment is based on the theory that the shape and size of the head between volumes does not change, so a rigid-body transformation is applied to align all brain volumes to the reference volume. Afterwards, the corrected images were co-registered to the individual anatomical T1 image. Next, the anatomical image was segmented and spatially normalized to a standard Montreal Neurological Institute (MNI) template and normalization parameters were applied to all functional images to create voxel-wise correspondence across subjects. There are several approaches involved in this step, including multi-parameter linear transformation, translation and non-linear registration. Finally, the functional images were spatially smoothed using a 3-dimensional isotropic Gaussian kernel model to increase the signal-to-noise ratio of the data.

Statistical model and inference of BOLD activation

A General Linear Model (GLM) was used for univariate analysis of the time course of each brain voxel responding to the applied/presented stimuli. Statistical inference regarding whether an individual voxel was activated in response to the stimulus, was calculated by correlating the BOLD time course of the individual voxel with the temporal sequence of

GENERAL INTRODUCTION

events in the stimulus paradigm. Since the BOLD signal is a reflection of the ratio of oxy-/deoxyhemoglobin, it is rather a relative measure than a quantitative measure. Inferences about the BOLD signal require a reference condition for comparison (e.g. comparison to a resting-state baseline or another experimental condition).

In more detail, the assumption of the GLM is that the time course of a voxel in response to an event (a stimulus), can be explained by a linear combination of hypothetical time-courses based on (a) the experimental effect, (b) confounding effects (such as movement parameters, heart rate, respiration etc.), and (c) residual noise. The BOLD response, an index of the underlying neuronal activity in response to the experimental task, is computed by convolving the experimental effects with an HRF. The output of the GLM model is a statistical map containing clusters of activated voxels whose time course shows a significant correlation with the event.

Statistical model and inference of task-dependent functional connectivity

In addition to task-related regional responses, fMRI also allows exploration of an interaction between brain regions in a task-dependent manner by using a generalized psychophysiological interaction (gPPI) approach (McLaren et al., 2012). The gPPI is also based on the GLM framework; it identifies brain regions that differ in functional connectivity depending on task context or conditions, which is tested by the β coefficient for the interaction term.

In the PPI model, the observed BOLD data for each brain voxel are simultaneously regressed onto (a) the convolved task predictors (i.e., main effect of task), (b) the BOLD data from ROI (i.e., main effect of ROI), and (c) each of the separate convolved interaction regressors (task condition \times neural estimate). The difference in the magnitude of the β coefficients for the interaction term of each task condition indicates the degree of task-dependent functional connectivity.

4 Aims of the thesis

The aims of this thesis can be divided into two parts:

Project I:

1. Investigating brain cortical volume recovery in terms of cortical thickness (gyral, sulcal pattern) and surface area, as well as subcortical volume recovery in the first two weeks of abstinence in ADP.
2. Investigating MRS-derived neurometabolites (focused on Glu markers and NAA) and volume recovery in the hippocampus during acute withdrawal and two weeks of abstinence in ADP, as well as an analogous rat model.
3. To further explore the neurochemical nature of abstinence-induced volume changes, i.e. whether increased glutamate levels in the hippocampus were associated with change in the hippocampal volume in the first two weeks of abstinence in ADP and rat model.

Project II:

1. Investigating whether BPD patients displayed alternations in impulsivity traits, ACC GABA levels, as well as BOLD activation and ACC functional connectivity during interference inhibition.
2. Exploring the inter-relationship between ACC GABA, neural correlates of interference inhibition, and impulsivity traits in BPD and HCs. illustrates the investigated model in this project. We hypothesized that the task-dependent activation and connectivity during interference inhibition serve as a mediator which could explain the associations between GABA and impulsivity.

The hypothesis is based on previous studies: increased impulsivity seemingly develops as a result from lower ability of inhibitory control (Olson et al., 2002; Olson et al., 1999), a cognitive function modulated by the frontal GABAergic system, which further drives the neural activity and synchronization of the fronto-striatal network (Bari and Robbins, 2013; Dalley et al., 2008a; Hayes et al., 2014).

GENERAL INTRODUCTION

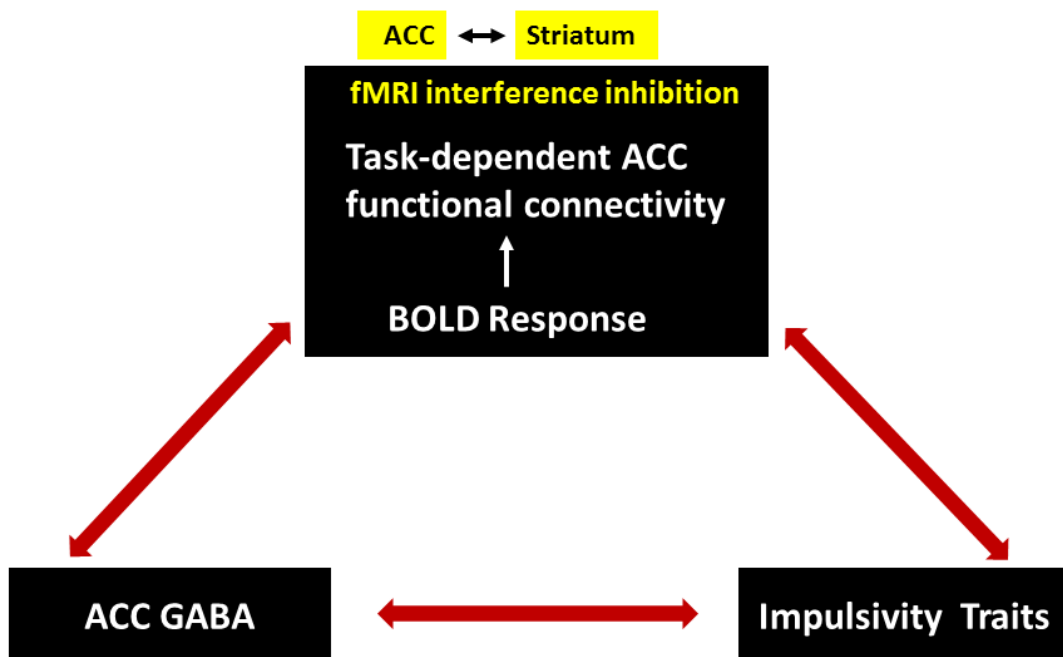


Figure 4-1 Illustration of the aim of the project. The main variables of interest are displayed in black boxes: GABA concentration, impulsivity traits and task-related BOLD signals, particularly in the ACC, striatum (including caudate, putamen, pallidus). Also the functional connectivity between these regions was of interest, indicated by the arrows.

GENERAL INTRODUCTION

CHAPTER II.

EMPIRICAL STUDIES

5 Longitudinal mapping of gyral and sulcal patterns of cortical thickness and brain volume regain during early alcohol abstinence²

Abstracts:

We explored brain volume recovery in terms of cortical thickness (gyral, sulcal pattern) and surface area, as well as subcortical volume recovery in the first two weeks of abstinence in 49 alcohol dependent patients. A wide-spread reduction of cortical thickness in alcohol dependent patients at day 1 of abstinence compared to healthy controls, with more pronounced differences in sulci relative to gyri was found. After 2 weeks of abstinence, partial recovery to varying degrees of cortical thickness loss in alcohol dependent patients was observed for several regions. The longitudinal cortical thickness changes were greater in sulci than in gyri of affected regions. No longitudinal change in surface areas and subcortical volumes was found. Alterations of cortical thickness contribute to brain volume loss in alcoholism and recovery during early abstinence. Sulci seem to be more vulnerable to

² Publication:

Wang, G.Y., Demirakca, T., van Eijk, J., Frischknecht, U., Ruf, M., Ucar, S., Hermann, D., Mann, K., Kiefer, F., Ende, G., 2016. Longitudinal Mapping of Gyral and Sulcal Patterns of Cortical Thickness and Brain Volume Regain during Early Alcohol Abstinence. *European addiction research* 22, 80-89.

EMPIRICAL STUDIES

excessive alcohol consumption and to drive abstinence induced volume recovery. No subcortical volume regain during the initial two weeks of abstinence was observed. Either the time span was too short, or lower subcortical volume could represent a pre-disposing trait marker.

Keywords:

Cortical thickness; early alcohol abstinence; gyri; sulci; subcortical volume

5.1 Introduction

It is well recognized that excessive alcohol consumption causes widespread structural changes in the brain, and hence leads to related functional deficits. Plenty of studies have consistently reported loss of gray matter (GM) and white matter (WM) and increased cerebrospinal fluid (CSF) in alcohol dependent individuals (for review see: (Buhler and Mann, 2011), (Krienke et al., 2014)). For example, alcohol dependent individuals showed a volume shrinkage in reward network brain regions, and volume change of those structures was associated with post-treatment alcohol consumption (Makris et al., 2008). Animal and human studies (Matthews and Morrow, 2000; Silvers et al., 2003; White et al., 2000) have indicated that chronic alcohol abuse impairs the hippocampus, which elicits deficits in visuospatial learning and memory. One study (Wrase et al., 2008) suggested that smaller amygdala volume in chronic alcoholics was associated with greater alcohol craving and relapse.

Notably, abstinent alcohol dependent individuals show a partial regeneration of brain volume changes, even during early abstinence (Demirakca et al., 2011a; Pfefferbaum et al., 1995; van Eijk et al., 2013). Brain volume regeneration appears to be greater during the first several weeks compared to continued long-term abstinence (Gazdzinski et al., 2005; Pfefferbaum et al., 1995). Moreover, a previous study (Gazdzinski et al., 2005) reported that alcoholics with pronounced brain volume loss at baseline experienced greater recovery during abstinence.

However, most cross-sectional and longitudinal brain volume studies obtained baseline measurements several weeks after cessation of drinking (Durazzo et al., 2010; Fein et al., 2006; Shear et al., 1994; Sullivan et al., 2005a; Wrase et al., 2008). Obviously, those studies may miss the early short-term recovery effect and might underestimate the extent of brain impairment and the potential magnitude of recovery. Thus, in our previous study (van Eijk et al., 2013), voxel-based morphometry (VBM) was used to highlight the widespread volumetric changes due to excessive alcohol consumption and partial volume reversibility within the first 2 weeks of alcohol abstinence. Volume recovery was only found in cortical areas with different recovery extents. No difference in any subcortical areas including pallidum, amygdala, as well as hippocampus was detected, especially not in the reward system

EMPIRICAL STUDIES

including caudate, putamen and nucleus accumbens, although these changes had been reported in other cross-sectional and long-term abstinence studies in alcoholism (Makris et al., 2008; Sameti et al., 2011).

Subcortical volume differences could be easily overlooked. One study (Bergouignan et al., 2009a) reported that disease-induced hippocampal changes could not be detected by standard VBM analysis. However, several studies pointed out that Freesurfer is a robust tool to analyze the subcortical structures (Dewey et al., 2010; Tae et al., 2008), with comparable accuracy to the manual labeling approach (Fischl et al., 2002). In contrast to the subcortical segmentation procedure in VBM, the technique applied by Freesurfer directly assigns a neuroanatomical label to each voxel based on probabilistic information derived from a manually labelled training set. Additionally, the classification technique in Freesurfer also employs a registration procedure to robustly distinguish the within-structure variability in the intrinsic tissue parameters to get a more accurate segmentation (Fischl et al., 2002).

In addition, VBM is not able to analyze cortical thickness. It is well documented that cortical volume includes two distinct properties: surface area (SA) and cortical thickness (CTh), which have different cellular and genetic bases and are affected by different lifespan factors (Hogstrom et al., 2013; Winkler et al., 2010). SA is associated with the numbers of radial columns, and appears to be influenced by various developmental factors. Whereas CTh is related to the number of cells in a column, being highly vulnerable to environmental factors over the lifespan (Momenan et al., 2012). Furthermore, cortical GM volume variation across healthy subjects is mostly driven by differences in the cortical SA rather than CTh (Im et al., 2006; Winkler et al., 2010). Thus, it is important to study the morphometric properties of cortical GM volume, CTh, and SA independently.

Moreover, structural differences exist between the sulci and gyri across the cortical brain areas, with gyri having greater number of neurons in deep layers (Welker, 1990), as well as different cell and dendrite morphology. A recent diffusion MRI study (Nie et al., 2012) pointed out that axonal connections are more concentrated in gyri relative to sulci. Another diffusion tensor imaging (DTI) study (Deng et al., 2014) indicated that gyri are global

EMPIRICAL STUDIES

functional connection centers and sulci are local functional hubs. Therefore, the sulci and gyri could be differentially affected by excessive alcohol consumption, and the initial recovery in early stage of abstinence could also differ. However, to our knowledge no study has reported and addressed this issue yet.

We used Freesurfer (<http://surfer.nmr.mgh.harvard.edu/>) to analyze our data, focusing on the volumetric changes in certain regions of interest (ROIs) in subcortical areas, CTh (sulcal & gyral pattern) and SA changes in cortical areas, associated with excessive alcohol consumption and early abstinence. Subcortical ROIs include caudate, putamen, pallidum, nucleus accumbens, amygdala, as well as hippocampus.

In summary, the main aims of our present study are: 1) to test (with Freesurfer) which parts of the subcortical regions are affected by excessive alcohol consumption and undergo significant recovery within the first 2 weeks of abstinence in alcohol dependent patients (ADPs). 2) to gain a deeper insight into the underlying mechanisms that contribute to dynamic cortical volumetric changes in ADPs within the first 2 weeks of abstinence (van Eijk et al., 2013) by examining the CTh and SA; 3) to test whether and how the pattern of gyri and sulci are differentially affected by excessive alcohol consumption, and whether the extents of recovery are different.

5.2 Materials and Methods

5.2.1 Participants

Forty-nine ADPs and 20 healthy controls (HCs) were included in our study. Group demographic data are summarized in Table 5-1. Treatment-seeking alcoholic inpatients were recruited from the Department of Addiction Medicine at the Central Institute of Mental Health in Mannheim, Germany. Patients met the DSM-IV and ICD10 criteria for alcohol dependence at the time of enrollment. They were first scanned within one day after their last alcoholic drink (TP1), and re-scanned after 14 days of abstinence (TP2). The severity of alcohol dependence was assessed with the Alcohol Dependence Scale (ADS) (Skinner Ha Fau - Allen and Allen, 1982) . Alcohol craving and drinking behavior was evaluated by the German

EMPIRICAL STUDIES

version of the Obsessive Compulsive Drinking Scale (OCDS) (Mann K, 2000). The age-matched HC group, who underwent two MRI measurements in a 14 days interval, was recruited by newspaper advertisement.

Exclusion criteria for all participants were: dependence on any substance other than alcohol or nicotine, any psychotropic medication in last 3 months, positive urine drug tests, brain injury history, other neurological or severe physiological illness (e.g. severe diabetes, HIV, etc.), hepatic encephalopathy, liver cirrhosis, and MRI-related exclusion criteria (e.g. metal implants, pace makers, etc.).

All participants provided written informed consent prior to the study. The study was approved by the ethics committee of the medical faculty Mannheim of Heidelberg University. Detailed information on the participants' medication has been provided in our earlier work (van Eijk et al., 2013).

Table 5-1 Demographic data for alcohol-dependent patients and healthy controls

| | Alcohol dependent patients | | Health controls | |
|---------------------------------------|----------------------------|--------|-----------------|-------|
| | Mean | SD | Mean | SD |
| Total Number | 49 | -- | 20 | -- |
| Number of female | 9 | -- | 3 | -- |
| Number of male | 40 | -- | 17 | -- |
| Age (years) | 47.02 | 10.00 | 46.65 | 12.37 |
| Alcohol(g) per drinking day * | 211.05 | 147.35 | 22.11 | 10.48 |
| Alcohol Dependence Scale * | 15.11 | 7.70 | 0.47 | 1.87 |
| Obsessive Compulsive Drinking Scale * | 21.45 | 9.36 | 2.60 | 2.80 |

* Significantly different between 2 groups ($p < 0.001$).

5.2.2 MRI Image Acquisition

MRI measurements were conducted at a Siemens Tim Trio 3T scanner (Erlangen, Germany) using a 12-channel head coil. A high-resolution 3D T1-weighted (MPRAGE) data set was acquired for each participant. Imaging parameters were as follows: repetition time TR = 2300

EMPIRICAL STUDIES

ms; echo time TE = 3.03 ms; inversion time TI = 900 ms; flip angle 9°; 192 slices; field of view 256 × 256 mm²; voxel size 1 × 1 × 1 mm³.

5.2.3 MRI Image Analysis

Before preprocessing with FreeSurfer, the data sets were inspected for the homogeneity and quality control via VBM8 (<http://www.neuro.uni-jena.de/vbm/>). Volume, CTh, SA and subcortical volume were processed with the FreeSurfer 5.1.0 software package. In brief, the processing stream includes motion correction, removal of non-brain tissue (Segonne et al., 2004), automated Talairach transformation, segmentation of the cortical GM and WM volumes and deep GM volumetric structures (Fischl et al., 2004), intensity normalization (Sled et al., 1998), tessellation of the GM/WM boundary, automated topology correction (Segonne et al., 2007), as well as surface deformation to define the grey/white and pial surface (Dale et al., 1999; Fischl and Dale, 2000). For each subject, CTh was calculated as the shortest distance from the GM/WM boundary to the GM/CSF boundary at each vertex on the tessellated surface (Fischl and Dale, 2000). SA was calculated by summing up the area of the vertices in each parcellation. Subcortical volume was calculated by voxel counting, based on an atlas containing probabilistic information for the structure classifications (Fischl et al., 2002). Additional, for the analysis of the longitudinal changes, an unbiased within-subject template space and average image was created using robust, inverse consistent registration (Reuter et al., 2012). The post-processing outputs were visually inspected and manually edited (if necessary) to assure the processing accuracy. To enable inter-subject and intra-subject comparison, the data for each subject was normalized to a standard surface template in a spherical surface-based coordinate system provided by FreeSurfer – to allow for a much higher localization accuracy of structural features of the brain across participants – and concatenated into a single image. Finally, this image was smoothed with a 10 mm full width at half maximum (FWHM) Gaussian kernel to improve the signal-to-noise ratio and reduce local variations (Du et al., 2007) in the measurements for further analysis. The quantitative estimates were driven in a set of spatially distinct ROI obtained using the sulcogyral-based atlas (68 ROI parcellations) (Desikan et al., 2006) and for further and more detailed investigations of gyri and sulci, an atlas with 148 ROI parcellations was used (Destrieux et al.,

2010). Figure 5-1 illustrates the visualization of the cortical surface, and its division into sulci and gyri.

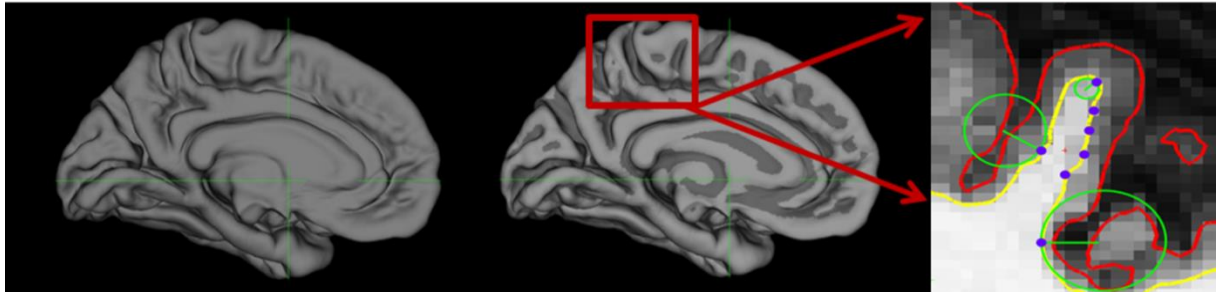


Figure 5-1 The brain surface in the middle aspect of the brain cortex (left). The same image after calculating and color-labelling the convexity and curvature of the sulci (dark-gray) and gyri (light-gray) (middle). An example of how to differentiate gyri and sulci based on the curvature value (right). Curvature=1/radius of circle (circle tangent to surface at each vertex). Vertices with a positive mean curvature value were served as sulci, and vertices with non-positive values were served as gyri.

5.2.4 Statistical Analysis

Statistical analysis was performed using FreeSurfer's Qdec (version 1.4) and SPSS (software Version 21 (IBM, Chicago, IL)). All demographic and neuroanatomical measures were tested for normal distribution using the Kolmogorov-Smirnov and Shapiro-Wilk tests. Group differences of demographic measures (before scan1) were assessed by independent two sample t-tests, with P-threshold set at 0.05.

In the previous VBM analysis (van Eijk et al., 2013) we tested whether there was a significant difference in GM volume between the smoking and non-smoking subgroup of ADP. We found no smoking effects on GM volume in our patients' sample. Thus, based on the prior analysis, we did not include the smoking behavior as a covariate in the current paper.

To avoid possible bias due to different brain volumes across subjects, the estimated total intracranial volume (eTIV) was calculated as the volume enclosed by the pial surface. In addition, to control for possible cortical folding features impacting on cortical thickness results, a general linear model (GLM) analysis was performed on cortical folding

EMPIRICAL STUDIES

characteristics, such as the depth of sulci of each vertex (SULC), the curvature of cortical surface (CURV), as well as the amount of convolution and displacement needed to warp the cortical surface during the registration (JACOBIAN_WHITE). These above three parameters (SULC, CURV, and JACOBIAN_WHITE) were automatically calculated by FreeSurfer.

We first analyzed the global measures (total GM volume, total cortical volume, total subcortical volume, total WM volume, total SA and mean total CTh) to get a first impression of the alcohol abuse and abstinence related effects on brain morphological alterations. Then, to corroborate these findings, local morphological measures (local CTh, local SA and ROI subcortical volume) were assessed. Furthermore, we did a separate analysis of gyral and sulcal CTh in these significant local ROIs to further investigate the underlying mechanisms. Age and gender were set as covariates for all analyses. Since the eTIV was found to be only related to the SA but not to the CTh both in our analysis and other studies (<https://surfer.nmr.mgh.harvard.edu/fswiki/eTIV>), the eTIV was only used as a covariate when we computed the volume and SA measures.

5.2.5 Cross-sectional analysis

A GLM with covariates of age and gender (and eTIV for volume and SA measures) was used to test group differences at each time point (TP) in global and regional / local measures between HCs and ADPs. Briefly, global measures and ROI subcortical volumes were assessed by multivariate analysis with covariates (MANCOVA) with the threshold set at $P < 0.05$ with Bonferroni correction. Statistical parametric maps of the local CTh and local SA were assessed at each surface vertex of the entire cortical mantle. Results were corrected for multiple comparisons with false discovery rate (FDR) at $P < 0.05$.

5.2.6 Longitudinal analysis

Mixed factorial ANCOVAs followed by paired t-tests were used for longitudinal analysis between patients and controls when global measures and ROI subcortical volumes were calculated. Covariates were also age and gender (and eTIV for volume and SA measures). The main effect for diagnosis, time, and the interaction of diagnosis-by-time were tested. The

EMPIRICAL STUDIES

significant threshold was set at $P < 0.05$ with Bonferroni correction. The extent of longitudinal changes in CTh and SA were defined as $(\text{measure at TP2} - \text{measure at TP1}) / \text{measure at TP1} * 100$, since all participants were scanned with the same interval (14 days) between both measurements. For comparisons of the local CTh and local SA, cluster-wise correction for multiple comparisons was performed with Monte Carlo simulations (vertex-wise threshold $P < 0.05$, 5000 iterations). Cluster-wise probabilities are reported, which represent the likelihood of finding a maximum cluster size during simulations (Hagler et al., 2006).

5.3 Results

5.3.1 Participants' characterization

Characteristics of participants for the two groups are shown in Table 5-1. No significant differences were noted in gender composition and age between the two groups. In comparison to controls, ADPs rated significant higher on the Alcohol Dependence Scale (ADS) as well as the OCDS (both $P < 0.001$).

5.3.2 Volume, surface area, and cortical thickness

5.3.2.1 Global measures

MANCOVA results revealed group differences in global measures between HCs and ADPs at both measurement TPs. Specifically, compared to HCs, ADPs exhibited lower global measures in total GM volume (TP1: $F(1,64) = 28.562$, $P < 0.001$; TP2: $F(1,64) = 28.170$, $P < 0.001$), total cortical volume (TP1: $F(1,64) = 24.187$, $P < 0.001$; TP2: $F(1,64) = 23.800$, $P < 0.001$), total subcortical volume (TP1: $F(1,64) = 23.516$, $P < 0.001$; TP2: $F(1,64) = 21.312$, $P < 0.001$), mean total CTh (TP1: $F(1,64) = 34.362$, $P < 0.001$; TP2: $F(1,64) = 28.562$, $P < 0.001$). No difference was found in global WM volume and total SA between HCs and ADPs for both TPs ($P > 0.05$).

Longitudinally, a 2×2 mixed factorial MANCOVA was conducted with the diagnosis as between-subjects factor and the time as a within-subjects factor. Significant diagnosis-by-time

EMPIRICAL STUDIES

interaction effect was found for mean total CTh ($F(1, 65) = 7.996$, $P = 0.036$). No interaction was seen in total GM volume, total WM volume, total cortical volume, total subcortical volume and total SA (all $P > 0.05$). Further, follow-up paired t-tests revealed no between-scan changes in any global measures in HCs, while ADPs demonstrated longitudinal increases in global measures of mean total CTh ($P < 0.001$).

5.3.2.2 Regional subcortical volumes

Smaller volumes in ADPs compared to HCs were evident for both TPs and located bilaterally in the putamen (TP1: left $P = 0.012$, right $P = 0.012$; TP2: left $P = 0.012$, right $P = 0.012$), nucleus accumbens (TP1: left $P < 0.001$, right $P = 0.012$; TP2: left $P = 0.012$, right $P = 0.024$), amygdala (TP1: left $P < 0.001$, right $P < 0.001$; TP2: left $P < 0.001$, right $P < 0.001$) as well as hippocampus (TP1: left $P = 0.012$, right $P < 0.001$; TP2: left $P = 0.012$, right $P = 0.012$). No group differences in the bilateral caudate and pallidum volumes were observed both at the TP1 and TP2 ($P > 0.05$).

Longitudinally, the 2×2 mixed factorial MANCOVA revealed that no significant diagnosis-time interaction was found for any of the 12 subcortical ROIs (bilateral caudate, putamen, pallidum, nucleus accumbens, amygdala, and hippocampus ($P > 0.05$)).

5.3.2.3 Local cortical thickness

Figure 5-2 illustrates areas of cortical thinning in ADPs relative to HCs at TP1 and TP2, respectively. On day 1 of abstinence (TP1), compared to HCs, ADPs demonstrated widespread lower CTh across the whole brain cortex. Differences between the ADPs and HCs were significant bilaterally in the medial orbitofrontal area, superior, middle and inferior part of frontal lobe, fusiform (extending to inferior temporal, lateral occipital lobe), inferior parietal (extending to postcentral, superior parietal lobe), in the left entorhinal and left lateral orbitofrontal area, as well as in the right rostral anterior cingulate (rostral ACC). After 14 days of abstinence (TP2), a partial recovery of cortical thinning was observed, but most of the regions remained significantly different between groups, including bilateral superior parietal, superior frontal, precentral, superior and inferior temporal areas. However, group differences

EMPIRICAL STUDIES

of cortical thickness for the bilateral medial orbitofrontal area and right rostral ACC could not be detected anymore.

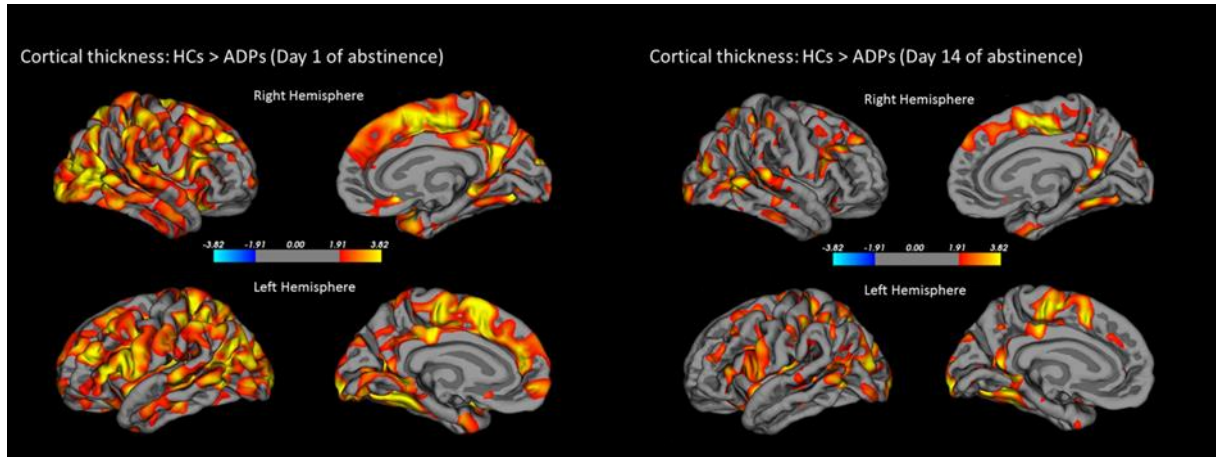


Figure 5-2 Areas of cortical thickness loss in ADPs at day 1 (left) and day 14 (right) of abstinence compared to HCs ($p < 0.05$, FDR corrected). The value of the scale bar represents $-\log_{10}(p) = 1.3$, with $P = 0.05$.

Longitudinally, the comparison of changes in CTh over the first 2 weeks of abstinence (TP2-TP1) between ADPs and HCs demonstrated an increase of cortical thickness in the ADP group in the bilateral lateral occipital, bilateral precentral, right postcentral, right cuneus, right caudal middle frontal, right superior frontal, right rostral ACC, left medial orbitofrontal, left parsopercularis, left lingual and left inferior parietal area (see Figure 5-3, Table 5-2). No longitudinal CTh changes were observed in HCs in this time period.

EMPIRICAL STUDIES

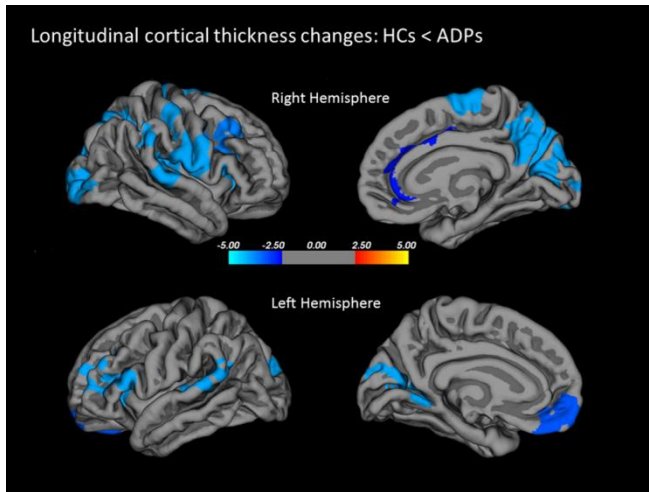


Figure 5-3 Areas of cortical thickness regaining in ADPs versus HCs after the first 14 days of abstinence (Monte Carlo simulation: vertex-wise threshold $p < 0.05$, 5000 iterations). The value of the scale bar represents $-\log_{10}(p) = 1.3$, with $P = 0.05$.

Table 5-2 Peak voxel of regions with cortical thickness regain in alcohol dependent patients versus healthy controls within the first 2 weeks of abstinence

| Hemisphere | Significant clusters | Max | Size (mm ²) | TalX | TalY | TalZ | CWP |
|------------|----------------------------|--------|-------------------------|-------|-------|-------|--------|
| Left | Lateral occipital | -4.561 | 613.72 | -23.7 | -87.2 | -6.2 | 0.0392 |
| | Medial orbitofrontal | -4.097 | 1034.17 | -6 | 56.5 | -11.9 | 0.001 |
| | Pars operculari | -3.368 | 2573.72 | -44.1 | 26 | 9.9 | 0.0001 |
| | Lingual | -3.127 | 1767.49 | -12.9 | -55 | 1.6 | 0.0001 |
| | Precentral | -2.969 | 715.03 | -41.9 | -5.1 | 44.8 | 0.015 |
| | Inferior parietal | -2.875 | 1197.98 | -43 | -50.8 | 22.4 | 0.0001 |
| Right | Postcentral | -5.023 | 5019.93 | 43.1 | -11.4 | 19.7 | 0.0001 |
| | Cuneus | -4.09 | 4918.99 | 10.7 | -66 | 19.4 | 0.0001 |
| | Lateral occipital | -3.455 | 1644.23 | 24.8 | -81.5 | -4 | 0.0001 |
| | Caudal-middle frontal | -3.361 | 681.71 | 33.9 | 1.3 | 41.8 | 0.046 |
| | Precentral | -3.121 | 1337.34 | 40.9 | 5.2 | 21.2 | 0.0003 |
| | Superior frontal | -2.971 | 2067.37 | 12.1 | 3.5 | 61 | 0.0001 |
| | Rostral anterior cingulate | -2.39 | 930.46 | 6.8 | 37 | -2.6 | 0.0059 |

Age and gender were set as covariates;

Monte Carlo simulations were used for cluster-wised correction: vertex-wise threshold $p < 0.05$, 5000 iterations.

CWP: clusterwise P-value

EMPIRICAL STUDIES

5.3.2.4 Gyral and Sulcal cortical thickness of the affected regions in ADPs

For the sake of clarity, the data of gyral and sulcal CTh were calculated and presented as average bilateral CTh in each lobe. Separate analysis of gyral and sulcal parts of the significant affected brain regions are shown in Figure 5-2 (day 1 of abstinence) suggested that each of those regions was thicker in gyri compared to sulci (all $P < 0.01$). On a descriptive level, cortical thickness differences between ADPs and HCs were more pronounced in sulcal relative to gyral parts in frontal lobe, parietal lobe, insular as well as temporal lobe (see Table 5-3).

Table 5-3 Gyral and sulcal cortical thickness of the affected regions mm²

| | Alcohol Dependent Patients (Day 1 of abstinence) | | Healthy Controls | | Difference (%) Healthy Controls v.s Alcohol Dependent Patients | |
|----------------|--|-----------------------------|----------------------------|-----------------------------|---|------------------|
| | Mean (SD) | | Mean (SD) | | Gyral | Sulcal |
| | Gyral thickness | Sulcal thickness | Gyral thickness | Sulcal thickness | thickness | thickness |
| Frontal lobe | 2.62 (0.18) | 2.11 (0.15) | 2.86 (0.19) | 2.37 (0.23) | 0.23 (8.12%) | 0.26 (10.84%) |
| Parietal lobe | 2.33 (0.17) | 1.81 (0.14) | 2.56 (0.20) | 2.06 (0.26) | 0.24 (9.18%) | 0.26 (12.45%) |
| Temporal lobe | 2.76 (0.21) | 2.29 (0.19) | 2.96 (0.16) | 2.55 (0.17) | 0.20 (6.70%) | 0.26 (10.29%) |
| Insular | 3.46 (0.23) | 2.59 (0.17) | 3.76 (0.21) | 2.81 (0.14) | 0.29 (7.77%) | 0.22 (7.86%) |
| Occipital lobe | 2.11 (0.15) | 2.05 (0.16) | 2.35 (0.28) | 2.27 (0.12) | 0.24 (10.27%) | 0.22 (9.56%) |

Difference: absolute differences value of cortical thickness in mm between the two groups;

%: represent the difference in percentage relative to the cortical thickness in healthy controls.

The regeneration extents of sulci in all affected regions were more pronounced in sulci than in gyri during the first 14 days of abstinence. The paired t-test showed that the recovery

EMPIRICAL STUDIES

magnitude of the frontal sulci was significantly greater than that of gyri ($P = 0.01$) (see Table 5-4).

Table 5-4 Abstinence-induced regain of gyral and sulcal cortical thickness for affected regions

| Regions | Changes in Gyri Mean (%) | Changes in Sulci Mean(%) | P Value |
|----------------|-------------------------------------|-------------------------------------|----------------|
| Frontal | 0.0009 (0.028%) | 0.0313(1.69%) | 0.01 |
| Insular | 0.0148(0.50%) | 0.0375(1.58%) | 0.27 |
| Parietal | 0.0283(1.25%) | 0.0265(1.56%) | 0.78 |
| Occipital | 0.0187(0.94%) | 0.0329(1.82%) | 0.36 |
| Temporal | 0.0295(1.12%) | 0.0421(1.97%) | 0.26 |

5.3.3 Local surface area

In local SA, no significant group differences between HCs and ADPs, as well as no significant longitudinal changes within the first 2 weeks of abstinence could be detected.

5.3.4 Cortical folding parameters

There were no between-group (ADPs vs. HCs) and longitudinal changes (TP2-TP1) in cortical folding parameters for SULC, CURV, and JACOBIAN_WHITE, indicating that folding parameters have no effect on cortical thickness.

5.4 Discussion

Our study aimed to investigate the subcortical volumes affected by chronic alcohol dependence and initial regain within the first 2 weeks of abstinence in ADPs. Moreover, this is also the first report to explore the nature of the partial recovery for the brain volume loss during the first 2 weeks of alcohol abstinence, as well as the gyral and sulcal pattern of affected CTh reduction and abstinence-induced recovery. The novel findings were as follows: (1) ADPs at day 1 of abstinence demonstrated significantly lower subcortical volumes than HCs in most reward system regions, including putamen, nucleus accumbens, amygdala, hippocampus. However, no area showed significant subcortical volume regain within the first

EMPIRICAL STUDIES

14 days of abstinence in ADPs. (2) In ADPs, the cortical volume recovery during the first 2 weeks of abstinence is predominantly driven by an increase in CTh. No significant longitudinal change in SA was seen either on a global or local level. (3) The CTh reduction is more pronounced in sulci than gyri across the affected regions. Greater sulcal than gyral CTh recovery in affected areas were seen during the first 2 weeks of sobriety.

The impairment of subcortical structures has been consistently reported in alcohol dependent individuals, especially the reward circuit is associated with chronic alcohol dependence and relapse (Bauer et al., 2013; Durazzo et al., 2011; Kuceyeski et al., 2013; Makris et al., 2008; Segobin et al., 2014). Our study, replicating previous findings, found that ADPs at day 1 of abstinence have smaller volumes of reward-related structures (including amygdala, putamen, nucleus accumbens, hippocampus), and these statistically significant differences still persist after 2 weeks of alcohol abstinence. This is in good concordance with lower volumes of the reward system in alcohol abstainers with maintained sobriety for 12 months (Durazzo et al., 2011; Sullivan et al.). There are also results by a cross-sectional study that reveal only minimal differences in subcortical volumes between alcoholics with about 6 years of sustained abstinence and nonalcoholic controls (Sameti et al., 2011). Moreover, consistent with our previous observation (van Eijk et al., 2013), no significant volumetric recovery of the subcortical structures was observed in current study, even with different approaches to analyze it. Remaining subcortical volume reductions despite long-term abstinence either suggests a non-reversible alcohol-induced damage of subcortical structures, or as just recently discovered a genetically determined smaller volume of subcortical structures (Hibar et al., 2015). Thus it should be considered that subjects developing alcohol dependence could have genetically determined smaller subcortical volumes potentially predisposing for alcoholism. Hence, longitudinally studies with a first measurement of subcortical volumes before starting alcohol use, further measurements after the development of alcoholism and long-term abstinence would be necessary to clarify this issue.

To further describe the nature of abstinence-induced volume changes, we examined both SA and CTh in this study. Our results suggest that no longitudinal changes occurred in any global and local SA during the first 2 weeks of abstinence, but region-specific increase in CTh is the

EMPIRICAL STUDIES

main feature. Specifically, there were pronounced increases in CTh in the medial orbitofrontal, middle frontal, superior frontal, rostral ACC, precentral, postcentral, cuneus, inferior parietal and lateral occipital regions in ADPs within the first 2 weeks of abstinence. The possible mechanisms behind the structural recovery are rehydration effect, axonal and dendritic regrowth, remyelinations, glial cell alterations, cerebral perfusion increase via improving microvasculature function or metabolite increase (Bartsch et al., 2007; Durazzo et al., 2010; Ende et al., 2005; Harper, 2009; Kohler et al.; Schweinsburg et al., 2000). These factors may differentially contribute to structural recovery at different TPs during abstinence. Increased myo-inositol (an index for glial cell activation) in ACC was only found in recently detoxified but not long-term abstinent alcoholics (Schweinsburg et al., 2000). However, the mechanism underlying the recovery of CTh during the first 2 weeks of abstinence is still unclear.

It is interesting to note that after only 14 days of abstinence, the CTh differences in the bilateral middle orbitofrontal cortex and right rostral ACC between HC and ADPs cannot be observed anymore. This might be a hint that the frontal lobe appears to be a very susceptible region to recover over the first 2 weeks of abstinence. Early pathology work also indicates that alcohol preferentially effects on pyramidal neurons in the frontal cortex. Alcohol related changes in neocortical neuronal loss and dendritic shrinkage may lead to cortical thinning, but the dendrite shrinkage could be fast reversible by alcohol abstinence (Harper, 2009).

Last, we extend our observations to the gyral and sulcal pattern of CTh loss and abstinence-induced partial recovery. Our results indicate that ADPs have more prominent shrinkage in sulcal than gyral parts of affected regions, suggesting that the atrophy effect of excessive alcohol consumption differs between gyri and sulci. Additionally, after 14 days of abstinence, ADPs demonstrated a greater thickness recovery in the sulcal part of affected areas than the gyral part, particular evident in frontal regions. Taken together, those results indicate that sulci are more susceptible to excessive alcohol consumption, and abstinence-induced recovery. In the future, a longitudinal animal model study is needed to explore the mechanisms behind this sulci-gyri differential vulnerability effect to alcohol.

EMPIRICAL STUDIES

In fact, there are distinct lines of evidence in support of our observation of a differential effect for sulci compared to gyri. A previous study indicated that the cytoarchitecture of gyri and sulci is greatly different in the human brain (White et al., 2003). Additionally, a significant difference between gyri and sulci in the axonal connectivity function and gene expression was found both in animals and humans (Deng et al., 2014; Zeng et al., 2014). A multimodal DTI/fMRI study (Deng et al., 2014) suggested that gyri are more related to longer connections that exchange information among distant structurally connected cortical regions via dense fibers, while sulci are more related to shorter connections that communicate directly with their neighboring gyri and indirectly exchange information with remote regions through gyri. Based on those indications, our data suggest short distance connections are more susceptible for excessive alcohol consumption and abstinence. Actually, functional connectivity alterations in alcoholism have repeatedly been reported (Beck et al., 2012; Chanraud et al., 2011; Muller-Oehring et al., 2014).

5.5 Limitations

For the statistics, mixed factorial MANCOVA was only used for global measures and regional subcortical volume analysis. Since the linear mixed effect analysis is not available for the FS5.1 version, local cortical thickness was estimated by the longitudinal percentage CTh change. In addition, head motion could also affect the cortical thickness measurement (Reuter et al., 2015). The homogeneity and quality of the data sets was inspected via VBM8. However, it would be more accurate to account for the motion effect if we could estimate the motion levels and use them as a covariate.

5.6 Conclusion

In conclusion, in this study we suggest that CTh alteration could be the mechanism corresponding to the previously observed partial volumetric recovery (van Eijk et al., 2013) during the first 2 weeks of abstinence in ADPs. The observation that the differences observed in the frontal lobe between patients and controls on day one of abstinence were not evident any more on day 14 might hint that the frontal lobe is a very susceptible region to abstinence-related recovery. Moreover, this is also the first report to reveal that alcohol differentially

EMPIRICAL STUDIES

impacts on sulci and gyri of the neocortex. Sulci are more susceptible to excessive alcohol consumption and abstinence-induced recovery. In light of current theories of the functional model of gyri and sulci, these changes may reflect aberrations in cerebral and subcortical connectivity. In addition, in contrast to multiple regional cortical GM regeneration within 14 days of abstinence, no subcortical volumetric recovery in the reward system was found, suggesting that the subcortical structures are damaged irreversible by alcohol or that genetically determined smaller volume of subcortical structures mediates susceptibility for alcoholism. These sustained subcortical GM alterations may attribute to the self-sustaining alcohol seeking behavior, cognitive and behavioral deficits in ADPs.

Acknowledgements

This work was supported by the Deutsche Forschungsgemeinschaft. (SFB636, project D7 to GE and KM).

References

- Bartsch, A.J., Homola, G., Biller, A., Smith, S.M., Weijers, H.G., Wiesbeck, G.A., Jenkinson, M., De Stefano, N., Solymosi, L., Bendszus, M., 2007. Manifestations of early brain recovery associated with abstinence from alcoholism. *Brain : a journal of neurology* 130, 36-47.
- Bauer, J., Pedersen, A., Scherbaum, N., Bening, J., Patschke, J., Kugel, H., Heindel, W., Arolt, V., Ohrmann, P., 2013. Craving in alcohol-dependent patients after detoxification is related to glutamatergic dysfunction in the nucleus accumbens and the anterior cingulate cortex. *Neuropsychopharmacology : official publication of the American College of Neuropsychopharmacology* 38, 1401-1408.
- Beck, A., Wustenberg, T., Genauck, A., Wrase, J., Schlagenhauf, F., Smolka, M.N., Mann, K., Heinz, A., 2012. Effect of brain structure, brain function, and brain connectivity on relapse in alcohol-dependent patients. *Archives of general psychiatry* 69, 842-852.
- Bergouignan, L., Chupin, M., Czechowska, Y., Kinkingnehun, S., Lemogne, C., Le Bastard, G., Lepage, M., Garnero, L., Colliot, O., Fossati, P., 2009. *NeuroImage* 45, 29-37.
- Buhler, M., Mann, K., 2011. Alcohol and the human brain: a systematic review of different neuroimaging methods. *Alcoholism, clinical and experimental research* 35, 1771-1793.
- Chanraud, S., Pitel, A.L., Pfefferbaum, A., Sullivan, E.V., 2011. Disruption of functional connectivity of the default-mode network in alcoholism. *Cerebral cortex* 21, 2272-2281.

EMPIRICAL STUDIES

- Dale, A.M., Fischl, B., Sereno, M.I., 1999. Cortical surface-based analysis. I. Segmentation and surface reconstruction. *NeuroImage* 9, 179-194.
- Demirakca, T., Ende, G., Kammerer, N., Welzel-Marquez, H., Hermann, D., Heinz, A., Mann, K., 2011. Effects of alcoholism and continued abstinence on brain volumes in both genders. *Alcoholism, clinical and experimental research* 35, 1678-1685.
- Deng, F., Jiang, X., Zhu, D., Zhang, T., Li, K., Guo, L., Liu, T., 2014. A functional model of cortical gyri and sulci. *Brain structure & function* 219, 1473-1491.
- Desikan, R.S., Segonne, F., Fischl, B., Quinn, B.T., Dickerson, B.C., Blacker, D., Buckner, R.L., Dale, A.M., Maguire, R.P., Hyman, B.T., Albert, M.S., Killiany, R.J., 2006. An automated labeling system for subdividing the human cerebral cortex on MRI scans into gyral based regions of interest. *NeuroImage* 31, 968-980.
- Destrieux, C., Fischl, B., Dale, A., Halgren, E., 2010. Automatic parcellation of human cortical gyri and sulci using standard anatomical nomenclature. *NeuroImage* 53, 1-15.
- Dewey, J., Hana, G., Russell, T., Price, J., McCaffrey, D., Harezlak, J., Sem, E., Anyanwu, J.C., Guttmann, C.R., Navia, B., Cohen, R., Tate, D.F., 2010. Reliability and validity of MRI-based automated volumetry software relative to auto-assisted manual measurement of subcortical structures in HIV-infected patients from a multisite study. *NeuroImage* 51, 1334-1344.
- Du, A.T., Schuff, N., Kramer, J.H., Rosen, H.J., Gorno-Tempini, M.L., Rankin, K., Miller, B.L., Weiner, M.W., 2007. Different regional patterns of cortical thinning in Alzheimer's disease and frontotemporal dementia. *Brain : a journal of neurology* 130, 1159-1166.
- Durazzo, T.C., Gazdzinski, S., Mon, A., Meyerhoff, D.J., 2010. Cortical perfusion in alcohol-dependent individuals during short-term abstinence: relationships to resumption of hazardous drinking after treatment. *Alcohol (Fayetteville, N.Y.)* 44, 201-210.
- Durazzo, T.C., Tosun, D., Buckley, S., Gazdzinski, S., Mon, A., Fryer, S.L., Meyerhoff, D.J., 2011. Cortical thickness, surface area, and volume of the brain reward system in alcohol dependence: relationships to relapse and extended abstinence. *Alcoholism, clinical and experimental research* 35, 1187-1200.
- Ende, G., Welzel, H., Walter, S., Weber-Fahr, W., Diehl, A., Hermann, D., Heinz, A., Mann, K., 2005. Monitoring the effects of chronic alcohol consumption and abstinence on brain metabolism: a longitudinal proton magnetic resonance spectroscopy study. *Biological psychiatry* 58, 974-980.
- Fein, G., Landman, B., Tran, H., McGillivray, S., Finn, P., Barakos, J., Moon, K., 2006. Brain atrophy in long-term abstinent alcoholics who demonstrate impairment on a simulated gambling task. *NeuroImage* 32, 1465-1471.
- Fischl, B., Dale, A.M., 2000. Measuring the thickness of the human cerebral cortex from magnetic resonance images. *Proceedings of the National Academy of Sciences of the United States of America* 97, 11050-11055.
- Fischl, B., Salat, D.H., Busa, E., Albert, M., Dieterich, M., Haselgrove, C., van der Kouwe, A., Killiany, R., Kennedy, D., Klaveness, S., Montillo, A., Makris, N., Rosen, B., Dale, A.M., 2002.

EMPIRICAL STUDIES

Whole brain segmentation: automated labeling of neuroanatomical structures in the human brain. *Neuron* 33, 341-355.

Fischl, B., Salat, D.H., van der Kouwe, A.J., Makris, N., Segonne, F., Quinn, B.T., Dale, A.M., 2004. Sequence-independent segmentation of magnetic resonance images. *NeuroImage* 23 Suppl 1, S69-84.

Gazdzinski, S., Durazzo, T.C., Meyerhoff, D.J., 2005. Temporal dynamics and determinants of whole brain tissue volume changes during recovery from alcohol dependence. *Drug and alcohol dependence* 78, 263-273.

Hagler, D.J., Jr., Saygin, A.P., Sereno, M.I., 2006. Smoothing and cluster thresholding for cortical surface-based group analysis of fMRI data. *NeuroImage* 33, 1093-1103.

Harper, C., 2009. The neuropathology of alcohol-related brain damage. *Alcohol and alcoholism* 44, 136-140.

Hibar, D.P., Stein, J.L., Renteria, M.E., Arias-Vasquez, A., Desrivieres, S., Jahanshad, N., Toro, R., Wittfeld, K., Abramovic, L., Andersson, M., Aribisala, B.S., Armstrong, N.J., Bernard, M., Bohlken, M.M., Boks, M.P., Bralten, J., Brown, A.A., Mallar Chakravarty, M., Chen, Q., Ching, C.R., Cuellar-Partida, G., den Braber, A., Giddaluru, S., Goldman, A.L., Grimm, O., Guadalupe, T., Hass, J., Woldehawariat, G., Holmes, A.J., Hoogman, M., Janowitz, D., Jia, T., Kim, S., Klein, M., Kraemer, B., Lee, P.H., Olde Loohuis, L.M., Luciano, M., Macare, C., Mather, K.A., Mattheisen, M., Milaneschi, Y., Nho, K., Pappmeyer, M., Ramasamy, A., Risacher, S.L., Roiz-Santianez, R., Rose, E.J., Salami, A., Samann, P.G., Schmaal, L., Schork, A.J., Shin, J., Strike, L.T., Teumer, A., van Donkelaar, M.M., van Eijk, K.R., Walters, R.K., Westlye, L.T., Whelan, C.D., Winkler, A.M., Zwiers, M.P., Alhusaini, S., Athanasiu, L., Ehrlich, S., Hakobjan, M.M., Hartberg, C.B., Haukvik, U.K., Heister, A.J., Hoehn, D., Kasperaviciute, D., Liewald, D.C., Lopez, L.M., Makkinje, R.R., Matarin, M., Naber, M.A., Reese McKay, D., Needham, M., Nugent, A.C., Putz, B., Royle, N.A., Shen, L., Sprooten, E., Trabzuni, D., van der Marel, S.S., van Hulzen, K.J., Walton, E., Wolf, C., Almasy, L., Ames, D., Arepalli, S., Assareh, A.A., Bastin, M.E., Brodaty, H., Bulayeva, K.B., Carless, M.A., Cichon, S., Corvin, A., Curran, J.E., Czisch, M., de Zubicaray, G.I., Dillman, A., Duggirala, R., Dyer, T.D., Erk, S., Fedko, I.O., Ferrucci, L., Foroud, T.M., Fox, P.T., Fukunaga, M., Raphael Gibbs, J., Goring, H.H., Green, R.C., Guelfi, S., Hansell, N.K., Hartman, C.A., Hegenscheid, K., Heinz, A., Hernandez, D.G., Heslenfeld, D.J., Hoekstra, P.J., Holsboer, F., Homuth, G., Hottenga, J.J., Ikeda, M., Jack, C.R., Jr., Jenkinson, M., Johnson, R., Kanai, R., Keil, M., Kent, J.W., Jr., Kochunov, P., Kwok, J.B., Lawrie, S.M., Liu, X., Longo, D.L., McMahon, K.L., Meisenzahl, E., Melle, I., Mohnke, S., Montgomery, G.W., Mostert, J.C., Muhleisen, T.W., Nalls, M.A., Nichols, T.E., Nilsson, L.G., Nothen, M.M., Ohi, K., Olvera, R.L., Perez-Iglesias, R., Bruce Pike, G., Potkin, S.G., Reinvang, I., Reppermund, S., Rietschel, M., Romanczuk-Seiferth, N., Rosen, G.D., Rujescu, D., Schnell, K., Schofield, P.R., Smith, C., Steen, V.M., Sussmann, J.E., Thalamuthu, A., Toga, A.W., Traynor, B.J., Troncoso, J., Turner, J.A., Valdes Hernandez, M.C., van 't Ent, D., van der Brug, M., van der Wee, N.J., van Tol, M.J., Veltman, D.J., Wassink, T.H., Westman, E., Zielke, R.H., Zonderman, A.B., Ashbrook, D.G., Hager, R., Lu, L., McMahon, F.J., Morris, D.W., Williams, R.W., Brunner, H.G., Buckner, R.L., Buitelaar, J.K., Cahn, W., Calhoun, V.D., Cavalleri, G.L., Crespo-Facorro, B., Dale, A.M., Davies, G.E., Delanty, N., Depondt, C., Djurovic, S., Drevets, W.C., Espeseth, T., Gollub, R.L., Ho, B.C., Hoffmann, W., Hosten, N., Kahn, R.S., Le Hellard, S., Meyer-Lindenberg, A., Muller-Myhsok, B., Nauck, M., Nyberg, L., Pandolfo, M., Penninx, B.W., Roffman, J.L., Sisodiya, S.M., Smoller, J.W., van Bokhoven, H., van Haren, N.E., Volzke, H., Walter, H., Weiner, M.W., Wen, W., White, T., Agartz, I., Andreassen, O.A., Blangero, J., Boomsma, D.I., Brouwer, R.M., Cannon, D.M.,

EMPIRICAL STUDIES

Cookson, M.R., de Geus, E.J., Deary, I.J., Donohoe, G., Fernandez, G., Fisher, S.E., Francks, C., Glahn, D.C., Grabe, H.J., Gruber, O., Hardy, J., Hashimoto, R., Hulshoff Pol, H.E., Jonsson, E.G., Kloszewska, I., Lovestone, S., Mattay, V.S., Mecocci, P., McDonald, C., McIntosh, A.M., Ophoff, R.A., Paus, T., Pausova, Z., Ryten, M., Sachdev, P.S., Saykin, A.J., Simmons, A., Singleton, A., Soininen, H., Wardlaw, J.M., Weale, M.E., Weinberger, D.R., Adams, H.H., Launer, L.J., Seiler, S., Schmidt, R., Chauhan, G., Satizabal, C.L., Becker, J.T., Yanek, L., van der Lee, S.J., Ebling, M., Fischl, B., Longstreth, W.T., Jr., Greve, D., Schmidt, H., Nyquist, P., Vinke, L.N., van Duijn, C.M., Xue, L., Mazoyer, B., Bis, J.C., Gudnason, V., Seshadri, S., Arfan Ikram, M., The Alzheimer's Disease Neuroimaging, I., The, C.C., Epigen, Imagen, Sys, Martin, N.G., Wright, M.J., Schumann, G., Franke, B., Thompson, P.M., Medland, S.E., 2015. Common genetic variants influence human subcortical brain structures. *Nature* 520, 224-229.

Hogstrom, L.J., Westlye, L.T., Walhovd, K.B., Fjell, A.M., 2013. The structure of the cerebral cortex across adult life: age-related patterns of surface area, thickness, and gyrification. *Cerebral cortex* 23, 2521-2530.

Im, K., Lee, J.M., Yoon, U., Shin, Y.W., Hong, S.B., Kim, I.Y., Kwon, J.S., Kim, S.I., 2006. Fractal dimension in human cortical surface: multiple regression analysis with cortical thickness, sulcal depth, and folding area. *Human brain mapping* 27, 994-1003.

Kohler, S., Klimke S Fau - Hellweg, R., Hellweg R Fau - Lang, U.E., Lang, U.E., 2013. Serum brain-derived neurotrophic factor and nerve growth factor concentrations change after alcohol withdrawal: preliminary data of a case-control comparison. *Eur Addict Res.* 19, 98-104.

Krienke, U.J., Nikesch F Fau - Spiegelhalter, K., Spiegelhalter K Fau - Hennig, J., Hennig J Fau - Olbrich, H.M., Olbrich Hm Fau - Langosch, J.M., Langosch, J.M., 2014. Impact of alcohol-related video sequences on functional MRI in abstinent alcoholics. *Eur Addict Res.* 20(1), 33-40.

Kuceyeski, A., Meyerhoff, D.J., Durazzo, T.C., Raj, A., 2013. Loss in connectivity among regions of the brain reward system in alcohol dependence. *Human brain mapping* 34, 3129-3142.

Makris, N., Oscar-Berman, M., Jaffin, S.K., Hodge, S.M., Kennedy, D.N., Caviness, V.S., Marinkovic, K., Breiter, H.C., Gasic, G.P., Harris, G.J., 2008. Decreased volume of the brain reward system in alcoholism. *Biological psychiatry* 64, 192-202.

Mann K, A.K., 2000. Die OCDS-G: Psychometrische Kennwerte der deutschen Version der Obsessive Compulsive Drinking Scale. *Sucht* 46, 90-100.

Matthews, D.B., Morrow, A.L., 2000. Effects of acute and chronic ethanol exposure on spatial cognitive processing and hippocampal function in the rat. *Hippocampus* 10, 122-130.

Momenan, R., Steckler, L.E., Saad, Z.S., van Rafelghem, S., Kerich, M.J., Hommer, D.W., 2012. Effects of alcohol dependence on cortical thickness as determined by magnetic resonance imaging. *Psychiatry research* 204, 101-111.

Muller-Oehring, E.M., Jung, Y.C., Pfefferbaum, A., Sullivan, E.V., Schulte, T., 2014. The Resting Brain of Alcoholics. *Cerebral cortex*.

Nie, J., Guo, L., Li, K., Wang, Y., Chen, G., Li, L., Chen, H., Deng, F., Jiang, X., Zhang, T., Huang, L., Faraco, C., Zhang, D., Guo, C., Yap, P.T., Hu, X., Li, G., Lv, J., Yuan, Y., Zhu, D., Han, J.,

EMPIRICAL STUDIES

- Sabatinelli, D., Zhao, Q., Miller, L.S., Xu, B., Shen, P., Platt, S., Shen, D., Hu, X., Liu, T., 2012. Axonal fiber terminations concentrate on gyri. *Cerebral cortex* 22, 2831-2839.
- Pfefferbaum, A., Sullivan, E.V., Mathalon, D.H., Shear, P.K., Rosenbloom, M.J., Lim, K.O., 1995. Longitudinal changes in magnetic resonance imaging brain volumes in abstinent and relapsed alcoholics. *Alcoholism, clinical and experimental research* 19, 1177-1191.
- Reuter, M., Schmansky, N.J., Rosas, H.D., Fischl, B., 2012. Within-subject template estimation for unbiased longitudinal image analysis. *NeuroImage* 61, 1402-1418.
- Reuter, M., Tisdall, M.D., Qureshi, A., Buckner, R.L., van der Kouwe, A.J., Fischl, B., 2015. Head motion during MRI acquisition reduces gray matter volume and thickness estimates. *NeuroImage* 107, 107-115.
- Sameti, M., Smith, S., Patenaude, B., Fein, G., 2011. Subcortical volumes in long-term abstinent alcoholics: associations with psychiatric comorbidity. *Alcoholism, clinical and experimental research* 35, 1067-1080.
- Schweinsburg, B.C., Taylor, M.J., Videen, J.S., Alhassoon, O.M., Patterson, T.L., Grant, I., 2000. Elevated myo-inositol in gray matter of recently detoxified but not long-term abstinent alcoholics: a preliminary MR spectroscopy study. *Alcoholism, clinical and experimental research* 24, 699-705.
- Segobin, S.H., Chetelat, G., Le Berre, A.P., Lannuzel, C., Boudehent, C., Vabret, F., Eustache, F., Beaunieux, H., Pitel, A.L., 2014. Relationship between brain volumetric changes and interim drinking at six months in alcohol-dependent patients. *Alcoholism, clinical and experimental research* 38, 739-748.
- Segonne, F., Dale, A.M., Busa, E., Glessner, M., Salat, D., Hahn, H.K., Fischl, B., 2004. A hybrid approach to the skull stripping problem in MRI. *NeuroImage* 22, 1060-1075.
- Segonne, F., Pacheco, J., Fischl, B., 2007. Geometrically accurate topology-correction of cortical surfaces using nonseparating loops. *IEEE transactions on medical imaging* 26, 518-529.
- Shear, P.K., Jernigan, T.L., Butters, N., 1994. Volumetric magnetic resonance imaging quantification of longitudinal brain changes in abstinent alcoholics. *Alcoholism, clinical and experimental research* 18, 172-176.
- Silvers, J.M., Tokunaga, S., Berry, R.B., White, A.M., Matthews, D.B., 2003. Impairments in spatial learning and memory: ethanol, allopregnanolone, and the hippocampus. *Brain research. Brain research reviews* 43, 275-284.
- Skinner Ha Fau - Allen, B.A., Allen, B.A., 1982. Alcohol dependence syndrome: measurement and validation. *J Abnorm Psychol.* 91, 199-209.
- Sled, J.G., Zijdenbos, A.P., Evans, A.C., 1998. A nonparametric method for automatic correction of intensity nonuniformity in MRI data. *IEEE transactions on medical imaging* 17, 87-97.
- Sullivan, E.V., Deshmukh, A., De Rosa, E., Rosenbloom, M.J., Pfefferbaum, A., 2005. Striatal and forebrain nuclei volumes: contribution to motor function and working memory deficits in alcoholism. *Biological psychiatry* 57, 768-776.

EMPIRICAL STUDIES

Tae, W.S., Kim, S.S., Lee, K.U., Nam, E.C., Kim, K.W., 2008. Validation of hippocampal volumes measured using a manual method and two automated methods (FreeSurfer and IBASPM) in chronic major depressive disorder. *Neuroradiology* 50, 569-581.

van Eijk, J., Demirakca, T., Frischknecht, U., Hermann, D., Mann, K., Ende, G., 2013. Rapid partial regeneration of brain volume during the first 14 days of abstinence from alcohol. *Alcoholism, clinical and experimental research* 37, 67-74.

Welker, W., 1990. Why Does Cerebral Cortex Fissure and Fold? *Cerebral cortex* 8, 3-136.

White, A.M., Matthews, D.B., Best, P.J., 2000. Ethanol, memory, and hippocampal function: a review of recent findings. *Hippocampus* 10, 88-93.

White, T., Andreasen, N.C., Nopoulos, P., Magnotta, V., 2003. Gyrfication abnormalities in childhood- and adolescent-onset schizophrenia. *Biological psychiatry* 54, 418-426.

Winkler, A.M., Kochunov, P., Blangero, J., Almasy, L., Zilles, K., Fox, P.T., Duggirala, R., Glahn, D.C., 2010. Cortical thickness or grey matter volume? The importance of selecting the phenotype for imaging genetics studies. *NeuroImage* 53, 1135-1146.

Wrase, J., Makris, N., Braus, D.F., Mann, K., Smolka, M.N., Kennedy, D.N., Caviness, V.S., Hodge, S.M., Tang, L., Albaugh, M., Ziegler, D.A., Davis, O.C., Kissling, C., Schumann, G., Breiter, H.C., Heinz, A., 2008. Amygdala volume associated with alcohol abuse relapse and craving. *The American journal of psychiatry* 165, 1179-1184.

Zeng, T., Chen, H., Fakhry, A., Hu, X., Liu, T., Ji, S., 2014. Allen mouse brain atlases reveal different neural connection and gene expression patterns in cerebellum gyri and sulci. *Brain structure & function*.

Statement of Contribution

In this study, I was involved in the MRI data acquisition, my main responsibility was the pre-processing and statistical analysis with FreeSurfer of all data, as well as data interpretation. I did the according literature research and study, prepared and wrote the manuscript.

6 Negative association between MR-spectroscopic glutamate markers and grey matter volume after alcohol withdrawal in the hippocampus: a translational study in humans and rats³

Abstract

Both chronic alcohol consumption and alcohol withdrawal lead to neural tissue damage which partly recovers during abstinence. This study investigated withdrawal associated changes in glutamatergic compounds, markers of neuronal integrity and grey matter volumes during acute alcohol withdrawal in the hippocampus, a key region in development and maintenance of alcohol dependence in humans and rats. Alcohol dependent patients (N=39) underwent MR imaging (MRI) and MR spectroscopy (MRS) measurements within 24h after the last drink and after two weeks of abstinence. MRI and MRS data of healthy controls (N=34) were acquired once. Our thorough quality criteria led to a reduction of available spectra of N=15 from the first and N=21 from the second measurement in patients and N=19 in healthy controls. In a translational approach, chronic intermittent ethanol exposed rats and respective controls (8/group) underwent 5 MRS measurements covering baseline, intoxication, 12h and

³ Publication :

Frischknecht, U., Hermann, D., Tunc-Skarka, N., Wang, G.-Y., Sack, M., van Eijk, J., Demirakca, T., Falfan-Melgoza, C., Krumm, B., Dieter, S., Spanagel, R., Kiefer, F., Mann, K.F., Sommer, W.H., Ende, G., Weber-Fahr, W., 2017. Negative Association Between MR-Spectroscopic Glutamate Markers and Gray Matter Volume After Alcohol Withdrawal in the Hippocampus: A Translational Study in Humans and Rats. *Alcoholism: Clinical and Experimental Research* 41, 323-333.

EMPIRICAL STUDIES

60h of withdrawal and 3 weeks of abstinence. In both species higher levels of markers of glutamatergic metabolism were associated with lower grey matter volumes in the hippocampus in early abstinence. Trends of reduced N-acetylaspartate (NAA) levels during intoxication persisted in patients with severe alcohol withdrawal symptoms over two weeks of abstinence. We observed a higher ratio of glutamate to glutamine during alcohol withdrawal in our animal model. Due to limited statistical power we regard the results as preliminary and discuss them in the framework of the hypothesis of withdrawal induced hyperglutamatergic neurotoxicity, alcohol induced neural dehydration and training associated effects of abstinence on hippocampal tissue integrity.

Key Words:

Alcohol Withdrawal, Magnetic Resonance Spectroscopy, Hippocampus, Glutamate, Gray Matter.

6.1 Introduction

Acute withdrawal in alcohol dependent patients is characterized by highly dynamic changes in brain structure, chemistry and function (Zahr et al., 2011; Zahr et al., 2010). It is unclear whether and to what extent the processes observed during acute withdrawal, while transient in nature, are related to those that remain during protracted abstinence and likely determine long-term clinical outcomes (Heilig et al., 2010a). Numerous studies reported reductions in grey matter volumes in alcohol dependent patients in different brain areas (Bühler and Mann, 2011; van Eijk et al., 2013) and recovery with abstinence. While MRI detects volumetric brain changes associated with alcohol abuse and abstinence, magnetic resonance spectroscopy MRS allows to study the neurometabolic state of the brain *in vivo*, including regional levels of the major excitatory neurotransmitter in the brain, Glu, and of related glutamatergic compounds (Meyerhoff et al., 2013). In the context of neuroplasticity and alcohol withdrawal, Glu is of prominent relevance, because on the one hand it may facilitate pathological learning underlying the addiction, and on the other hand excessive Glu in the brain during alcohol withdrawal can cause excitotoxicity and neuronal cell death (Cippitelli et al., 2010; Hoffman, 1995; Prendergast et al., 2004; Spanagel, 2009; Tsai et al., 1998). Previously, we reported elevated Glu levels in the medial prefrontal cortex of alcoholic patients and alcohol dependent rats during acute withdrawal (Hermann et al., 2012b). In the animal model this effect was more distinct when Glu was referenced to Gln, which is connected to Glu via the Glu-Gln cycle.

The second most abundant biochemical compound in the brain is NAA, which as a neuronal osmolyte is involved in fluid balance in the brain, and is seen as a marker of neuronal integrity, viability and function (Moffett et al., 2007). NAA reductions in the human brain were consistently reported after administration of alcohol in healthy subjects (Gomez et al., 2012), in alcohol dependent patients (Meyerhoff et al., 2004; Mon et al., 2012; Yeo et al., 2013), and in animal models of alcohol addiction (Zahr et al., 2010). In our previous study, we found NAA reductions in the mPFC of alcohol dependent patients in the early phase of acute alcohol withdrawal, as well as during acute alcohol intoxication in alcohol dependent

EMPIRICAL STUDIES

rats (Hermann et al., 2012b). NAA recovery within some days of abstinence has been reported in both animal and human studies (Hermann et al., 2012b; Mon et al., 2012; Zahr et al., 2010).

The hippocampus, a key region of neuroplasticity in the brain, also plays a major role in the development and maintenance of alcohol addiction (Canales, 2012; Koob and Volkow, 2010), for example, by mediating several important addiction related processes, such as learning (Krank et al., 2005; Nees and Pohlack, 2014) and memory (Bahner et al., 2015) as well as adult neurogenesis (Canales, 2012; Mandyam and Koob, 2012), which are all impaired during acute withdrawal (Dominguez et al., 2014; Hansson et al., 2010; Tipps et al., 2015). Similar impairments are found during alcohol intoxication, however underlying mechanisms are thought to differ (for a review see (Zorumski et al., 2014)). Learning during ethanol intoxication blocks N-methyl-D-aspartate (NMDA) receptor activity and thereby long term potentiation, which may weaken dendritic arbour (McAllister, 2000) and could thus be reflected by reduced NAA levels. Learning impairments during withdrawal may result from neuronal damage due to excessive glutamate release (Lovinger, 1993) and thus could be reflected by elevated Glu levels.

In this study we investigated structural alterations and MRS derived glutamatergic markers and NAA as a metabolite indicating neuronal health during acute withdrawal and early abstinence in the hippocampus of alcohol dependent patients and a rat model designed to highly parallel the patient situation. Based on our previous study (Hermann et al., 2012b) we expected elevated glutamate markers and reduced NAA (a well replicated finding, for review see (Meyerhoff et al., 2013)) in the hippocampus during withdrawal and normalization with ongoing abstinence. We hypothesized high levels of glutamatergic compounds and/or low levels of NAA in the hippocampus to be associated with severity of alcohol withdrawal symptoms and hippocampal volume reduction.

6.2 Materials and Methods:

6.2.1 Participants:

Sample and procedure are largely overlapping with our previous study (for details see supplemental information and (Hermann et al., 2012b)). Treatment seeking alcohol dependent patients (N=39) underwent two MRS scans. The first was at the day of admission to our inpatient clinic (ADP-day1) and an identical second scan after two weeks of controlled abstinence (ADP-day14). The first took place, when breath alcohol levels dropped below 1.0 g/L and before medical treatment of withdrawal symptoms with benzodiazepines became necessary. Via newspaper and online announcements we recruited age and sex matched healthy controls (HC, N=34) and scanned them once. Exclusion criteria for all participants were current or lifetime diagnosis of substance dependence except nicotine dependence (and alcohol dependence in patients), any psychotropic medication in the previous 3 months, positive urine drug screen, other psychiatric or neurological brain diseases, hepatic encephalopathy, liver cirrhosis, severe medical illnesses and common exclusion criteria for magnetic resonance imaging (e.g., metal implants). The study was approved by the Ethics Committee of the Mannheim Medical Faculty of the University of Heidelberg, and informed written consent was obtained from all participants. Sample characteristics are provided in Table 6-1.

EMPIRICAL STUDIES

Table 6-1 Characteristics of human sample

| | Total Measured | | Analysed sample | |
|--|------------------|----------------------------|------------------|----------------------------|
| | Healthy Controls | Alcohol dependent patients | Healthy Controls | Alcohol dependent patients |
| | N=34 | N=39 | N=19 | N=21 |
| Sex | 79% male | 77% male | 84% male | 71% male |
| Age | 44.5 (12.3) | 46.3 (11.4) | 46.7 (12.2) | 47.5 (9.8) |
| ADS | 0.66 (1.60) | 14.47 (7.19) | 0.58 (1.26) | 13.53 (8.06) |
| OCDS | 0.81 (1.45) | 13.19 (8.05) | 1.06 (1.70) | 11.84 (9.11) |
| EtOH/DD | 23.17 (14.61) | 188.44 (106.84) | 22.09 (10.89) | 195.56 (82.75) |
| PDA | 80.8 (23.3) | 23.2 (32.3) | 76.2 (24.2) | 27.3 (35.3) |
| PHDD | 0.7 (0.2) | 71.9 (34.8) | 0.6 (1.9) | 72.0 (36.2) |
| GGT | 25.1 (11.9) | 267.69 (616.9) | 28.3 (12.5) | 202.4 (394.2) |
| Smokers | 21% smokers | 80% smokers | 16% smokers | 86% smokers |
| FTND Score | 3.14 (1.77) | 6.17 (2.04) | 2.67 (0.58) | 6.50 (2.16) |
| CIWA-Score prior to 1. MRS | -- | 5.84 (3.80) | -- | 5.33 (3.94) |
| CIWA-Score after 1. MRS | -- | 6.92 (5.00) | -- | 6.55 (5.75) |
| BrAC prior to 1. MRS | -- | 0.40 (0.45) | -- | 0.37 (0.42) |
| BrAC after 1. MRS | -- | 0.18 (0.32) | -- | 0.17 (0.32) |
| Diazepamequivalent needed during withdrawal. | -- | 22.1 (35.2) | -- | 22.1 (42.3) |

ADS = Alcohol dependence scale; OCDS = Obsessive Compulsive Drinking Scale; EtOH/DD = Alcohol consumption per drinking day during previous 90 days; PDA = Percent days abstinent during previous 90 days;

PHDD = Percent heavy drinking days defined by more than 48/60 g Alcohol per day for women/men during the previous 90 days; GGT= gamma glutamyl-transferase; FTND = Fagestrom test of nicotine dependence;

CIWA = Clinical institute withdrawal assessment ; BrAC = Breath alcohol concentration;

6.2.2 ^1H MR Spectroscopy at 3T and morphometric analysis of hippocampal volumes in humans

All participants were scanned in a clinical 3T whole-body scanner (Siemens, Erlangen, Germany). The position of the MRS voxel ($15 \times 25 \times 10 \text{ mm}^3$, Figure 6-1a) in the hippocampus was defined on the basis of anatomical images from an isotropic (1 mm^3 resolution) T1-weighted three dimensional dataset (MPRAGE). Voxel positioning was performed by aligning axial MR images based on the long axis of the hippocampus as seen in sagittal images and by maximising the grey matter (GM) content in the voxel. Metabolite spectra were acquired with a point-resolved spectroscopy (PRESS) sequence using TE/TR=30/2000 ms, bandwidth = 2400 Hz, 2048 data points, and 256 averages (see also supplemental information). In addition fully relaxed unsuppressed water spectra (2 averages) were acquired with TR=10 s and TE=30 ms (for quantification via water scaling and eddy currents correction). Quantification of spectra was based on LCModel spectral fitting and a quality control procedure was applied (for details see supplement).

MPRAGE images were corrected for bias effects, normalized to the MNI template and smoothed to calculate estimates for individual total intracranial volume (TIV). Individual GM images of the hippocampus were calculated using SPM8 and the WFU Pic Atlas. In this voxel-based morphometric approach, the GM volume was estimated by integrating the GM voxel values over all voxels within the hippocampus (Hipp). To account for brain size effects, the values were normalized to the TIV for each participant respectively (for details see (van Eijk et al., 2013)).

EMPIRICAL STUDIES

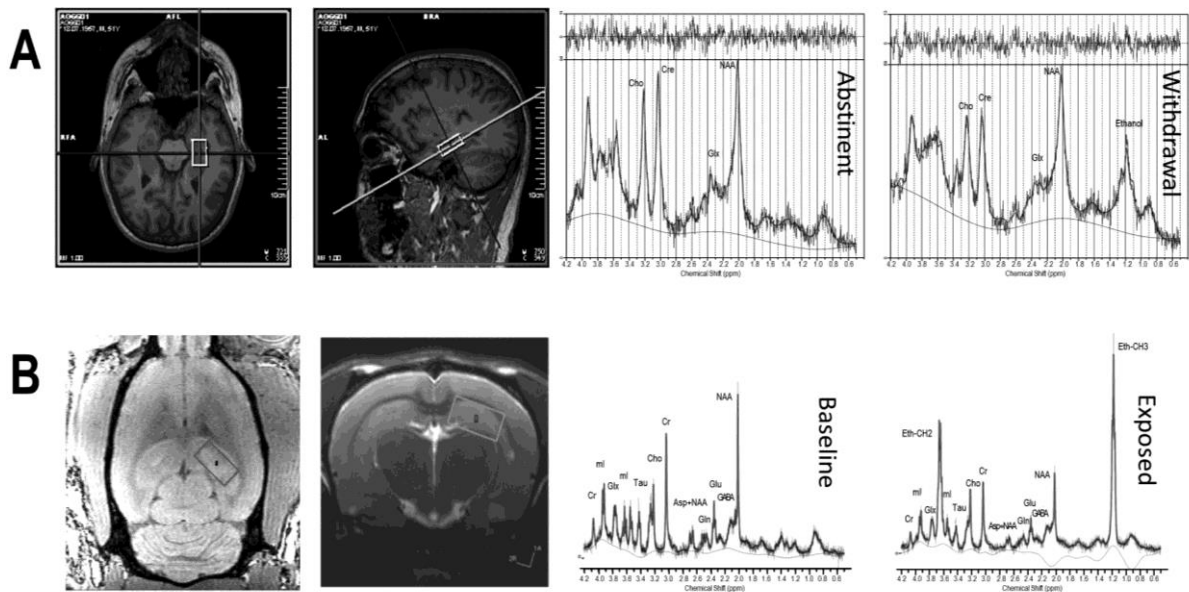


Figure 6-1 Typical spectra and voxel positioning in the hippocampus of humans (A) and rats (B). Spectra peaks define choline-containing compounds(Cho), creatine (Cre), glutamate and glutamine (Glx), N-acetylaspartate (NAA), myo-inositol (mI), taurine (Tau), aspartate (Asp), glutamate (Glu), gamma-aminobutyric acid (GABA), and ethanol (Eth-CH₃, Eth-CH₂).

6.2.3 Statistical Analysis of Human Data

Based on the results from our previous study(Hermann et al., 2012b) and the findings of Kuhn et al. (2014), we used separate one way analysis of variance (ANOVA) with planned comparisons contrasting ADP-day1 vs. HC & ADP-day14 (contrast coefficients: 1/-0.5/-0.5 for Glx; -1/0.5/0.5 for NAA and Hipp/TIV). Pearson correlations and Spearman's rank correlations were applied where appropriate to investigate associations. We accounted for family wise error rates (FWE) as described in the supplement.

6.2.4 Animals

Sixteen male Wistar rats (Charles River, Sulzfeld, Germany), 3 months of age at the beginning of the experiment were housed under standard conditions (2 per cage, 12 h artificial light-dark cycle, with lights on at 07:00 a.m., temperature: 22±1°C, humidity: 55±5%, food and water ad libitum). All experimental procedures were approved by the Committee on Animal Care and Use (Regierungspräsidium Karlsruhe), and carried out in accordance with

EMPIRICAL STUDIES

the local Animal Welfare Act and the European Communities Council Directive of 24 November 1986 (86/609/EEC).

To induce dependence rats were exposed to chronic intermittent exposure (CIE) to ethanol vapour for 16 hours per day over a period of 7 weeks according to the protocol of Rimondini et al. (Rimondini et al., 2002), a paradigm that allows a high degree of control over brain alcohol levels, and induces behavioural and molecular changes relevant for the pathophysiology of alcoholism (Meinhardt and Sommer, 2015). The experiment and subjects have been described in detail before (Hermann et al., 2012b) (also see supplement).

6.2.5 ^1H MRS at 9.4 T and morphometric analysis of hippocampal volumes in rats

Rats were scanned five times in a 9.4 T horizontal bore animal scanner (Bruker, Ettlingen, Germany). Scans were performed before the initiation (baseline) and during the last CIE intoxication cycle (intox), as well as 12 hours (12 h) and 60 hours (60 h) after the last intoxication cycle, and after a 3-week period of abstinence (3 wk). Measurements in control rats were conducted age-matched to the 1st, 3rd and 5th scan. For details on animal treatment during scanning see (Hermann et al., 2012b). The position of the hippocampus voxel (16 μl ; 2 x 2 x 4 mm³) was based on anatomic images from a T1-weighted fast imaging with steady precession (FISP) three-dimensional sequence (TE = 4ms, TR = 8ms, alpha = 20°, four averages; MTX = 256 x 256 x 128; FOV = 3cm; see Figure 6-1b). Spectra were acquired using a PRESS sequence at TE/TR = 10/4000 with 256 averages. To minimize chemical shift displacement artefacts the PRESS sequence was modified to deliver the slice selective excitation and refocusing pulses with a frequency shift of -2 ppm. The chemical shift displacement of the spectroscopy voxel was 0.22 mm/PPM for the 2 mm edges (180° refocusing pulse) and 0.23 mm/PPM for the 4mm edge (90° selection pulse). An additional one-shot unsuppressed water signal was acquired with no frequency shift, which was used for eddy-current correction and water-scaling. Quantification was done similar to the human analysis with LCModel spectral fitting. For further details, see (Hermann et al., 2012b).

EMPIRICAL STUDIES

3D structural images were acquired using the FISP-sequence. 16 rats were measured (8 controls, 8 ethanol-intoxicated) at different time-points. After acquisition, the 3D images were resized by factor 10, coregistered, and skull stripped (FSL BET, Smith (2002)). A template of tissue classification maps (GM, white matter (WM) and cerebrospinal fluid (CSF)) created from the structural images (Biedermann et al., 2012) was used as priors to run an individual segmentation, and the resulting segmented images were smoothed with a 4mm Gaussian kernel filter. Using the segmented, unsmoothed structural data, a ROI of the right anteriodorsal hippocampus was defined based on the Paxinos atlas (Paxinos and Watson, 2004). The respective voxel values of the data provide an estimation of the absolute tissue volume in this ROI that overlaps with the voxel from the MRS.

6.2.6 Statistical Analysis of animal data

Group differences in metabolite concentrations were tested using separate mixed model analyses (Proc Mixed module, SAS9.2, SAS Cary, North Carolina) for Glu, Gln and NAA including weight as a covariate (for rationale of including weight as covariate and FWE correction see supplement). Because the control group was only measured three times, values for the missing time points were interpolated. If there was a significant or trend level indication for a main effect of treatment or interaction of treatment and time, exploratory post-hoc analyses, uncorrected for multiple comparisons were used to compare alcohol exposure effects at the various time points against the respective time point of the naïve control group using analysis of covariance including weight as a covariate. Glu/Gln ratios and anteriodorsal hippocampal volumes were analysed by repeated measures ANOVA followed by Bonferroni corrected pairwise comparisons. FWE corrected Pearson correlations (see supplement) were used to investigate associations of Glu, Gln and the Glu/Gln ratio with GM volume in the hippocampus at each time point of measurement.

6.3 Results

In the human study, 15 MRS spectra from the first measurement and 21 spectra from the second measurement of patients and 19 spectra from the HC group passed our thorough quality criteria. However, t-tests showed no significant differences in the assessed

EMPIRICAL STUDIES

characteristics between excluded subjects and those being used for further analysis (all p-values > 0.1, see Table 6-1).

6.3.1 Hippocampal volumes are marginally reduced during withdrawal and recovered to normal levels with abstinence

In humans, no statistical difference ($F[2, 102] = 0.82$, $P = 0.45$) between the hippocampal volume/TIV ratio of patients (at both time points) compared to control subjects was found. A widely used alternative of brain volume correction by controlling for age and sex instead of TIV yielded significantly reduced hippocampal volume in patients at both time points ($F[2,100] = 8.56$), $P < 0.001$).

Anteriodorsal hippocampal volumes of rats showed significant time effect ($F[4,9] = 11.52$, $P = 0.001$), but only a trend effect of treatment ($F[1,12] = 3.42$, $P = 0.089$) and no time x treatment interaction ($F[4,9] = 2.57$, $P = 0.11$). Post-hoc t-tests showed reduced anteriodorsal hippocampal volume at the 12h ($P = 0.013$) and the 60h ($P = 0.027$) withdrawal time points compared to control animals. A trend level effect was already observed at the time of intoxication ($P = 0.070$). After three weeks of abstinence hippocampal volumes did not differ from those of controls ($P = 0.181$).

6.3.2 The ratio of glutamate to glutamine is elevated during withdrawal while the metabolite concentrations themselves are not.

We found no difference in Glx between patients during withdrawal and after 14 days of controlled abstinence and controls ($F[1,49] = 1.57$, $P = 0.216$, see Table 6-2). In the animal study, we found no main effects on Glu for treatment ($F[1,52] = 0.24$; $P = 0.63$) or time ($F[4, 52] = 0.96$; $P = 0.44$) in the mixed model analysis with weight as a time dependent covariate, but a trend towards an interaction between time and treatment ($F[4, 52] = 2.92$, $P = 0.03$; $P_{\text{FWE}} = 0.06$). Exploratory post-hoc ANOVAs with weight as covariate showed lower Glu levels in the ethanol exposed group at baseline ($F[1, 13] = 5.13$; $P = 0.041$). Therefore, in the post-hoc ANOVAs of the other time-points, we included baseline Glu levels as an additional covariate, which revealed a trend of higher Glu levels in the hippocampus of ethanol exposed

EMPIRICAL STUDIES

rats compared to controls after 12h of withdrawal ($F[3, 11] = 4.17$; $P = 0.066$) but not at the other time-points (all P -values > 0.1).

For Gln levels we found no treatment ($P = 0.98$) but time ($F[4, 52] = 4.20$; $P = 0.005$; $P_{\text{FWE}} = 0.015$) and time x treatment interaction ($F[4, 52] = 11.12$; $P < 0.001$; $P_{\text{FWE}} < 0.004$) effects. Exploratory post-hoc ANOVAs with weight as covariate revealed a trend for higher Gln during intoxication ($F[1, 13] = 4.52$, $P = 0.053$) but no group differences at any other time-points (all P -values > 0.1).

For the Glu/Gln ratio we found no main effect of treatment ($F[1, 13] = 2.46$; $P = 0.14$) but a significant time ($F[4, 10] = 6.05$; $P = 0.01$; $P_{\text{FWE}} = 0.02$) and significant time x treatment interaction effect ($F[4, 10] = 5.21$; $P = 0.016$; $P_{\text{FWE}} = 0.048$). Post-hoc pairwise comparisons revealed significantly higher Glu/Gln ratios in comparison to controls 12h and 60h after withdrawal ($P = 0.013$ and $P = 0.032$, respectively, see supplement Figure S1 and additional results for Glx in animals

EMPIRICAL STUDIES

Table 6-2 Metabolite values, volumetric values and their associations in alcohol dependent subjects and controls

| | | Alcohol dependent subjects | | | control subjects | | | | | Statistics | |
|-------------------------------------|---|----------------------------|--------------------------|--------------------------|--------------------------|--------------------|--------------|------------------------|--------------------------------|--|--|
| Human study | Marker – Mean (SE) | Acute Withdrawal | | | 14 days abstinence | | | single measurement | | ANOVA | |
| | Glx [mmol/L] | 10.62 (0.47) (N=14) | | | 11.80 (0.57) (N=21) | | | 11.50 (0.77) (N=17) | | n.s. | |
| | NAA [mmol/L] | 7.21 (0.19) (N=15) | | | 7.73 (0.17)* (N=21) | | | 7.75 (0.22) (N=19) | | p _{FWE} =0.08 | |
| | TIV ¹ [ml] | 1414.3 (22.7) | | | 1408.1 (19.8) | | | 1501.3 (26.4) | | n.s. | |
| | Hippo ¹ [ml] | 7.95 (0.14) | | | 7.91 (0.12) | | | 8.6 (0.14)* | | P < 0.001 | |
| | Hipp/TIV [ratio] | 0.0056 (0.000081) | | | 0.0057 (0.000063) | | | 0.0057 (0.000054) | | n.s. | |
| Correlation – Pearsons R (p-values) | | | | | | | | | | | |
| | Glx*Hipp/TIV | -0.16 (0.96) | | | -0.57 (0.007) | | | | | | |
| Animal Study | Marker – Mean (SE) | Baseline | Intoxication | 12 hours withdrawal | 60 hours withdrawal | 3 weeks abstinence | Baseline | parallel to withdrawal | parallel to 3 weeks abstinence | Model statistics (treatment; time; time*treatment) | |
| | Glu ² [mmol/L] | 7.63 (0.21) ^a | 7.52 (0.16) | 7.84 (0.26) ^b | 7.33 (0.37) | 7.17 (0.23) | 8.24 (0.20) | 7.04 (0.28) | 6.84 (0.14) | n.s.; n.s.; p _{FWE} = 0.06 | |
| | Gln ² [mmol/L] | 1.91 (0.08) | 2.75 (0.08) ^c | 2.02 (0.12) | 1.78 (0.11) | 2.21 (0.11) | 2.34 (0.24) | 2.30 (0.14) | 2.37 (0.12) | n.s.; p _{FWE} = 0.015; p _{FWE} < 0.004 | |
| | Glu/Gln ³ [ratio] | 4.06 (0.21) | 2.74 (0.11) | 3.95 (0.20) ^d | 4.26 (0.40) ^d | 3.30 (0.23) | 3.69 (0.28) | 3.13 (0.21) | 2.94 (0.17) | n.s.; p _{FWE} = 0.02; p _{FWE} = 0.048 | |
| | NAA ² [mmol/L] | 10,42 (0.15) | 9,18 (0.19) ^a | 9,98 (0.28) | 9,82 (0.26) | 10,00 (0.08) | 10.63 (0.26) | 10.43 (0.18) | 10.31 (0.19) | n.s.; p _{FWE} < 0.004; p _{FWE} = 0.075 | |
| | ad Hipp ³ [µm ³] | 5.53 (0.19) | 5.59 (0.15) ^e | 5.35 (0.17) ^a | 5.41 (0.18) ^a | 5.88 (0.19) | 5.89 (0.17) | 6.03 (0.16) | 6.22 (0.13) | P = 0.089, P = 0.001, n.s. | |
| | Correlation – Pearsons R (p-values) | | | | | | | | | | |
| | | Glu*adHipp | 0.63 (0.38) | -0.64 (0.08) | -0.09 (0.84) | -0.46 (0.25) | -0.44 (0.28) | | | | |
| | Gln*adHipp | 0.15 (0.73) | 0.48 (0.23) | 0.58 (0.13) | 0.19 (0.66) | 0.21 (0.61) | | | | | |
| | Glu/Gln*adHipp | 0.10 (0.82) | -0.71 (0.05) | -0.90 (0.003) | -0.34 (0.40) | -0.37 (0.36) | | | | | |

EMPIRICAL STUDIES

SE = Standard Error; Glu = glutamate; Gln = glutamine; Glx = glutamate + glutamine; Glu/Gln = ratio of glutamate to glutamine; NAA = N-acetylaspartate; TIV = Total Intracranial volume; Hippo = hippocampal volume; Hipp/TIV = ratio of hippocampal volume to total intracranial volume; ad Hipp = antero-dorsal hippocampal volume; FWE = family wise error corrected p-value according to Bonferroni-Holm method; n.s. = not significant ($P > 0.10$); * indicates significant different group; Bold = indicates significant correlation (after bonferroni correction); ¹ Total intracranial volume and hippocampal volume ANOVA includes age and sex as covariates; ² metabolites were analysed by mixed effect model analysis with weight as time dependent covariate; ³ ratio and ad Hipp were analysed by general linear model repeated measure analysis; ^a significantly lower than respective control measurement with weight as covariate; ^b significantly higher than respective control measurement with baseline difference and weight as covariates; ^c trend ($P < 0.10$) higher than respective control measurement with weight as covariate; ^d significantly higher than respective control measurement; ^e trend ($P < 0.10$) lower than respective control measurement

6.3.3 Inverse correlation of glutamatergic compounds with hippocampal volume

In the human study correlation analyses of Glx with the hippocampal volume/TIV ratio revealed a significant negative correlation at the two-week time point indicating lower volumes in the presence of higher Glx ($R = -0.57$, $P = 0.007$; see Table 6-2 and Figure 6-2A), this remained significant even when controlling for age.

In alcohol dependent animals we found a significant correlation between the ratio of Glu/Gln and anteriodorsal hippocampus volume 12hrs after withdrawal ($R = -0.83$, $P < 0.003$; see Table 6-2 Metabolite values, volumetric values and their associations in alcohol dependent subjects and controls and Figure 6-2B), while there was no correlation with either glutamate or glutamine levels at any time point (all P -values > 0.1).

No significant correlations in the respective variables were found in controls of either humans ($P > 0.7$) or rats ($P > 0.2$).

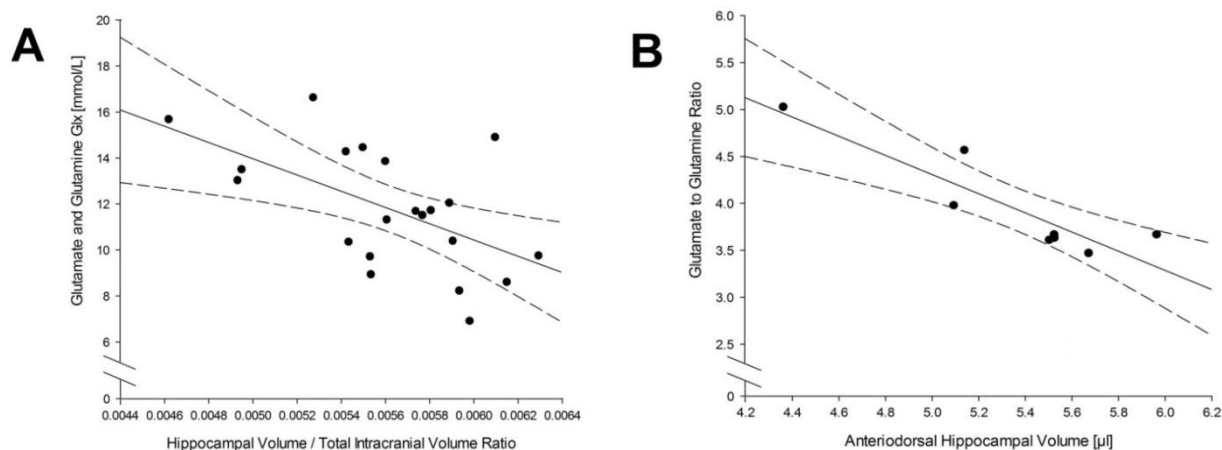


Figure 6-2 (A) After 14 days of abstinence in alcohol-dependent patients, the levels of glutamate and glutamine (Glx) were associated negatively with hippocampal volumes referenced individually to total intracranial volume. (B) A similar pattern was found in rats 12 hours after withdrawal from alcohol that underwent 49 cycles of ethanol vapor exposure: The ratio of glutamate to glutamine was negatively associated with anteriodorsal hippocampus volume.

6.3.4 Trend reduction in NAA levels during intoxication recovers in the absence of severe withdrawal symptoms

In the human study, the planned contrast for reduced NAA during acute withdrawal ADP-day1 compared to ADP-day14 and HC reached trend level significance after correction for multiple comparisons ($F[1,52] = 4.42$, $P = 0.040$; $P_{\text{FWE}} = 0.08$, see Figure 6-3A). An exploratory analysis of alcohol dependent patients after 14 days of abstinence showed significantly reduced NAA levels in those who developed severe alcohol withdrawal symptoms and therefore were treated with benzodiazepine in comparison to those not developing clinically relevant withdrawal symptoms ($t[19] = 2.72$, $P = 0.014$, see supplement).

In the animal study linear mixed model analysis with weight as time dependent covariate revealed a significant time effect ($F[4,52] = 7.55$; $P < 0.001$; $P_{\text{FWE}} < 0.004$) and a trend for time x treatment interaction ($F[4,52] = 2.26$; $P = 0.075$; $P_{\text{FWE}} = 0.075$) but no treatment effect ($F[1,52] = 0.8$; $P = 0.38$). Exploratory post- hoc ANOVAs with weight as covariate revealed significantly lower concentrations of NAA in the hippocampus of ethanol exposed rats only during intoxication compared to naive controls ($F[1, 13] = 6.2$, $P = 0.027$; all other time-points: p -values > 0.1 ; see Figure 6-3B).

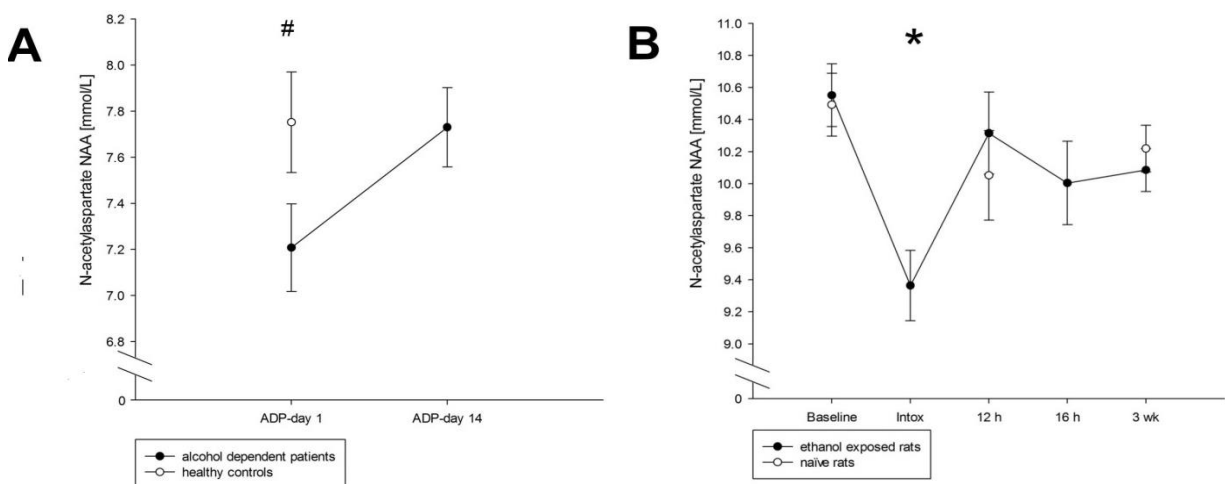


Figure 6-3 (A) Reduced N-acetylaspartate (NAA) levels in the hippocampus during acute alcohol withdrawal in alcohol-dependent patients who stopped drinking within 24 hours before the first MRS measurement (ADP-day 1) compared with their levels after 2 weeks of abstinence (ADP-day 14) and to a single measurement of HCs. (B) Reductions in NAA levels

EMPIRICAL STUDIES

during the last intoxication (Intox) after 49 cycles of chronic intermittent ethanol exposure compared to naive control rats were not present any more 12 hours, 60 hours, or 3 weeks after alcohol withdrawal. Asterisk indicates significant effects at $P > 0.05$; number sign indicates trend-level significant effect after FWE correction at $P < 0.10$.

6.4 Discussion

This is the first study using both MR spectroscopy and MR imaging to investigate glutamatergic compounds, N-acetylaspartate and grey matter morphometry of the hippocampus during acute alcohol withdrawal. We hypothesise that our results from both humans and rats are in line with the hypothesis of alcohol withdrawal related neurotoxicity: hyperglutamatergic metabolism affects GM volume and abstinence induces recovery. We found higher glutamate-markers associated with lower GM volumes in the hippocampus of both species in early abstinence. In the animal study a hyperglutamatergic state of the hippocampus during alcohol withdrawal was suggested by an increased Glu/Gln ratio, which is in accordance with previous findings from the medial prefrontal cortex in these animals (Hermann et al., 2012b). In both species the major neuronal cell osmolyte NAA tended to be reduced during intoxication and recovered quickly after cessation of alcohol consumption. The human study provided preliminary evidence for fast recovery of NAA in patients without severe alcohol withdrawal symptoms.

Hyperglutamatergic states are associated with reduced hippocampal volume

We found high levels of glutamate + glutamine to be associated with reduced hippocampal volumes in humans that recently underwent alcohol withdrawal. This was paralleled by higher values of the glutamate/glutamine ratio in rats with lower anterodorsal hippocampal volumes 12hrs post ethanol vapour exposure. The lack of such associations in controls of both species points to the specificity of the finding in of alcohol dependence after withdrawal. This adds to a line of previous evidence: in a human study, hippocampal volume reductions after alcohol withdrawal were associated with alcohol withdrawal severity (Barnes et al., 2010). Moreover, we found elevated glutamate levels during alcohol withdrawal in the anterior cingulate cortex of humans and rats in our previous study (Hermann et al., 2012b). Further, several in vitro

EMPIRICAL STUDIES

studies showed the neurotoxic nature of elevated glutamate concentrations after alcohol withdrawal (Lukoyanov et al., 1999; Prendergast and Mulholland, 2012; Tsai et al., 1998).

The association of high Glx with low hippocampal volume after two weeks of abstinence in the human sample and not in the initial phase of withdrawal suggests that neural damage is rather a consequence of withdrawal than of chronic alcohol intoxication. Although the lack of a significant association in the first measurement may as well result from reduced power for this analysis, the parallel animal study, where there was no difference in power between the measurement during intoxication and after withdrawal yielded only a significant association at the later measurement time point. Thus we hypothesise that these findings may reflect neural damage due to excessive glutamatergic activity during alcohol withdrawal, as proposed by the glutamate hypothesis of alcoholism (Lovinger, 1993; Prendergast et al., 2004; Tsai and Coyle, 1998). The notion of a hyperglutamatergic state in the hippocampus is supported by elevated Glu to Gln ratios during acute withdrawal 12h and 60h after withdrawal from alcohol and by the trend elevation in Glu levels at 12h in our animal study. Keeping in mind that MRS does not provide insights into the cellular mechanisms and that evidence for this notion is still lacking, we hypothesise that an elevated Glu/Gln ratio may reflect an acceleration of the glutamate-glutamine cycle indicating enhanced glutamatergic neurotransmission. In line with previous results from frontal areas (Hermann et al., 2012b) our results extend it to another brain region that plays an important role in development and maintenance of addiction.

Here, we did not detect any differences in Glx levels between alcoholics and healthy controls or during the withdrawal phase. Glx represents a MRS signal derived from both metabolites Glu and Gln. If during alcohol withdrawal Glu levels increase and Gln levels decrease by a comparable amount, the sum of both remains constant. This is supported by our exploratory analysis of Glx in animals, where no difference during withdrawal could be detected. Therefore short-term alterations of glutamatergic neurotransmission which may result from an acceleration or deceleration of the glutamate-glutamine cycle might not change Glx – however longer lasting alteration may be a signal to increase storage of glutamatergic compounds reflected by increased Glx levels. Other possible explanations, why we did not detect differences in Glx in our human study come from the different methods applied here in terms of MR spectroscopy and sample size. The MR protocol of the human study differed

EMPIRICAL STUDIES

from our previous study (Hermann et al., 2012b) showing elevated Glu levels during alcohol withdrawal in the anterior cingulate cortex in terms of the echo time used. Here we used a TE of 30ms, which provides better overall signal-to-noise ratio but also more resonance overlap from Glu and Gln. Furthermore, due to a lower spectral quality the total N and thus statistical power was less in the hippocampal analysis compared to our previous study on the anterior cingulate cortex (Hermann et al., 2012b).

Hippocampal volumes during alcohol withdrawal

Previous studies reported hippocampal GM volume reduction in alcohol dependence in early abstinence (Durazzo et al., 2011), and after weeks of abstinence (Barnes et al., 2010; Sullivan et al., 1995) as well as a recovery in hippocampal volume in BDNF val homozygous patients after 7 months of abstinence (Hoefer et al., 2014). Although we did not find a significant reduction in our primary analysis based on a correction of hippocampal volume to TIV, lower hippocampal volumes in alcohol dependent patients were evident when considering age and sex but not TIV as a covariate. In rats we found reductions in anteriodorsal hippocampal volumes during intoxication and withdrawal compared to controls. The results are in line with previous studies reporting hippocampal volumes to be reduced in alcohol dependence only when they are not corrected for whole brain volume (Agartz et al., 1999; Harding et al., 1997). A large study in healthy controls found that several structures including the hippocampus are not directly proportional to TIV (Barnes et al., 2010) and thus using it to normalize regional volumes may be misleading when investigating the hippocampus.

Fast recovery of reduced levels of the brain metabolite NAA in the absence of severe alcohol withdrawal

In patients that had their last alcoholic drink within 24 hours before the first measurement, there was a trend towards a reduction in NAA levels compared to two weeks of abstinence and compared to healthy controls, the latter two groups did not differ. This effect was supported by a trend increase of NAA during the 14 days of abstinence in the patient group. Although metabolism rates between humans and rats are different and so is the time scale between (2 weeks in humans, vs. 12hrs in rats), this rapid regeneration of NAA is paralleled

EMPIRICAL STUDIES

in the animal model for alcohol dependence by reduced NAA levels in the hippocampus of rats during alcohol intoxication compared to controls. In animals this effect had already disappeared after a 12 hour withdrawal period.

These results are in line with previous MR spectroscopy studies reporting reduced NAA in other brain regions of alcohol dependent subjects (Meyerhoff et al., 2004; Mon et al., 2012; Zahr et al., 2010) as well as acute alcohol effects in healthy controls (Gomez et al., 2012). However, the fast recovery of hippocampal NAA has not been reported previously and needs some discussion. Most other studies found reduced brain NAA in alcohol dependent patients after several days or weeks of abstinence (Meyerhoff et al., 2004; Mon et al., 2012) but previous animal studies found no NAA reductions during abstinence in models of alcohol dependence (Hermann et al., 2012b; Zahr et al., 2009). While fast recovery from NAA reductions was reported in (Hermann et al., 2012b), (Zahr et al., 2009) did not detect changes in NAA during intoxication after 12 weeks of CIE when using a human scanner at lower field strength compared to our study. In another animal study NAA was reduced within 10 hours of the last ethanol ingestion after a four day binge intoxication episode, but not any more after 7 days of abstinence (Zahr et al., 2010). Taken together these results suggest reduced NAA levels to be a consequence of ethanol rather than of withdrawal. However in the human studies reduced NAA levels were often reported after several days or weeks of abstinence. This could be explained by our exploratory finding: patients who needed treatment with benzodiazepines for their severe alcohol withdrawal symptoms had lower NAA levels after two weeks of abstinence compared to those without benzodiazepine treatment. This could be an effect of benzodiazepines itself, e.g. through inhibition of neurogenesis (Wu and Castren, 2009), although a previous MR spectroscopy study did not find an effect of benzodiazepines on brain metabolites (Yildiz et al., 2010). Thus we hypothesise it to be an effect of severe alcohol withdrawal that impairs NAA recovery. This view is supported in our study by associations of CIWA-scores before the first scan and NAA levels after 14 days indicating that patients with a more severe alcohol withdrawal still had reduced NAA levels after two weeks of abstinence. A similar association has been reported by (Kuhn et al., 2014) where withdrawal severity was negatively associated with hippocampal volumes. Therefore reduced NAA levels in patients after several weeks of abstinence are most likely due to alcohol

EMPIRICAL STUDIES

withdrawal severity, which was not assessed in the studies reporting such reductions (Meyerhoff et al., 2004; Mon et al., 2012). Gazdzinski et al (2008) report NAA recovery to occur only in non-smoking individuals and thereby provide another explanation for variations between studies. However, in our study, smoking was not associated with reduced NAA levels at any measurement point, but then again only 14% of patients were nonsmokers prohibiting a sufficient analysis of this possibility. Although the time scale of the NAA recovery in humans differed from that in rats and possible different mechanism between species could account for it, we hypothesise that NAA reductions after alcohol abuse recover shortly after alcohol cessation, if no severe alcohol withdrawal syndrome occurs. Considering the role of NAA as a major neuronal osmolyte (Baslow, 2011) rehydration could be an explanation for our findings. However, based on the lack of support in previous studies (Mann et al., 1993; Rooney et al., 2000), the rehydration hypothesis was rejected. Other explanations, such as training or learning induced neuroplasticity or neurogenesis are possible since patients participated in a treatment program that includes mental and physical exercise. This exercise may be lower than in studies showing such effects on grey matter volume (for reviews see (Anderson, 2011; Zatorre et al., 2012)), but for patients the exercise may have been more than before admission to the clinic. However, we did not collect data on this issue that could support this explanation.

6.5 Limitations

Besides the major strengths of this study: the highly parallel approach in humans and rats, longitudinal design with high temporal resolution, advanced measurement techniques high quality criteria, several limitations need to be discussed. The challenging nature of this study is best reflected by the low number of spectra passing our quality control. The hippocampus is located near the skull base and next to major blood vessels both interfering with the magnetic field where movement artefacts due to alcohol withdrawal symptoms such as tremor, restlessness and anxiety reduce the quality of MR spectra. This resulted in a lack of power for some analyses, which was further diminished by the necessity to apply alpha adjustments since we were interested in several metabolites within one study. This is especially important for our group comparisons in Glu and NAA levels, which, although the alterations point all into the same direction, do not reach significance after controlling for multiple testing.

EMPIRICAL STUDIES

Another limitation of the present study not only is the use of Glx but also Glu and Gln concentrations as indicators for glutamatergic neurotransmission. Glx as a summed signal does not allow attributing the observed changes to a distinct metabolite, neither glutamate nor glutamine. Separation of Glu and Gln requires higher field strength or dedicated spectral editing sequences. Generally, all MR spectroscopic measures including Glu, Gln, Glx and NAA are derived from volumes that encompass millions of neurons and glia cells as well as blood vessels and cerebrospinal fluid, each with their distinct metabolic profile. Thus, it remains unknown how the measures of Glu, Gln and Glx relate to glutamatergic neurotransmission (for further discussion on interpretation of MRS derived metabolite values see Myers et al. (2016)).

We cannot rule out the possibility that metabolite concentrations are affected by a dehydration-induced change in water signal. However, this would bias all metabolites similarly. In addition, the observation of reduced levels of NAA would indicate dehydration of neuronal cell bodies but not of the whole volume investigated by MRS. Using metabolite ratios can rule out confounding effects of the water signal, but does not allow for the attribution of the observed effect to either of the two metabolites.

Another set of limitations are due to ethical questions: (a) measurement during alcohol withdrawal needs close medical supervision and in the presence of severe withdrawal symptoms medical management becomes necessary. This narrows the time window for an unmedicated MR scan. Therefore, we could disentangle the effects of intoxication and withdrawal in rats, but not in humans. (b) medical treatment of withdrawal severity has to be according to clinical need and therefore does not allow for experimental manipulation. This is especially important when interpreting the potential effect of the benzodiazepine treatment on hippocampal NAA recovery.

6.6 Conclusion:

The origin of alcohol-associated brain atrophy is yet to be elucidated. One main hypothesis suggests hyperglutamatergic neurotoxicity resulting in neuronal tissue damage and non-reversible cell death (Tsai and Coyle, 1998). Keeping in mind the limitations of MR

EMPIRICAL STUDIES

technology in detecting cellular mechanisms, we feel our results of negative associations between glutamate markers and grey matter volume in the hippocampus after withdrawal from alcohol in both species to be best explained by this hypothesis.

The rapid recovery of NAA levels after cessation of alcohol consumption in the absence of severe alcohol withdrawal syndrome could result from different mechanisms such as alcohol induced rehydration (Mann et al. 1993, Harper et al. 1985), abstinence induced learning and training experiences that increase axonal and dendritic growth (Anderson, 2011; Zatorre et al., 2012) or by neuroplasticity in the hippocampus (Hansson et al., 2010; Mandyam and Koob, 2012). However the present study does not allow to favour one of these explanations.

References

- Agartz I, Momenan R, Rawlings RR, Kerich MJ, Hommer DW (1999) Hippocampal volume in patients with alcohol dependence. *Archives of general psychiatry* 56:356-363.
- Anderson BJ (2011) Plasticity of gray matter volume: the cellular and synaptic plasticity that underlies volumetric change. *Developmental psychobiology* 53:456-465.
- Bahner F, Demanuele C, Schweiger J, Gerchen MF, Zamoscik V, Ueltzhoffer K, Hahn T, Meyer P, Flor H, Durstewitz D, Tost H, Kirsch P, Plichta MM, Meyer-Lindenberg A (2015) Hippocampal-Dorsolateral Prefrontal Coupling as a Species-Conserved Cognitive Mechanism: A Human Translational Imaging Study. *Neuropsychopharmacology : official publication of the American College of Neuropsychopharmacology*.
- Barnes J, Ridgway GR, Bartlett J, Henley SM, Lehmann M, Hobbs N, Clarkson MJ, MacManus DG, Ourselin S, Fox NC (2010) Head size, age and gender adjustment in MRI studies: a necessary nuisance? *NeuroImage* 53:1244-1255.
- Baslow MH (2011) The Vertebrate Brain, Evidence of Its Modular Organization and Operating System: Insights into the Brain's Basic Units of Structure, Function, and Operation and How They Influence Neuronal Signaling and Behavior. *Frontiers in Behavioral Neuroscience* 5:5.
- Biedermann S, Fuss J, Zheng L, Sartorius A, Falfan-Melgoza C, Demirakca T, Gass P, Ende G, Weber-Fahr W (2012) In vivo voxel based morphometry: detection of increased hippocampal volume and decreased glutamate levels in exercising mice. *NeuroImage* 61:1206-1212.
- Bühler M, Mann K (2011) Alcohol and the Human Brain: A Systematic Review of Different Neuroimaging Methods. *Alcoholism: Clinical and Experimental Research* 35:1771-1793.
- Canales JJ (2012) Deficient Plasticity in the Hippocampus and the Spiral of Addiction: Focus on Adult Neurogenesis. *Current topics in behavioral neurosciences*.

EMPIRICAL STUDIES

Cippitelli A, Damadzic R, Frankola K, Goldstein A, Thorsell A, Singley E, Eskay RL, Heilig M (2010) Alcohol-induced neurodegeneration, suppression of transforming growth factor-beta, and cognitive impairment in rats: prevention by group II metabotropic glutamate receptor activation. *Biological psychiatry* 67:823-830.

Dominguez G, Dagnas M, Decorte L, Vandesquille M, Belzung C, Beracochea D, Mons N (2014) Rescuing prefrontal cAMP-CREB pathway reverses working memory deficits during withdrawal from prolonged alcohol exposure. *Brain structure & function*.

Durazzo TC, Tosun D, Buckley S, Gazdzinski S, Mon A, Fryer SL, Meyerhoff DJ (2011) Cortical thickness, surface area, and volume of the brain reward system in alcohol dependence: relationships to relapse and extended abstinence. *Alcoholism, clinical and experimental research* 35:1187-1200.

Gazdzinski S, Durazzo TC, Yeh PH, Hardin D, Banys P, Meyerhoff DJ (2008) Chronic cigarette smoking modulates injury and short-term recovery of the medial temporal lobe in alcoholics. *Psychiatry research* 162:133-145.

Gomez R, Behar KL, Watzl J, Weinzimer SA, Gulanski B, Sanacora G, Koretski J, Guidone E, Jiang L, Petrakis IL, Pittman B, Krystal JH, Mason GF (2012) Intravenous ethanol infusion decreases human cortical gamma-aminobutyric acid and N-acetylaspartate as measured with proton magnetic resonance spectroscopy at 4 tesla. *Biological psychiatry* 71:239-246.

Hansson AC, Nixon K, Rimondini R, Damadzic R, Sommer WH, Eskay R, Crews FT, Heilig M (2010) Long-term suppression of forebrain neurogenesis and loss of neuronal progenitor cells following prolonged alcohol dependence in rats. *Int J Neuropsychopharmacol* 13:583-593.

Harding AJ, Wong A, Svoboda M, Kril JJ, Halliday GM (1997) Chronic alcohol consumption does not cause hippocampal neuron loss in humans. *Hippocampus* 7:78-87.

Heilig M, Egli M, Crabbe JC, Becker HC (2010) Acute withdrawal, protracted abstinence and negative affect in alcoholism: are they linked? *Addiction biology* 15:169-184.

Hermann D, Weber-Fahr W, Sartorius A, Hoerst M, Frischknecht U, Tunc-Skarka N, Perreau-Lenz S, Hansson AC, Krumm B, Kiefer F, Spanagel R, Mann K, Ende G, Sommer WH (2012) Translational magnetic resonance spectroscopy reveals excessive central glutamate levels during alcohol withdrawal in humans and rats. *Biological psychiatry* 71:1015-1021.

Hoefler ME, Pennington DL, Durazzo TC, Mon A, Abe C, Truran D, Hutchison KE, Meyerhoff DJ (2014) Genetic and behavioral determinants of hippocampal volume recovery during abstinence from alcohol. *Alcohol* 48:631-638.

Hoffman PL (1995) Glutamate receptors in alcohol withdrawal-induced neurotoxicity. *Metabolic brain disease* 10:73-79.

Koob GF, Volkow ND (2010) Neurocircuitry of addiction. *Neuropsychopharmacology* : official publication of the American College of Neuropsychopharmacology 35:217-238.

Krank M, Wall AM, Stewart SH, Wiers RW, Goldman MS (2005) Context effects on alcohol cognitions. *Alcoholism, clinical and experimental research* 29:196-206.

EMPIRICAL STUDIES

Kuhn S, Charlet K, Schubert F, Kiefer F, Zimmermann P, Heinz A, Gallinat J (2014) Plasticity of hippocampal subfield volume cornu ammonis 2+3 over the course of withdrawal in patients with alcohol dependence. *JAMA Psychiatry* 71:806-811.

Lovinger DM (1993) Excitotoxicity and alcohol-related brain damage. *Alcoholism, clinical and experimental research* 17:19-27.

Lukoyanov NV, Madeira MD, Paula-Barbosa MM (1999) Behavioral and neuroanatomical consequences of chronic ethanol intake and withdrawal. *Physiology & behavior* 66:337-346.

Mandyam CD, Koob GF (2012) The addicted brain craves new neurons: putative role for adult-born progenitors in promoting recovery. *Trends Neurosci* 35:250-260.

Mann K, Mundle G, Langle G, Petersen D (1993) The reversibility of alcoholic brain damage is not due to rehydration: a CT study. *Addiction (Abingdon, England)* 88:649-653.

McAllister AK (2000) Cellular and Molecular Mechanisms of Dendrite Growth. *Cerebral Cortex* 10:963-973.

Meinhardt MW, Sommer WH (2015) Postdependent state in rats as a model for medication development in alcoholism. *Addiction biology* 20:1-21.

Meyerhoff DJ, Blumenfeld R, Truran D, Lindgren J, Flenniken D, Cardenas V, Chao LL, Rothlind J, Studholme C, Weiner MW (2004) Effects of heavy drinking, binge drinking, and family history of alcoholism on regional brain metabolites. *Alcoholism, clinical and experimental research* 28:650-661.

Meyerhoff DJ, Durazzo TC, Ende G (2013) Chronic alcohol consumption, abstinence and relapse: brain proton magnetic resonance spectroscopy studies in animals and humans. *Current topics in behavioral neurosciences* 13:511-540.

Moffett JR, Ross B, Arun P, Madhavarao CN, Namboodiri AM (2007) N-Acetylaspartate in the CNS: from neurodiagnostics to neurobiology. *Progress in neurobiology* 81:89-131.

Mon A, Durazzo TC, Meyerhoff DJ (2012) Glutamate, GABA, and other cortical metabolite concentrations during early abstinence from alcohol and their associations with neurocognitive changes. *Drug and alcohol dependence* 125:27-36.

Myers JF, Nutt DJ, Lingford-Hughes AR (2016) gamma-aminobutyric acid as a metabolite: Interpreting magnetic resonance spectroscopy experiments. *Journal of psychopharmacology (Oxford, England)* 30:422-427.

Nees F, Pohlack ST (2014) Functional MRI studies of the hippocampus. *Frontiers of neurology and neuroscience* 34:85-94.

Paxinos G, Watson C (2004) *The Rat Brain in Stereotaxic Coordinates - The New Coronal Set*, Elsevier Science.

Prendergast MA, Harris BR, Mullholland PJ, Blanchard JA, 2nd, Gibson DA, Holley RC, Littleton JM (2004) Hippocampal CA1 region neurodegeneration produced by ethanol withdrawal requires activation of intrinsic polysynaptic hippocampal pathways and function of N-methyl-D-aspartate receptors. *Neuroscience* 124:869-877.

EMPIRICAL STUDIES

Prendergast MA, Mulholland PJ (2012) Glucocorticoid and polyamine interactions in the plasticity of glutamatergic synapses that contribute to ethanol-associated dependence and neuronal injury. *Addiction biology* 17:209-223.

Rimondini R, Arlinde C, Sommer W, Heilig M (2002) Long-lasting increase in voluntary ethanol consumption and transcriptional regulation in the rat brain after intermittent exposure to alcohol. *FASEB J* 16:27-35.

Rooney WD, Lee JH, Li X, Wang GJ, Franceschi D, Springer CS, Jr., Volkow ND (2000) 4.0 T water proton T1 relaxation times in normal human brain and during acute ethanol intoxication. *Alcoholism, clinical and experimental research* 24:830-836.

Smith SM (2002) Fast robust automated brain extraction. *Human Brain Mapping* 17:143-155.

Spanagel R (2009) Alcoholism: a systems approach from molecular physiology to addictive behavior. *Physiological reviews* 89:649-705.

Sullivan EV, Marsh L, Mathalon DH, Lim KO, Pfefferbaum A (1995) Anterior hippocampal volume deficits in nonamnesic, aging chronic alcoholics. *Alcoholism, clinical and experimental research* 19:110-122.

Tipps ME, Raybuck JD, Buck KJ, Lattal KM (2015) Acute ethanol withdrawal impairs contextual learning and enhances cued learning. *Alcoholism, clinical and experimental research* 39:282-290.

Tsai G, Coyle JT (1998) The role of glutamatergic neurotransmission in the pathophysiology of alcoholism. *Annual review of medicine* 49:173-184.

Tsai GE, Ragan P, Chang R, Chen S, Linnoila VM, Coyle JT (1998) Increased glutamatergic neurotransmission and oxidative stress after alcohol withdrawal. *The American journal of psychiatry* 155:726-732.

van Eijk J, Demirakca T, Frischknecht U, Hermann D, Mann K, Ende G (2013) Rapid partial regeneration of brain volume during the first 14 days of abstinence from alcohol. *Alcoholism, clinical and experimental research* 37:67-74.

Wu X, Castren E (2009) Co-treatment with diazepam prevents the effects of fluoxetine on the proliferation and survival of hippocampal dentate granule cells. *Biological psychiatry* 66:5-8.

Yeo RA, Thoma RJ, Gasparovic C, Monnig M, Harlaar N, Calhoun VD, Kalyanam R, Mayer AR, Durazzo TC, Hutchison KE (2013) Neurometabolite concentration and clinical features of chronic alcohol use: a proton magnetic resonance spectroscopy study. *Psychiatry research* 211:141-147.

Yildiz A, Gokmen N, Kucukguclu S, Yurt A, Olson D, Rouse ED, Moore C, Dicle O, Renshaw PF (2010) In vivo proton magnetic resonance spectroscopic examination of benzodiazepine action in humans. *Psychiatry research* 184:162-170.

Zahr NM, Bell RL, Ringham HN, Sullivan EV, Witzmann FA, Pfefferbaum A (2011) Ethanol-induced changes in the expression of proteins related to neurotransmission and metabolism in different regions of the rat brain. *Pharmacology, biochemistry, and behavior* 99:428-436.

EMPIRICAL STUDIES

Zahr NM, Mayer D, Rohlfing T, Hasak MP, Hsu O, Vinco S, Orduna J, Luong R, Sullivan EV, Pfefferbaum A (2010) Brain injury and recovery following binge ethanol: evidence from in vivo magnetic resonance spectroscopy. *Biological psychiatry* 67:846-854.

Zahr NM, Mayer D, Vinco S, Orduna J, Luong R, Sullivan EV, Pfefferbaum A (2009) In vivo evidence for alcohol-induced neurochemical changes in rat brain without protracted withdrawal, pronounced thiamine deficiency, or severe liver damage. *Neuropsychopharmacology* : official publication of the American College of Neuropsychopharmacology 34:1427-1442.

Zatorre RJ, Fields RD, Johansen-Berg H (2012) Plasticity in Gray and White: Neuroimaging changes in brain structure during learning. *Nature neuroscience* 15:528-536.

Zorumski CF, Mennerick S, Izumi Y (2014) Acute and Chronic Effects of Ethanol on Learning-Related Synaptic Plasticity. *Alcohol (Fayetteville, N.Y.)* 48:1-17.

Statement of Contribution

In this study, I was involved in the multimodal data acquisition (MRS & MRI) in the human study. I developed the concept for the multimodal integration analysis, helped with the according data interpretation, and the revision of the manuscript.

Supplementary information:

Methods and Materials:

Containing the descriptions of the overlap of the human sample with the previous study, the quantification of human spectra, the quality control procedure for human spectra, the rationale for the planned comparisons and the description of the chronic intermittent ethanol exposure paradigm in rats.

EMPIRICAL STUDIES

Overlap of human sample with previous study

The human sample used in this study consisted of a subsample of N=30 healthy controls and N=27 patients that were already part of the Hermann et al. (2012) study. Another N=4 healthy controls and N=12 patients were recruited in addition for the present study.

Rationale for choosing a TE of 30ms in human MRS measurements

The proximity of the hippocampus to major blood vessels and its position in the magnetic field makes spectra acquisition difficult. Therefore, we chose a TE of 30ms that provides a higher signal/noise ratio, at the cost of having a high overlap of the signals from both Glu and Gln, allowing for quantification of a summed Glx signal only.

Quantification of human spectra

Quantification of spectra was based on LCModel spectral fitting, using a simulated bases-set including Alanine, Aspartate, Creatine, Phosphocreatine, Glucose, Glutamine (Gln), Glutamate (Glu), gamma-Aminobutyric acid, Glucero-phocholine, Phosphocholine, myo-Inositol, Lactate, N-acetylaspartate (NAA), N-acetylaspartatylglutamine, Scyllo-Inositol, Taurine, Guanidinoacetate plus macromolecules, a set of lipids and ethanol. Tissue contribution of grey matter, white matter and cerebrospinal fluid to LCModel spectral fitting was accounted for according to the in-house developed protocol described in Weber-Fahr et al. (2002).

Quality control procedure for human spectra

Spectra were rejected if Cramer-Rao lower bounds (CRLB) of either NAA, creatine+phosphocreatine (Cr), choline-containing compounds (Cho) or myo-Inositol (mI) were higher than 10% or higher than 20% for Glu + Gln (=Glx). Four raters (NTS, MS, GO, GE), experienced in MR spectroscopy, visually checked the quality of all obtained spectra. Ratings revealed an intra-class-correlation of $ICC[3,k] = 0.96$ for the quality ratings ranging from 0 = good, 1 = mostly acceptable and 2 = unacceptable. This indicates high interrater reliability. Additionally to the CRLB criteria, the obtained values were only included in the

EMPIRICAL STUDIES

statistical analysis if the respective spectrum was defined as “good” by at least one rater and by none as “inacceptable”.

Modelling the hypotheses on planned contrasts in order to increase statistical power

Our hypothesis for Glx in humans was as follows: healthy controls are the reference point. During acute withdrawal on day1 Glx levels are increased but after two weeks of abstinence Glx levels normalize again (= resembles that of healthy controls). In order to test this we used ANOVA with planned comparisons where the coefficients have to add up to 0 and allocated

“-0.5” to both healthy control measurements and to 14 days abstinence measurements and “+1” to acute withdrawal measurements. For the comparison in NAA we expected the opposite direction. Therefore coefficients of “+0.5” were allocated to both healthy control measurements and to 14 days abstinence measurements and “-1” to acute withdrawal measurements.

Accounting for multiple comparisons in humans

For the comparison of the two metabolites of interest (Glx and NAA) in two separate ANOVAs, Bonferroni-Holm adjustments were applied to account for familywise error rate (FWE).

Significance levels for correlations between Glx and Hippo/TIV were adjusted for two tests corresponding to the correlations for both time points in alcohol dependent patients. This resulted in an adjusted alpha of 0.025 below which we regard an effect as significant.

Chronic intermittent ethanol exposure paradigm in rats:

Eight of sixteen rats were exposed to daily intermittent exposure cycles to alcohol vapor intoxication and withdrawal. The exposure to alcohol vapor intoxication resulted in daily oscillating blood alcohol levels from 2.0–3.5 g/l to zero. Near the end of the 49-cycle exposure period, signs of withdrawal in the form of tail stiffness and piloerection were visible towards the end of the alcohol off phase. Weight gain during the exposure period was significantly less in the alcohol exposed group (3 % of their baseline body weight) compared

EMPIRICAL STUDIES

to control rats (22.5 %) leading to significant differences in body weights at the end of the exposure period (464.4 ± 15.4 g and 557.8 ± 7.7 g, exposed vs. control, respectively, $P < 0.001$). Rats recovered quickly after cessation of the alcohol exposure, thus body weights did not significantly differ between groups after the 3-week abstinence period (529.3 ± 11.8 g and 562.6 ± 7.9 g, n.s., exposed vs. control, respectively).

Rational for inclusion of weight as a time dependent covariate in our analysis

While age was matched between the two groups of rats, weight differed during the course of CIE but not anymore after 3 weeks of abstinence and might have been a covariate explaining possible differences rather than intoxication or withdrawal state, on which this study focused on. Therefore, we regarded the inclusion of weight as a covariate as necessary.

Accounting for multiple comparisons in Animals:

For the comparisons of the metabolites of interest between the groups across different time points, we applied Bonferroni-Holm adjustments to account for familywise error rate (FWE), when comparing three metabolites and one metabolite ratio in four different models.

For the correlations of interest at any time point within the CIE rats we applied a Bonferroni adjustment for three correlations at 5 measurements resulting in an adjusted alpha of 0.003 below which we regard a correlation as significant.

Results:

Containing Figure S1, depicting the course of the glutamate to glutamine ratio during the animal procedure, revealing elevated Glu/Gln ratios during withdrawal compared to naïve rats, analysis of Glx in animals, absent increase in NAA levels during 14 days abstinence in patients that needed benzodiazepine treatment for their severe withdrawal, Figure S2 depicting the NAA level reduction and dose dependent relationship after 14 days abstinence in patients that needed treatment with benzodiazepine for their severe alcohol withdrawal, and Figure S3 depicting anteriodorsal hippocampal volume changes in rats.

EMPIRICAL STUDIES

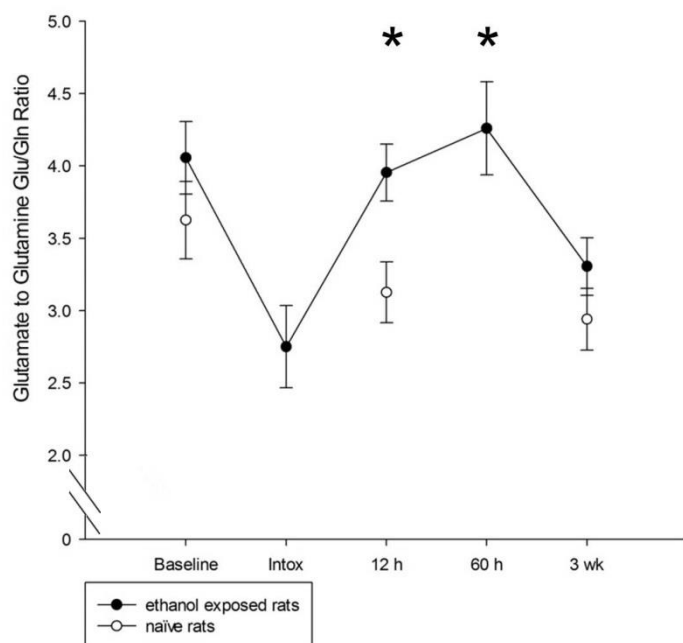


Figure S1: Elevated glutamate to glutamine ratios in the hippocampus during alcohol withdrawal in ethanol exposed rats compared to naïve rats. MRS measurements took place at baseline, during the last intoxication period of a 49 cycles intermittent ethanol exposure paradigm (Intox), after 12 hours of ethanol withdrawal (12 h) after 60 hours of ethanol withdrawal (60 h) and after 3 weeks of abstinence (3 wk). Elevated ratios during withdrawal indicate elevated glutamatergic neurotransmission. Asterisks indicate significant higher levels in ethanol exposed rats compared to naïve rats at the respective measurement time point.

Analysis in Glx parallels human findings in so far as there are no differences detectable during withdrawal

In order to better compare human and animal findings, we repeated the analysis for Glx in rats and found no effect for time ($P = 0.20$) or treatment ($P = 0.68$) but a significant interaction of time and treatment ($P < 0.001$). Post hoc ANOVAS with weight as covariate revealed this interaction to be driven by trend level Glx reductions in exposed rats at baseline ($P = 0.09$) but no differences at any other measurement point (all $P > 0.1$). When adding baseline Glx levels as covariate for the other measurement points there was a significant elevation in Glx levels in exposed rats during intoxication ($P = 0.03$) but no difference at any other time point ($P > 0.1$). Taken together this corroborates the findings from both metabolite concentrations where the baseline difference is most probably driven by the difference found in Glu and the difference at intoxication is most probably driven by the difference found in Gln. This adds to the

EMPIRICAL STUDIES

conclusion, that withdrawal associated increases in Glu concentrations as we reported previously in Hermann et al. (2012) are more difficult to detect when using sequences that only allow for the quantification of the summed signal of Glx.

Absent increase in NAA levels during 14 days abstinence in patients that needed benzodiazepine treatment for their severe withdrawal

Separate paired sample t-tests in patients whose spectra quality allowed for longitudinal analysis revealed a trend increase in NAA levels between patients that did not need benzodiazepine treatment during withdrawal ($F[5] = -2.45$, $P = 0.054$), but not in those who needed such medication for their severe withdrawal ($F[4] = -0.54$, $P = 0.62$). NAA levels did not differ during acute withdrawal between those who subsequently needed benzodiazepine treatment and those who did not ($t[13] = -0.20$, $P = 0.85$).

Additional support for Benzodiazepine dosage as a proxy for withdrawal severity

The frequency of benzodiazepine treatment depended on clinical withdrawal symptoms as assessed with CIWA-Ar, therefore the dose of benzodiazepines given can be regarded as a proxy of withdrawal severity. The observation of persistent NAA decrease in alcohol dependent patients with severe withdrawal symptoms was further supported by a significant negative correlation between the dose of benzodiazepines needed for withdrawal treatment and NAA concentration after 14 days of abstinence ($\rho = -0.52$, $P = 0.015$, see Figure S2). We also found a trend association of the CIWA-Ar score before the first MRS and the NAA levels after 14 days of abstinence ($\rho = -0.42$, $P = 0.059$).

EMPIRICAL STUDIES

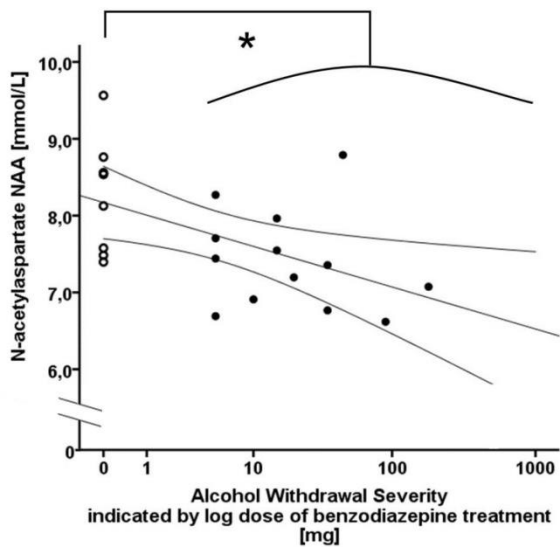


Figure S2: N-Acetylaspartate (NAA) levels after 14 days abstinence in alcohol dependent patients are reduced in a dose dependent manner if alcohol withdrawal symptoms made treatment with benzodiazepines necessary. The frequency and dose of benzodiazepine treatment depended on clinical withdrawal symptoms as assessed repeatedly every 2 hours with CIWA-Ar. Therefore the sum of benzodiazepines given can be regarded as a measure of withdrawal severity. The asterisk indicates a significant difference between patients who needed benzodiazepines and those who did not.

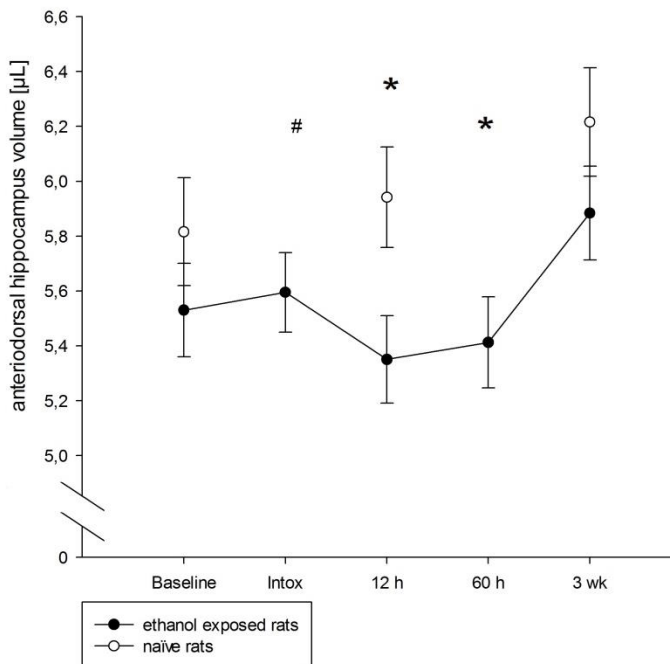


Figure S3: Reduced anteriodorsal hippocampal volumes during alcohol withdrawal in ethanol exposed rats compared to naïve rats. MRS measurements took place at baseline, during the last intoxication period of a 49 cycles intermittent ethanol exposure paradigm (Intox), after 12 hours of ethanol withdrawal (12 h) after 60 hours of ethanol withdrawal (60 h) and after 3 weeks of abstinence (3 wk). Asterisks indicate significant lower anteriodorsal hippocampal volumes in ethanol exposed rats compared to naïve rats at the respective measurement time point. At intoxication this was only a trend.

7 ACC GABA levels are associated with functional activation and connectivity in the fronto-striatal network during interference inhibition in patients with borderline personality disorder⁴

Abstract

Impulsivity often develops from disturbed inhibitory control, a function mainly regulated by γ -Aminobutyric acid (GABA) levels in the anterior cingulate cortex (ACC) and the fronto-striatal system. In this study, we combined MRS GABA measurements and fMRI to investigate neurochemical and neurofunctional correlates of interference inhibition, further emphasizing the direct relationship between those two systems, as well as their relations to impulsivity in patients with BPD. In addition to BOLD activation, task-dependent functional connectivity was assessed by a generalized psychophysiological interactions approach. Full factorial analyses were performed via SPM to examine the main effect (within-group associations) as well as the interaction term (group differences in the association slope). The UPPS scales were used to evaluate impulsivity traits. Compared to healthy controls (HCs), BPD patients exhibited significantly less ACC-caudate functional connectivity during

⁴ Publication :

Wang, G.Y., van Eijk, J., Demirakca, T., Sack, M., Krause-Utz, A., Cackowski, S., Schmahl, C., Ende, G., 2017. ACC GABA levels are associated with functional activation and connectivity in the fronto-striatal network during interference inhibition in patients with borderline personality disorder. *NeuroImage* 147, 164-174.

EMPIRICAL STUDIES

interference inhibition. ACC GABA levels in BPD patients but not in HCs were positively related to the magnitude of activation in several fronto-striatal regions (e.g. ACC, frontal regions, putamen, caudate,) and the strength of ACC-caudate functional connectivity during interference inhibition. The strength of the correlations of GABA with connectivity significantly differs between the two groups. Moreover, among all the UPPS impulsivity subscales, UPPS sensation seeking in the BPD group was related to GABA and was also negatively related to the task-dependent BOLD activation and functional connectivity in the fronto-striatal network. Finally, mediation analyses revealed that the magnitude of activation in the caudate and the strength of ACC-caudate functional connectivity mediated the relationship between ACC GABA levels and UPPS sensation seeking in patients with BPD. Our findings suggest a disconnectivity of the fronto-striatal network in BPD patients during interference inhibition, particularly for patients with higher impulsivity. The ACC GABAergic system seems to play a crucial role in regulating regional BOLD activations and functional connectivity in this network, which are further associated with impulsive sensation seeking in BPD.

Key words

Borderline personality disorder; interference inhibition; anterior cingulate cortex; GABA; fronto-striatal networks; impulsivity

7.1 Introduction

It has consistently been reported that dysfunctional inhibitory processes are associated with heightened impulsivity in neuropsychological disorders involving excessive impulsive behavior, such as borderline personality disorder (BPD) (Holtmann et al., 2013; Wingenfeld et al., 2009). However, the underlying neurobiological mechanisms are largely unknown.

Functional imaging studies exploring neural correlates of inhibitory control suggest that these processes involve activation of the fronto-striatal network (Aron et al., 2007; Sebastian et al., 2014b; van Eijk et al., 2015b). The activation of this network is found to be altered in BPD patients. In particular, dysfunction of the anterior cingulate cortex (ACC) is a central pathophysiological feature in BPD (for review see (Sebastian et al., 2014b)). Activation in the ACC has been associated with conflict detection and monitoring (Botvinick et al., 2004; Kerns et al., 2004), and BPD patients often display less activation in the ACC compared to healthy controls (HCs) during emotional interference inhibition tasks (Holtmann et al., 2013; Wingenfeld et al., 2009).

The integration of the fronto-striatal network is also suggested to play a prominent role in inhibitory control (Aron et al., 2007; Behan et al., 2015; Courtney et al., 2013; Cubillo et al., 2010; Jahfari et al., 2011). More specifically, the ACC was shown to have widespread anatomical and functional connections to striatal nuclei, mainly involved in conflict-related inhibitory control (Harrison et al., 2009a; Marsh et al., 2014; Tekin and Cummings, 2002). Aberrant functional connectivity between ACC (or functionally connected PFC regions) and striatum were repeatedly observed in several psychiatric disorders with inhibitory control deficits (Courtney et al., 2013; Cubillo et al., 2010; Marsh et al., 2014). However, no study has specifically examined ACC based connectivity within this network in BPD.

In addition, although the neurochemical basis of inhibitory control deficits in BPD is still largely unknown, studies in healthy subjects using magnetic resonance spectroscopy (MRS) have indicated that levels of the inhibitory neurotransmitter γ -Aminobutyric acid (GABA), especially in the fronto-striatal network, play an important role in the regulation of inhibitory control (Dharmadhikari et al., 2015; Hayes et al., 2014; Kuhn et al., 2016; Quetscher et al.,

EMPIRICAL STUDIES

2015). For example, Silveri et al. (2013) reported that in healthy adolescents a lower GABA/creatine ratio in the ACC was associated with worse performance on a go/nogo task. Our recent investigation by (Ende et al., 2016) is supportive of these findings suggesting that lower ACC GABA levels in BPD patients and HCs are associated with higher impulsivity total scores. Boy et al. (2011) also reported that in healthy men higher prefrontal GABA levels correlate with lower rash impulsivity. Furthermore, the GABAergic neurons contribute dramatically to neural firing rates and hemodynamic response, which are also believed to be related to BOLD signal changes (Attwell and Iadecola, 2002; Logothetis, 2002; Logothetis et al., 2001). Therefore, examinations of associations between metabolites and fMRI measures provide us an opportunity to gain deeper insight in the role of brain metabolites on brain activity during behavioral performance. Indeed, a growing number of studies indicate that GABA levels in key regions (e.g. ACC) can predict task-modulated brain activation (Donahue et al., 2010; Muthukumaraswamy et al., 2009; Northoff et al., 2007) and task-dependent functional connectivity (Duncan et al., 2014; Sampaio-Baptista et al., 2015), while other studies did not observe correlations between those two measures (Cousijn et al., 2014; Harris et al., 2015). Yet, the relationship of ACC GABA levels with functional activation and connectivity within the fronto-striatal network during inhibitory control is not fully understood.

Moreover, it has been suggested that impulsivity traits greatly rely on individual variances in BOLD signal changes ((Brown et al., 2015); for review see (Dalley et al., 2008a)). In support of this notion, a great amount of literature suggests that dysfunction in the fronto-striatal network during inhibitory control is associated with heightened impulsivity traits in clinical patients (DeVito et al., 2013; Ding et al., 2014; Horn et al., 2003; Kaladjian et al., 2011), highlighting that the fronto-striatal system is particularly important in regulation of impulsivity. However, no studies have yet examined the relationship between these processes and psychometric measures of impulsivity in BPD.

As demonstrated by previous studies, increased impulsivity seems to develop from lower ability of inhibitory control (Olson et al., 2002; Olson et al., 1999), a cognitive function modulated by the frontal GABAergic system, which further drives the neural activity and synchronization of the fronto-striatal network (Bari and Robbins, 2013; Dalley et al., 2008a;

EMPIRICAL STUDIES

Hayes et al., 2014). This raises the possibility that the negative association of GABA and impulsivity indicated in our prior investigation using the same MRS dataset (Ende et al., 2016), might be mediated by regional BOLD activation as well as ACC based functional connectivity with key regions in the fronto-striatal network. For this combined analysis we included a subsample of the BPD and HC subjects included in (Ende et al., 2015b; van Eijk et al., 2015b) who underwent both, GABA MRS and an fMRI experiment.

Neither the GABA levels nor the BOLD activation had been found to be significantly different between HCs and BPD patients in the previous evaluation (Ende et al., 2015b; van Eijk et al., 2015b).

We now report a combined evaluation, where we used a multimodal neuroimaging approach to explore the inter-relationship between ACC GABA, neural correlates of interference inhibition, and impulsivity in BPD and HCs. We hypothesized that the task-dependent activation and connectivity during interference inhibition serve as a mediator which could explain the associations between GABA and impulsivity. We took a hierarchical approach to test our hypothesis: (1) to explore whether ACC GABA would be associated with the activation in the ACC and other fronto-striatal regions; (2) to test if there was functional connectivity to the ACC for these regions, and whether this task-dependent connectivity was weaker in BPD; (3) to test whether ACC GABA was also correlated with this functional connectivity strength; (4) to explore which impulsivity subscale was associated with ACC GABA; (5) to test whether the GABA-associated impulsivity subscale was also correlated with activations and connectivity in the fronto-striatal network during interference inhibition; (6) to test our hypothesis that the task-dependent activation and connectivity during interference inhibition served as a mediator, mediating the associations between GABA and impulsivity.

7.2 Materials and methods

7.2.1 Participants

Participants included 33 women with BPD (aged 18-42 years) and 32 age-matched healthy women (aged 18-41years). Diagnostic assessments were conducted by well-trained

EMPIRICAL STUDIES

psychologists and psychiatrists. The diagnostic assessments included two structured interviews: the German version of the Structured Clinical Interview for DSM-IV (SCID-I) (First et al., 1997; Wittchen et al., 1997) was used to screen for major Axis I psychiatric disorders; the BPD section of the International Personality Disorder Examination (Loranger, 1999) was used to confirm the diagnosis of BPD. Exclusion criteria for BPD patients were lifetime diagnosis of bipolar disorder, psychotic disorder, substance abuse within the last 2 months, attention-deficit / hyperactivity disorder (ADHD), serious physical and neurological diseases as well as current psychotropic medication (within two weeks prior to study). A further exclusion criterion for the control group was any current Axis I or II psychiatric diagnosis.

BPD patients were recruited at the Central Institute of Mental Health in Mannheim, Germany. HCs were recruited via advertisements in newspapers and at websites. After full explanation of the study procedures, written informed consent was obtained from all participants. The study was approved by the ethics committee of the Medical Faculty Mannheim/Heidelberg University and conducted according to the Declaration of Helsinki.

Seven women with BPD and 7 healthy subjects had to be excluded from the fMRI and MRS analyses due to misunderstandings of task instructions, movement artifacts, positive drug screening, early termination of the measurement and insufficient spectral quality. Finally, 26 BPD patients and 25 HCs were included in imaging analyses. Twenty-four BPD patients and 25 HCs both have MRS and fMRI data which could be used for correlation and mediation analyses.

7.2.2 Experimental procedure

Participants underwent clinical and neuropsychological testing, followed by an MRS scan at rest, used to assess GABA levels in the bilateral ACC. Finally, a hybrid inhibition paradigm was presented during fMRI measurement to evaluate inhibitory control, which includes the properties of the Simon-, Go/nogo-, and Stopsignal tasks. The clinical and psychological assessment took place prior to the MRI session within the same week but not on the same day. The MRS and fMRI were measured on the same day in one session.

7.2.2.1 MR data acquisition

All MR data was acquired on a 3 T whole body MR scanner with a 32 channel receive-only head coil (Siemens Magnetom TIM Trio, Erlangen, Germany). First, a T1-weighted high-resolution anatomical data set was acquired using a 3D MPRAGE sequence (TR/TE = 2300/3.03 ms; flip angle = 9° ; FOV = $256 \times 256 \text{ mm}^2$; voxel size = $1 \times 1 \times 1 \text{ mm}^3$). The $40 \times 30 \times 20 \text{ mm}^3$ MRS voxel was placed in the bilateral ACC (see Figure 7-1a) based on the isotropic 1 mm^3 MPRAGE data set with reconstructed coronal and transverse planes aligned with the shape of the corpus callosum. GABA spectra were obtained with a MEGA-PRESS sequence (TR/TE = 3000/68 ms, NEX = 96 on, 96 off, total scan time 9.6 min) while subject was at rest. The editing pulse (Gauss shape, 20.3 ms length, bandwidth: 44 Hz) in the MEGA-PRESS sequence was switched between 1.9 (on) and 1.5 ppm (off) alternating every excitation which suppresses MM contribution to the GABA signal. Additionally, water-suppressed spectra were obtained with a PRESS sequence at TR/TE = 10000/30 ms for quantification. Then, for fMRI measurement, T2*-weighted gradient echo planar imaging (EPI) sequence was used to measure the BOLD signal during the Hybrid Response Inhibition (HRI) Task (TR/TE = 1520/30 ms, flip angle = 71° , voxel size = $3.4 \times 3.4 \times 4 \text{ mm}^3$, 28 transverse slices). For each run 346 EPI volumes were acquired.

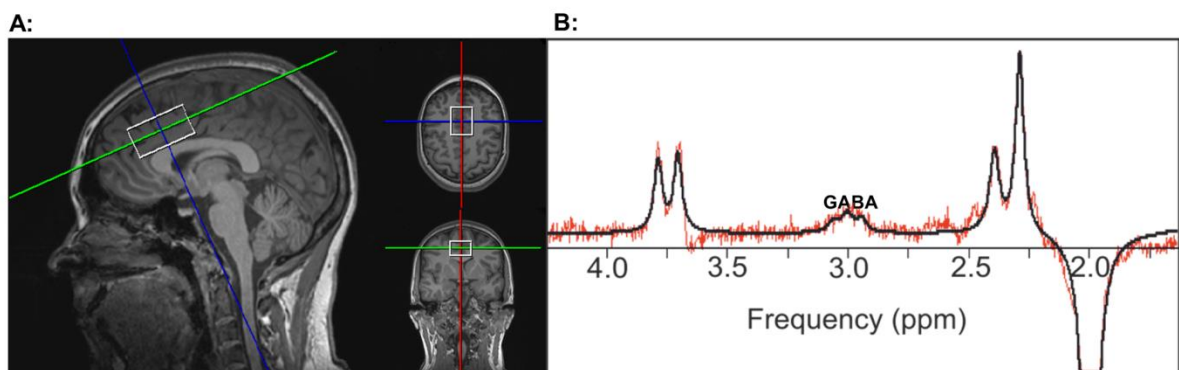


Figure 7-1 A: The MRS voxel; B: an exemplary MEGA-PRESS spectrum

7.2.2.2 Experimental paradigm

Participants performed three runs of the HRI task during the fMRI scanning session, which incorporated the properties of the Simon-, Go/nogo-, and Stopsignal tasks. Briefly, the task consisted of four conditions: a congruent go condition (62.5%), an incongruent go condition (12.5%), a nogo condition (12.5%) and a stop condition (12.5%). The length of the interstimulus interval was jittered with a mean duration of 1500ms and a standard deviation of 372 ms. Each run consisted of 160 trials, and was presented in a pseudo-randomized order (see Figure 7-2). The Presentation software was used to run the task, and VisuaStim digital goggles were used to present the task during the measurement.

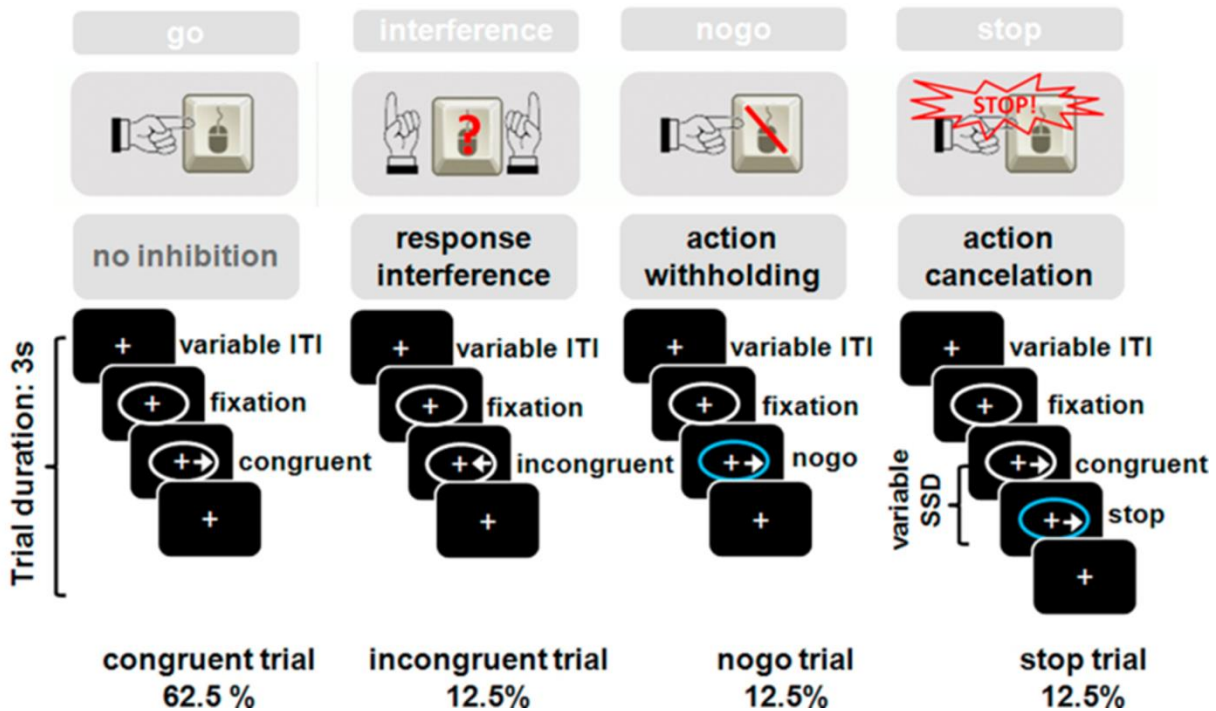


Figure 7-2 Schematic representation of the Hybrid Response Inhibition (HRI) task. The HRI task combined elements of the three separate tasks (Simon-, Go/nogo-, and Stopsignal tasks) using identical visual stimulus material across conditions. Participants were instructed to press a button according to the pointing direction of an arrow, except for when a blue circle is presented (in this case, participants were instructed to inhibit their responses). ITI = intertrial interval; SSD = stopsignal delay.

EMPIRICAL STUDIES

The task of interest for the present analysis is the Simon task (interference inhibition), thus we describe this task here in more detail. Participants were asked to fixate on a white cross at all times, which was presented in the center of the screen against a black background. Each trial started with a white ellipse encircling the cross. After 500ms, a white arrow was presented within the ellipse either on the right or left side of the fixation cross. Participants were instructed to respond corresponding to the direction of the arrow (congruent and incongruent conditions). In the congruent condition, the direction of the arrow and the presentation of the arrow on the screen were identical, e.g. arrow on the right side pointing in the right direction, while in the incongruent condition the pointing direction and the presentation side were opposite, e.g. the arrow on the right side was pointing in the left direction.

7.2.3 Measures and data processing

7.2.3.1 Clinical data and impulsivity assessment

Severity of BPD symptoms was assessed using the Borderline Symptom List-23 (Bohus et al., 2007). Impulsivity trait was assessed using the UPPS impulsiveness scale (Schmidt et al., 2008), with subscales: urgency, lack of perseverance, lack of premeditation and sensation seeking.

7.2.3.2 MRS data: absolute GABA levels in the ACC

For quantification of the spectra, the GABA signals were analyzed using the jMRUI-software (Stefan et al., 2009). The jMRUI procedure included zerofilling (2048 points), a slight apodization of 4Hz (Lorentzian shape), and HLSVD filtering of the residual water peak. Three peaks with Lorentzian shape were used to fit the GABA signal at 3 ppm. Quantification was based on phantom measurements including correction for the voxel's tissue compartmentation (Aufhaus et al., 2013). Briefly, the calculation of the GABA concentration in vivo is as follows:

$$C_{\text{GABA}}^{\text{iv}} = \frac{S_{\text{GABA}}^{\text{iv}}}{S_{\text{H}_2\text{O}}^{\text{iv}}} \frac{S_{\text{H}_2\text{O}}^{\text{ph}}}{S_{\text{GABA}}^{\text{ph}}} * C_{\text{GABA}}^{\text{ph}} * \frac{\rho_{\text{H}_2\text{O}}}{\text{BM}_{\text{GABA}}},$$

EMPIRICAL STUDIES

where S_X^{iv} and S_X^{ph} are the peak areas of the corresponding in vivo and phantom measurement, respectively. C_{GABA}^{ph} is the GABA concentration of the phantom. BM_{GABA} is *the brain matter* voxel composition (sum of white matter (WM) and gray matter (GM)) for the voxel position calculated for the GABA frequency (cerebrospinal fluid (CSF) content subtracted). The differing water fraction in the voxel's WM, GM, and CSF content is described by ρ_{H2O} ($0.71WM + 0.81GM + 0.98CSF$) and taken from (Christiansen et al., 1993). All spectra underwent visual inspection to control for spectral quality. Additionally, the spectra with an N-acetylaspartate (NAA) linewidth greater than 6.5 Hz were excluded. GABA levels are given in institutional units [i.u.].

7.2.3.3 fMRI data: BOLD activation & functional connectivity

Image preprocessing

SPM8 (Wellcome Department of Cognitive Neurology) was used to conduct all image preprocessing and statistical analysis, running with MATLAB R2012b (The Mathworks Inc., Natick, Massachusetts, USA). Prior to preprocessing, images were screened for motion artifacts and participants with a head motion > 2 mm were excluded. The first five functional images of each run were discarded to allow for equilibrium effects. In detail, several preprocessing procedures were run in the batch mode. First, functional images were corrected for timing differences between slices. Images were then motion-corrected and realigned to the mean image of each scanning run. Afterwards, the corrected images were co-registered to the individual anatomical T1 image. Following that, the anatomical image was segmented and spatially normalized to a standard Montreal Neurological Institute (MNI) template and normalization parameters were applied to all functional images. Finally, the functional images were spatially smoothed using a 3-dimensional isotropic Gaussian kernel with a full width half maximum (FWHM) of 6 mm.

BOLD activation analysis

On the subject level, a linear regression model (general linear model, GLM) was created to test within-subject effects. For the task of interest in this study, incongruent correct go and

EMPIRICAL STUDIES

congruent correct go trials were regarded as Simon successful inhibition and Simon go trials, respectively. Thus, correct reactions for incongruent go and congruent go trials were modeled as regressors of interest. The invalid trials (incorrect reactions for the 4 events), valid trials of non-interest (correct reactions for no-go and stop events), instruction, fixation cross, and the six movement parameters were modeled as regressors of no interest. All events were modeled as stick functions at stimulus onset and convoluted with a canonical hemodynamic response function. The model included a high-pass filter with a cut-off period of 128s to remove drifts or other low-frequency physical noise in the time course. The BOLD contrast of ‘successful interference inhibition’ was defined as correct reactions for [incongruent go > congruent go]. Additionally, BOLD contrasts were calculated for each task conditions ([incongruent go > baseline], [congruent go > baseline]) to characterize the corresponding task-related cognitive process.

Functional connectivity analysis: gPPI

A generalized psychophysiological interactions (gPPI) approach (McLaren et al., 2012) was used to assess task-dependent functional connectivity of the seed region, aiming to provide information of functional interaction between the seed region and all other brain voxels during each task condition as well as to clarify the psychological impact of such an interaction. This method has been shown to be more sensitive and accurate at estimating the pair-wise connectivity differences between conditions (e.g. incongruent go > congruent go) than the standard PPI implemented in the SPM software (McLaren et al., 2012). In the current study, the seed region of the bilateral ACC was drawn with masks provided by the WFU PickAtlas (https://www.nitrc.org/projects/wfu_pickatlas/). The gPPI model was created and estimated by the gPPI toolbox (<http://www.nitrc.org/projects/gppi>). The physiological variable was created by extracting the mean deconvolved time course from the seed region. Psychophysiological interactions were calculated as the multiplication vector of the physiological variable and each task regressor (e. g. congruent go, incongruent go). For the task of interest in this study, the PPI terms of successful Simon task trials (including [PPI incongruent go > congruent go], [PPI incongruent go], as well as [PPI congruent go]) were computed to characterize the corresponding task-dependent functional connectivity of the ACC.

7.2.3.4 Behavioral data

Reaction time (RT) and error index were recorded by the presentation software during the fMRI measurements. Behavioral parameters of interest were the mean RT on correct congruent and incongruent trials as well as the errors on incongruent trials. The interference effect in the Simon task was calculated by subtracting mean RT in congruent trials from mean RT in incongruent trials.

7.2.4 Statistical analysis

Two sample t-tests were performed via SPSS (PASW version 22) on the GABA levels and psychophysiological data (including age, BSL-23) to test group differences between BPD patients and HCs. Differences were considered significant if $P < 0.05$. Group differences in UPPS subscales were analyzed with a multivariate general linear model (MANOVA). The Bonferroni-corrected threshold for statistical significance was set at $P = 0.013$ to account for the 4 UPPS subscales investigated. Group differences in behavioral performance were also tested using MANOVA, and the Bonferroni-corrected threshold was considered significant if $P < 0.01$ to account for the 5 behavioral indices of the Simon task.

To examine the correlations of ACC GABA levels with behavioral interference inhibition and UPPS scores, Spearman's rho correlations including bootstrapping analyses were performed with SPSS due to the non-normal distributions for the BSL values and behavioral measures. The correlation coefficient and the 95% confidence interval were computed using 5000 bootstrapped samples. The initial significance threshold was set at $P < 0.05$. The Bonferroni-corrected threshold for statistical significance was set at $P = 0.01$ to account for the 5 behavioral indices, as well as $P = 0.013$ to account for the 4 UPPS subscales.

Whole brain BOLD activation and gPPI data were analyzed with SPM8. One- and two-sample t-tests were used to assess within- and between-group differences, respectively.

A full factorial model was performed with SPM8 to examine the association between fMRI results (BOLD or gPPI) and the covariate of interest (GABA or UPPS score). This approach was used to analyze the main effect (within-group associations) as well as the interaction term

EMPIRICAL STUDIES

(group differences in the association slope) in one statistical model. The model included the factor group with two levels and the continuous variables (GABA or UPPS) as covariates of interest.

For all the imaging analyses (e.g. group comparison & voxel-wise regression analysis), an initial threshold of $P < 0.001$, uncorrected, with a minimum of 10 contiguous voxels, was used to detect the potential significant clusters. Based on previous studies and our hypothesis, fronto-striatal regions were the regions of interest (ROIs) in this study, including dorsal lateral prefrontal cortex (DLPFC), inferior frontal cortex (IFC), middle frontal cortex (MFC), superior frontal cortex (SFC), ACC, putamen, caudate, and pallidum (Grant and Kim, 2014; Sebastian et al., 2013; van Eijk et al., 2015b). The clusters detected with those ROIs (obtained from the automated anatomical labeling atlas (AAL) (Tzourio-Mazoyer et al., 2002)) that survived small volume family-wise error correction ($P_{SVC_FWE} < 0.05$) were considered as significant and reported.

In order to further test the hypothesis that fronto-striatal processes (activation and functional connectivity) mediates the relationship between ACC GABA levels and impulsivity, the mediation was tested with bootstrapping analyses in the SPSS PROCESS macro written by Andrew F. Hayes ([http:// www.afhayes.com](http://www.afhayes.com)). Indirect effects and the 95% confidence interval were computed using 5000 bootstrapped samples. Statistics were considered significant for $P < 0.05$. First, we performed conjunction analyses to identify the brain regions, both correlated with GABA and UPPS scores. The conjunction map was thresholded at $P < 0.005$, uncorrected, cluster > 10 voxels. Then, we chose the significant cluster (left caudate) as the ROI, and extracted the mean parameter estimate (BOLD & PPI) values to use for the further mediation analyses in SPSS.

7.3 Results

7.3.1 Demographic and trait impulsivity characteristics

The characteristics of all participants are summarized in Table 7-1. BPD patients had significantly higher BSL-23 scores than HCs. Compared to HCs, BPD patients scored higher on UPPS urgency, lack of perseverance, and sensation seeking scores, but not on lack of

EMPIRICAL STUDIES

premeditation. No group difference in UPPS sensation seeking scores was found between patients with (N = 12) and without prior substance abuse history (P = 0.294).

In addition, correlation with bootstrapping analyses revealed that a higher BSL-23 score in BPD patients was associated with higher UPPS urgency (r = 0.421, P = 0.032) and UPPS sensation seeking scores (r = 0.432, P = 0.027). In HCs, a positive correlation was found between the BSL-23 score and UPPS urgency (r = 0.403, P = 0.046). But none of these correlations survived the Bonferroni correction.

Table 7-1 Demographic and impulsivity feature of BPD patients and healthy controls
[mean (SD)]

| Characteristics | BPD patients | Healthy controls | P-value |
|------------------------|--------------|------------------|----------|
| Age (years) | 26.77(6.55) | 27.53(6.59) | 0.65 |
| BSL-23 total | 47.17(21.04) | 2.6(4.1) | < 0.001* |
| UPPS-urgency | 38.19(7.58) | 23.24(4.91) | <0.001* |
| UPPS-Premeditation | 23.35(5.63) | 21.76(3.29) | 0.112 |
| UPPS-Perseverance | 21.50(5.70) | 16.24(3.66) | <0.001* |
| UPPS-Sensation seeking | 33.93(8.49) | 28.64(5.62) | 0.006* |

For UPPS impulsivity measures $P < 0.05/4$ was regarded as significant (marked with *) to control for multiple comparison.

7.3.2 Behavioural measures of interference inhibition

Behavioral data are summarized in Table 7-2. The interference effect, i.e. longer RT in the incongruent condition than in the congruent condition, was significant in both BPD patients and HC (BPD: $t(25) = 11.42$, $P < 0.001$, HC: $t(24) = 12.62$, $P < 0.001$), but no significant group difference was found. Both groups also showed more errors when performing incongruent trials relative to congruent trials (BPD: $t(25) = 3.72$, $P = 0.001$, HC: $t(24) = 5.27$, $P < 0.001$), but error ratios on the incongruent trails and congruent trials also did not differ between groups.

EMPIRICAL STUDIES

Table 7-2 Behavioral measures in BPD patients and healthy controls during interference inhibition [mean (SD)]

| | BPD Patients | Healthy controls | P-value |
|--------------------------|----------------------------|-----------------------------|----------------|
| Number | 25 | 26 | |
| Incongruent RT (ms) | 580.81(95.39) ^a | 609.53(104.49) ^a | 0.31 |
| Congruent RT (ms) | 468.22(113.22) | 493.55(120.40) | 0.44 |
| Interference effect (ms) | 112.59(75.93) | 115.99(63.21) | 0.86 |
| Incongruent errors (%) | 12.95(16.38) ^b | 8.93(7.80) ^b | 0.27 |
| Congruent errors (%) | 1.00(1.43) | 1.55(2.38) | 0.33 |

RT = Reaction time

Within group difference (incongruent vs. congruent), $P < 0.05/5$ was regarded as significant (marked with a or b, and Italics).

7.3.3 MRS measures

Table 7-3 GM ratio and GABA levels in BPD patients and healthy controls [mean (SD)]

| Metabolite | BPD patients | Healthy controls | P-value |
|-------------------|---------------------|-------------------------|----------------|
| GM ratio | 0.60(0.04) | 0.60(0.04) | 0.97 |
| GABA (i.u) | 1.67(0.31) | 1.72(0.27) | 0.57 |
| NAA linewidth | 4.91(0.44) | 4.87(0.55) | 0.22 |

GM ratio = GM / (GM + WM), GM = gray matter; WM = white matter;

NAA = N-acetylaspartate

Metabolite data are summarized in Table 7-3. ACC GABA levels were not significantly correlated with participants' age ($r = -0.14$, $P = 0.36$) or GM ratio ($r = -0.19$, $P = 0.19$) in the MRS voxel. Therefore, age and GM ratio were not used as covariates for further group comparisons. GM ratios, ACC GABA levels, and NAA linewidth were not significantly different between the two groups.

7.3.4 BOLD activation

Brain activation associated with interference inhibition was assessed by the BOLD contrast [incongruent go > congruent go]. BPD patients displayed similar activation patterns as HCs during interference inhibition. Both groups demonstrated significant enhanced activations in the key regions of the fronto-striatal network (van Eijk et al., 2015b). No significant group difference was found between the two groups during interference inhibition and the two task conditions.

7.3.5 Functional connectivity (gPPI)

Interference inhibition was assessed by the evaluation of [PPI incongruent go > congruent go]. In HCs the ACC showed greater functional connectivity with the left caudate during incongruent trials relative to congruent trials, whereas significantly less connectivity between the ACC and left caudate (MNI: -10, 13, 4, $t = 4.05$, $P_{\text{FWE_SVC}} = 0.032$) was found in BPD patients. Compared to HCs, BPD patients had less positive task-dependent connectivity changes between ACC and left caudate, indicating that BPD patients had weaker task-dependent ACC-caudate functional connectivity during interference inhibition (see Figure 7-3A).

To further explore by which task condition such connectivity changes are driven, each task condition of interference inhibition was also separately assessed by the contrasts of [PPI incongruent go] and [PPI congruent go]. During the incongruent go condition, in contrast to HCs, BPD patients demonstrated less functional connectivity between the ACC and left caudate (MNI: -10, 14, 3, $t = 4.35$, $P_{\text{FWE_SVC}} = 0.022$) (see Figure 7-3B). There was no group difference in ACC based connectivity during the congruent go condition.

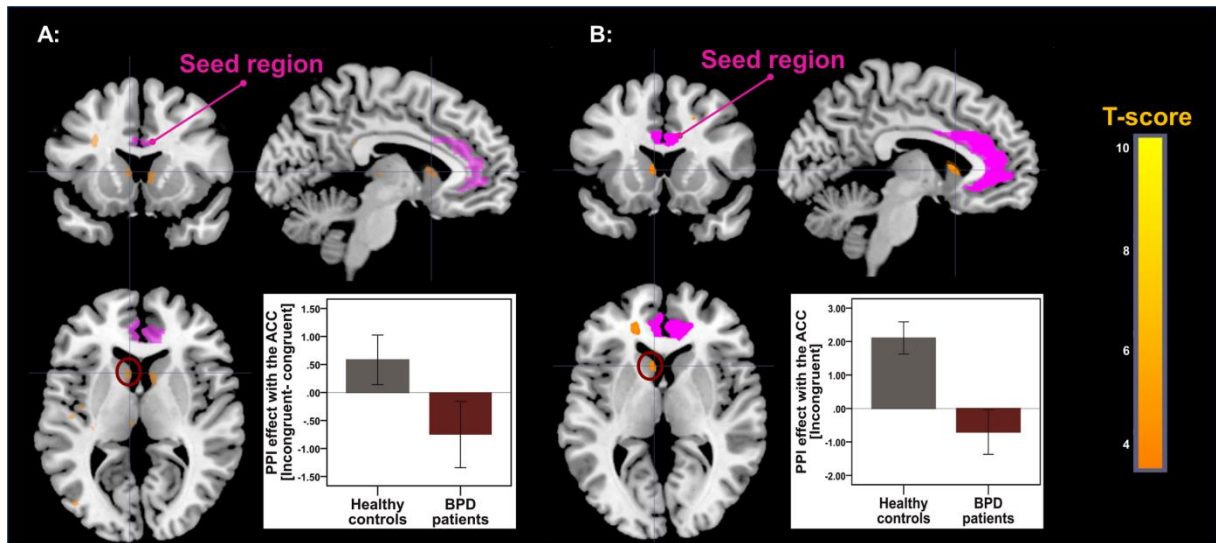


Figure 7-3 Whole-brain analysis of group differences in gPPI effects with the ACC (seed region) A: During interference inhibition [incongruent go – congruent go], significant differences in task-dependent ACC connectivity between BPD patients and healthy controls (HCs) were found in bilateral caudate. B: During the incongruent go condition, significant group differences in ACC connectivity was found in the left caudate. Statistical significance for those parametric maps was set at ($P < 0.001$, uncorrected; cluster size > 10 voxels). The cluster still survived after small volume corrections. For illustration of direction and magnitude of the difference between groups, mean parameter estimates of the PPI effects with the ACC for the significant cluster is plotted by group in bar-graphs.

7.3.6 Correlation Analysis

7.3.6.1 GABA – behavioral interference inhibition & impulsivity

In BPD patients the interference effect was found to be significantly positively correlated with GABA levels in the ACC ($r = 0.58$, $P = 0.005$). Of all the UPPS subscales, the UPPS sensation seeking score in BPD patients was significantly negatively associated with ACC GABA levels ($r = -0.49$, $P = 0.012$). The significance of these correlations still survived after Bonferroni corrections. No significant correlations were found in HCs for these measures (GABA-interference: $r = -0.223$, $P = 0.284$; GABA-UPPS sensation seeking: $r = -0.238$, $P = 0.251$). In addition, there were no significant correlations between any performance measures and UPPS subscores in either HCs or BPD patients.

7.3.6.2 GABA – fMRI (BOLD & Connectivity)

In BPD patients, the main effect of the full factorial analyses yielded several clusters in the fronto-striatal network in which the magnitude of BOLD activation during interference inhibition [incongruent go > congruent go] was positively correlated with ACC GABA levels. These significant clusters include bilateral ACC (L: MNI: -4, 24, 30; $t = 4.44$; $P_{\text{FWE_SVC}} = 0.003$; R: MNI: 4, 12, 24; $t = 4.70$; $P_{\text{FWE_SVC}} < 0.001$), left IFG (L: MNI: -32, 28, -6; $t = 4.75$; $P_{\text{FWE_SVC}} = 0.006$), left DLPFC (L: MNI: -36, 34, 16; $t = 4.82$; $P_{\text{FWE_SVC}} = 0.013$), left putamen (L: MNI: -14, 2, -10; $t = 3.73$; $P_{\text{FWE_SVC}} = 0.02$), left pallidum (L: MNI: -12, 8, -6; $t = 3.76$; $P_{\text{FWE_SVC}} = 0.008$) and bilateral caudate (L: MNI: -10, 6, 6; $t = 4.46$; $P_{\text{FWE_SVC}} = 0.008$; R: MNI: 12, 0, 20; $t = 3.81$; $P_{\text{FWE_SVC}} = 0.016$) (see Figure 7-4A). No significant correlation was found in HCs between ACC GABA levels and BOLD activation in these ROIs. The interaction term suggested that the GABA-BOLD associations did not differ between the groups. To further explore by which task condition (incongruent go or congruent go) the positive correlations are driven, we also performed the same analyses separately for each task condition. Higher ACC GABA levels were positively associated with the magnitude of BOLD activation during the incongruent condition in several regions for both groups, but neither of the groups showed significant correlations during the congruent condition. In addition to BOLD activation, full factorial analyses were also performed between ACC GABA levels and ACC seed based connectivity maps for the contrasts [PPI incongruent go > congruent go, PPI incongruent, PPI congruent]. A significant correlation was only found in BPD patients during the incongruent condition, and the significant cluster located in the bilateral caudate (L: MNI: -16, 24, 0; $t = 4.36$; $P_{\text{FWE_SVC}} = 0.010$; R: MNI: 12, 24, 4; $t = 4.05$; $P_{\text{FWE_SVC}} = 0.024$) in which the magnitude of functional connectivity with the ACC was positively correlated with ACC GABA levels (see Figure 7-4B). The interaction term suggested that the correlation between GABA levels and ACC connectivity with the left caudate (MNI: -18, 12, 20, $t = 3.91$; $P_{\text{FWE_SVC}} = 0.033$) during the incongruent condition was significantly stronger in BPD patients compared to HCs.

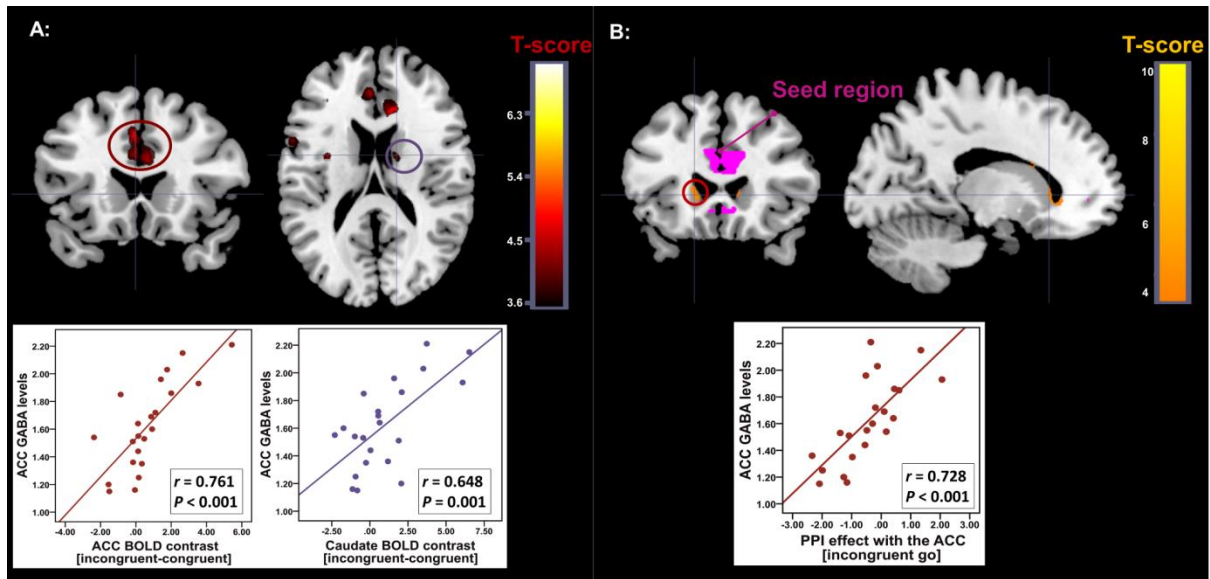


Figure 7-4 Associations of ACC GABA levels with BOLD activation and ACC based functional connectivity during interference inhibition in patients with BPD. A: Statistical parametric map resulting from the main effect of the full factorial model to demonstrate the association between ACC GABA levels (as the covariate of interest) and BOLD contrast [incongruent go > congruent go] in BPD patients. B: Statistical parametric map resulting from the main effect of the full factorial model to demonstrate the association between ACC GABA levels (as the covariate of interest) and the PPI effect [incongruent go] with the ACC in BPD patients. Clusters in those maps represent the significant positive correlation with GABA levels, and statistical significance was set at ($P < 0.001$, uncorrected; cluster size > 10 voxels). The clusters still survived after small volume corrections. Scatterplots illustrate the correlation effects between ACC GABA levels and mean parameter estimates of the BOLD contrast (A) and PPI effects with the ACC (B) for the significant cluster. The color of dots is equal to the highlighted cluster.

7.3.6.3 fMRI (BOLD & Connectivity) – impulsivity

Since the UPPS sensation seeking subscale was the only one significantly related to GABA, we focused on the associations of this subscale and fMRI results. The main effect of the full factorial model suggested that in BPD patients but not in HCs the UPPS sensation seeking score was negatively correlated with the magnitude of activations in the bilateral caudate (L: MNI: -10, 14, 4, $t = 4.45$, $P_{FWE_SVC} = 0.022$; R: MNI: 12, 14, 6; $t = 3.95$, $P_{FWE_SVC} = 0.043$), right DLPFC (MNI: 8, 28, 48, $t = 4.47$, $P_{FWE_SVC} = 0.045$), and right IFG (MNI: 44, 20, 14, $t = 4.7$, $P_{FWE_SVC} = 0.026$) during interference inhibition [incongruent go > congruent go] (see Figure 7-5A). No interaction was found in within-group associations.

EMPIRICAL STUDIES

Regarding the within-group association effect of the ACC seed based connectivity maps and UPPS scores, a significant correlation was found in BPD patients for the UPPS sensation seeking score during the incongruent condition. A unique cluster located in the left caudate (MNI: -18, 10, 24; $t = 4.59$; $P_{FWE_SVC} = 0.005$) in which the magnitude of functional connectivity with ACC during the incongruent condition negatively correlated with ACC GABA levels (see Figure 7-5B). No interaction was found in within-group associations in BPD. In HCs the full factorial analysis did not reveal any significant correlation between ACC based connectivity and UPPS sensation seeking scores as well as the between-group interaction effect.

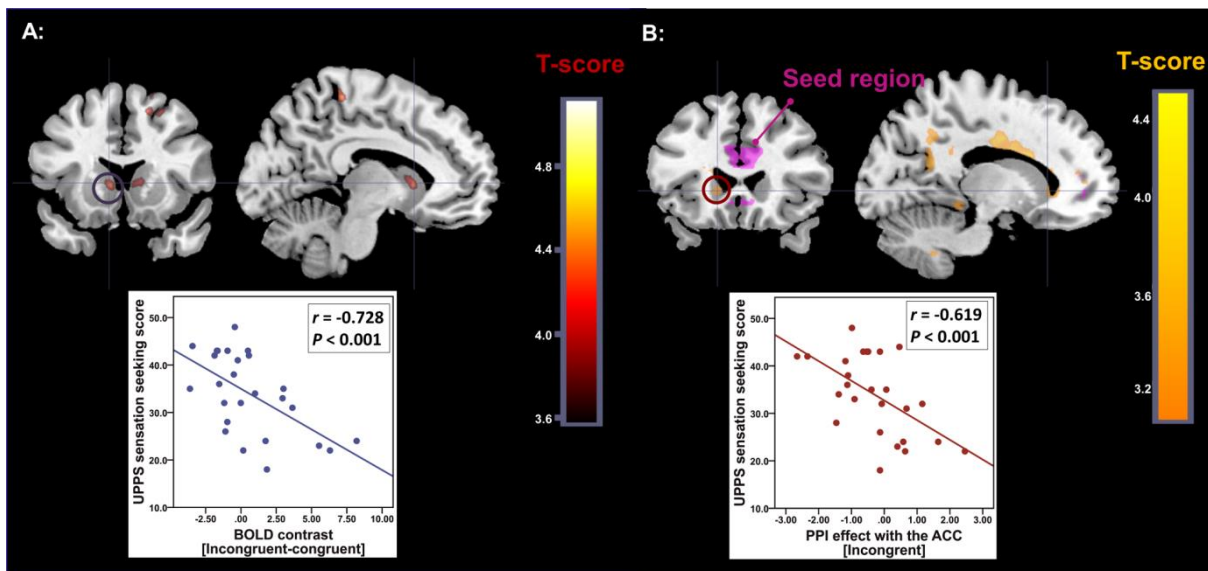


Figure 7-5 Associations of impulsivity scores with BOLD activation and ACC based functional connectivity during interference inhibition in patients with BPD. A: Statistical parametric map resulting from the main effect of the full factorial model to demonstrate the association between UPPS sensation seeking scores (as the covariate of interest) and BOLD contrast [incongruent > congruent] in BPD patients. B: Statistical parametric map resulting from the main effect of the full factorial model to demonstrate the association between the UPPS sensation seeking score (as the covariate of interest) and the PPI effect [incongruent] with the ACC in BPD patients. Clusters in those maps represent the significant negative correlation with GABA levels, and statistical significance was set at ($P < 0.001$, uncorrected; cluster size > 10 voxels) The cluster still survived after small volume corrections. Scatterplots illustrated correlation effects between ACC GABA levels and mean parameter estimates of the BOLD contrast (A) and PPI effects with the ACC (B) for the significant cluster. The color of dots is equal to the highlighted cluster.

7.3.6.4 Mediation analysis (ACC GABA – fronto-striatal- trait impulsivity)

In BPD patients, (see Figure 7-6) ACC GABA levels were negatively correlated with the UPPS sensation seeking score ($\beta = -12.24$, $P = 0.040$), and positively correlated with the magnitude of BOLD activation during interference inhibition [incongruent go > congruent go] in the left caudate ($\beta = 5.75$, $P = 0.004$). BOLD activation in the left caudate during interference inhibition [incongruent go > congruent go] showed a negative correlation with the UPPS sensation seeking score ($\beta = -1.46$, $P = 0.037$). The bootstrapping analysis of the indirect effect revealed a bias-corrected 95% confidence interval excluding zero (%CI = -18.799, -1.998), demonstrating the presence of an indirect effect of ACC GABA levels on impulsive sensation seeking. The direct effect of ACC GABA levels on UPPS sensation seeking score was no longer significant after controlling for BOLD activation in the left caudate during interference inhibition [incongruent go > congruent go] ($\beta = 3.827$, $P = 0.553$), indicating that the caudate activation fully mediates the relationship between ACC GABA levels and impulsive sensation seeking.

Similarly, as described in Figure 7-7, in BPD patients, ACC GABA levels were negatively correlated with the UPPS sensation seeking score ($\beta = -12.24$, $P = 0.040$), and positively correlated with the strength of ACC-left caudate functional connectivity during the incongruent go condition ($\beta = 2.72$, $P < 0.001$). ACC-left caudate connectivity strength showed a negative correlation with the UPPS sensation seeking score ($\beta = -4.27$, $P = 0.036$).

EMPIRICAL STUDIES

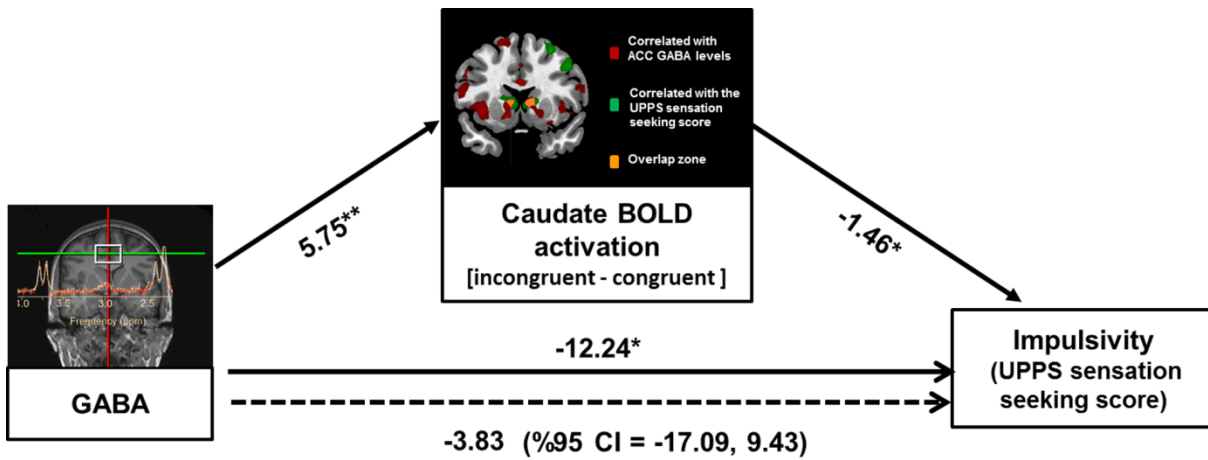


Figure 7-6 The relationship between ACC GABA levels and UPPS sensation seeking in BPD is fully mediated by BOLD activation in the caudate during interference inhibition. Unstandardized regression coefficients and confidence intervals are shown for each path ($P < 0.05^*$, $P < 0.01^{**}$). The clusters in the statistical parametric map represent where the magnitudes of activations have significant correlations with GABA, the UPPS sensation seeking score or both (For illustration, statistical significance was set at $P < 0.005$, uncorrected; cluster size > 10 voxels).

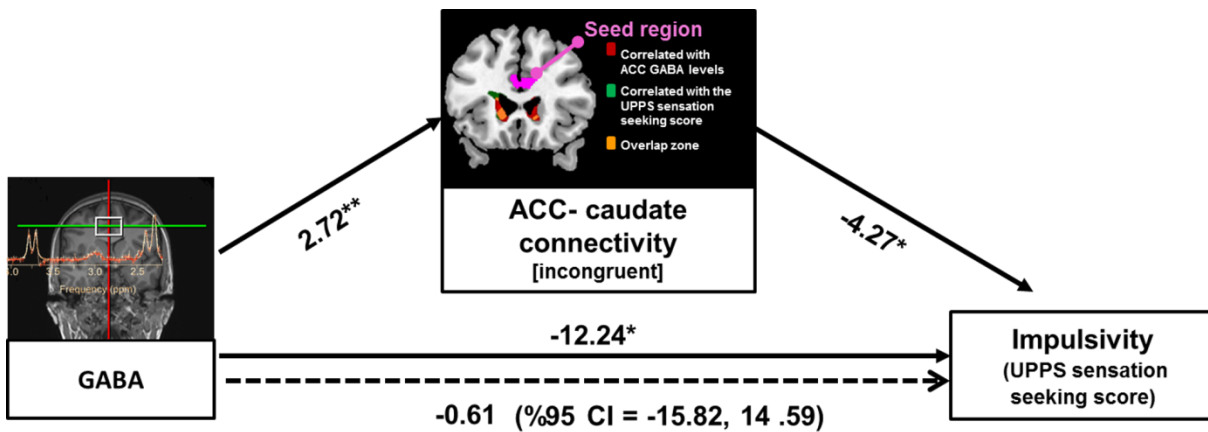


Figure 7-7 The relationship between ACC GABA levels and UPPS sensation seeking in BPD is fully mediated by the strength of ACC-caudate functional connectivity during the incongruent condition. Unstandardized regression coefficients and confidence intervals are shown for each path ($P < 0.05^*$, $P < 0.01^{**}$). Clusters in the statistical parametric map represent where the magnitudes of functional connectivity with the ACC have significant correlations with GABA, the UPPS sensation seeking score or both (For illustration, statistical significance was set at $P < 0.005$, uncorrected; cluster size > 10 voxels).

EMPIRICAL STUDIES

The bootstrapping analysis of the indirect effect revealed a bias corrected 95% confidence interval excluding zero (%CI = -22.473, -2.260), suggesting the presence of an indirect effect of ACC GABA levels on impulsive sensation seeking. The direct effect of ACC GABA levels on the UPPS sensation seeking score, controlling for the strength of ACC-left caudate connectivity, was no longer significant ($\beta = 0.61$, $P = 0.934$), indicating the strength of ACC-caudate connectivity fully mediates the relationship between ACC GABA levels and impulsive sensation seeking. No significant mediation effects were observed in HCs.

7.3.7 Summary of findings in the hierarchical analysis

All of the results in the hierarchical analyses are summarized in Figure 7-8.

Frontal–striatal correlates of interference inhibition in BPD and HC

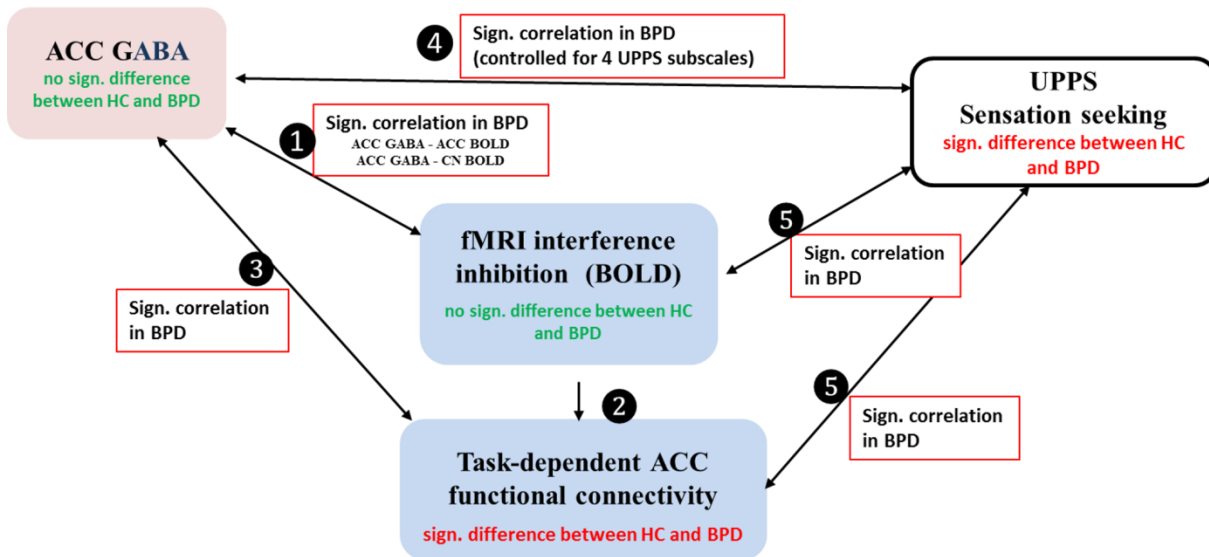


Figure 7-8. The summary of findings in the hierarchical analysis

1. ACC GABA is significantly correlated with BOLD activation in the ACC and bilateral caudate nucleus (CN) during interference inhibition in BPD.
2. Strong functional connectivity between the ACC and CN. Significantly less ACC- left CN connectivity in BPD compared to HCs.
3. Connectivity strength between ACC and bilateral CN is significantly correlated with ACC GABA in BPD.
4. Among all UPPS scales, ACC GABA is only significantly correlated with the UPPS sensation seeking score in BPD
5. UPPS sensation seeking score is also significantly correlated with bilateral CN BOLD activations and ACC- left CN connectivity.
6. Mediation analysis revealed the left CN BOLD and ACC-left CN connectivity served as mediator, mediating the association between GABA and UPPS sensation seeking.

7.4 Discussion

To our knowledge, this is the first study combining fMRI BOLD response as well as functional connectivity with MRS GABA measurements to investigate neurofunctional and neurochemical correlates of interference inhibition, further emphasizing the relationship between these systems, as well as their relation to impulsivity in patients with BPD. There are several novel findings in our study: (1) compared to HCs, BPD patients exhibited weaker fronto-striatal functional connectivity during interference inhibition. (2) Among all the UPPS subscales, ACC GABA levels in BPD patients were only significantly associated with the UPPS sensation seeking score. (3) ACC GABA levels in BPD patients were positively related to the magnitude of activation in several fronto-striatal regions (e.g. caudate, ACC, frontal regions, putamen) and the strength of ACC-caudate functional connectivity during interference inhibition. (4) The magnitude of activation (e.g. caudate, DLPFC, IFC) and ACC-caudate functional connectivity in the fronto-striatal network during inference inhibition was negatively associated with the UPPS sensation seeking score. (5) Consistent with our hypothesis, our results suggest the magnitude of activation in the caudate and the ACC-caudate functional connectivity strength mediate the relationship between ACC GABA levels and impulsive sensation seeking in patients with BPD.

In the present study, BPD patients reported heightened impulsivity scores, and demonstrated weaker ACC-caudate functional connectivity during interference inhibition. The results are consistent with previous findings suggesting disconnectivity of the fronto-striatal network is an important pathological factor contributing to neuropsychiatric disorders associated with impulsive behavior (Cubillo et al., 2010; Delmonte et al., 2013; Harrison et al., 2009b; Marsh et al., 2014). However, notably, although BPD patients have higher impulsivity and alterations in the functional fronto-striatal network, they did not show behavioral performance deficits.

Quantifying relationships between ACC neurochemistry and neural substrates of interference inhibition could aid in identifying neurobiological mechanisms related to higher impulsivity in BPD. Opposite to most previous findings showing ACC GABA levels negatively coupled with task-induced activation (Arrubla et al., 2014; Donahue et al., 2010; Duncan et al., 2014;

EMPIRICAL STUDIES

Hu et al., 2013; Northoff et al., 2007), our study suggests that ACC GABA levels in BPD patients are positively related to conflict-related activation in this area. This contradiction may be due to the different cognitive tasks used, with our study being the first to use an inhibitory control task. In line with our findings, Lipp et al. (2015) also reported a positive correlation between GABA⁺ and fear-related BOLD activation in the insula. Other studies found no correlation between these two measures (Cousijn et al., 2014; Harris et al., 2015). On the other hand, we only found a significant GABA – BOLD association effect in BPD patients, whereas several prior neuroimaging studies have also found significant associations in healthy volunteers (Duncan et al., 2014; Lipp et al., 2015). The discrepancies between our and prior studies are difficult to explain, because different tasks were applied. One possible explanation is that the absence of correlation in our healthy sample results from the heterogeneities in the patterns of brain activations during interference inhibition. Alternatively, the GABA-BOLD association is suggested to increase with cognitive loads (Hu et al., 2013), it is likely that when performing the same task, BPD patients have to maintain performance by engaging more brain resources than HCs.

Results in the present study suggest that ACC GABA levels in BPD patients are not only associated with subsequent task-induced activation itself, but also positively related to activation in other functionally connected fronto-striatal regions (e.g. caudate) during interference inhibition. In combination with our functional connectivity findings, this positive interregional effect may result from local GABAergic interneurons within the ACC modulating long-range excitatory connections to the striatum. Alternatively, this effect could also be mediated by the long-range fronto-striatal GABAergic projection (Caputi et al., 2013; Lee et al., 2014), which have been found in animal models. Until these long-range GABAergic projections can be corroborated in humans, this interpretation needs to be considered with some caution. Thus, our results suggest that the neurotransmitter profile in key regions of a network may affect the whole network activity through functional connectivity. Moreover, in line with the BOLD activation effect, GABA levels also showed a positive correlation with the strength of ACC-caudate functional connectivity. The ACC GABAergic system seems to play a crucial role in modulating the activity and integrity of the fronto-striatal network.

EMPIRICAL STUDIES

Furthermore, in contrast to HCs, BPD patients demonstrated a stronger correlation of GABA levels with ACC-caudate connectivity strength. Although the strength of correlation does not necessarily reflect the extent of the GABA levels impact on the fronto-striatal network, at least, it is implicated that the ACC GABAergic system is very crucial for modulating the functional state of the fronto-striatal network in BPD.

In our prior exploratory MRS study (Ende et al., 2016) ACC GABA is suggested to be important in regulation of impulsivity (evaluated by total scores of Barratt impulsiveness scale (BIS)). Different impulsivity facets are subject to have distinct, occasionally overlapping neurobiological underpinnings (Dalley et al., 2011b; L. Birkley and T. Smith, 2011; Norbury and Husain, 2015; Wilbertz et al., 2014). To extend our observation, impulsivity subscales rather than total score were applied in the present study. Furthermore, the UPPS subscales have been suggested to account for 64% BPD features (Peters et al., 2013) and no such clear information can be found for BIS subscales. Therefore, the UPPS scales possibly have more potential to clarify BPD-related impulsive behaviors.

Among all the UPPS subscales, we found that GABA levels in the ACC were only significantly associated with UPPS sensation seeking score in BPD patients, suggesting that impulsive sensation seeking may have a different neurochemical basis from other forms of impulsivity, and is greatly associated with the GABAergic system in the ACC. This view is supported by previous preclinical research (Weerts et al., 2007), indicating that administration of GABA receptor agonists can attenuate cocaine-sensation seeking behavior in baboons. Consistent with preclinical research, in human studies (for review see (Norbury and Husain, 2015)), impulsive sensation seeking also demonstrated distinct developmental trajectories in contrast to other forms of impulsivity (Harden and Tucker-Drob, 2011; Quinn and Harden, 2013). Only weak or non-significant correlations were found between impulsive sensation seeking and other impulsivity subscores both in healthy subjects and clinical patients (Whiteside and Lynam, 2001).

We did not observe the correlation between the task performance and UPPS scores. However, the missing association between self-report impulsivity and behavioral data is not limited to our study, and several previous studies in BPD as well as in healthy volunteers, and

EMPIRICAL STUDIES

schizophrenia also reported the same non-correlation results (Jacob et al., 2010; Kaladjian et al., 2011; Sebastian et al., 2013a). The plausible explanation is that self-report questionnaires represent impulsivity as a stable trait while behavioral tasks evaluate state-dependent variations. Alternatively, the behavioral performance might be the final outcome of several dimensions of impulsivity traits. Moreover, the fMRI task was not designed to push subjects to work at the limit of their own inhibitory capacity. At a low task demand, BPD patients with higher impulsivity may inhibit successfully by recruiting more brain resource. In this context, it is likely that compared to behavioral measures, the BOLD signal and connectivity changes is a more sensitive index to reflect the resources involved in the task performance. In support of this view, UPPS sensation seeking scores were found to be negatively associated with the BOLD activation and connectivity during interference inhibition. Given that weaker connectivity in BPD patients relative to HCs, our findings suggest that connectivity strength of the fronto-striatal network during the task is reduced in BPD patients with higher impulsivity.

Finally, our findings suggest that the clusters in the fronto-striatal network associated with sensation seeking largely overlap with the clusters associated with ACC GABA levels. The association of GABA and impulsive sensation seeking in BPD patients was found to be mediated by the regional BOLD activation as well as ACC functional connectivity in the fronto-striatal network during interference inhibition. It seems that the fronto-striatal network during inhibitory control mediates the association between ACC GABA levels and impulsivity in patients with BPD. However, it is important to note that the current study was not able to establish causal directions between those variables due to the cross-sectional design.

Although our findings are novel and robust, the present findings have several limitations. First, the current study lacked a control region for the GABA measurement which would be important to determine the anatomical specificity of the effects found in this study. Additionally, given that MRS can only measure the whole GABA pool within a region, it cannot be determined by which neural compartment (e.g. the intracellular or the extra-synaptic GABA pool) our findings were driven. The use of animal models (translational approach) might provide further insight here. We only acquired one GABA value before the

fMRI measurement thus no GABA changes due to behavioral inhibition could be assessed. It would be interesting to assess the neurotransmitter levels and brain activity at the same functional level. A further limitation is that our sample only comprised female BPD patients with relatively typical clinical features, thus we cannot make conclusive inferences for male BPD patients. Besides that, the contribution of co-occurring psychiatric disorders in BPD patients to the neuroimaging findings is still unclear, although ADHD (sharing a lot of clinical feature with BPD) was excluded in this study and no group difference in UPPS sensation seeking scores was found between patients with and without prior substance abuse history. However, co-occurring psychiatric disorders are frequent in the BPD population, and exclusion of any comorbidity would lead to a non-representative patient sample.

7.5 Conclusion

This study emphasizes the additional value of more advanced data analyses to unravel group difference between BPD patients and HCs which could not be detected in the BOLD response and in the ACC GABA levels per se. We could show that task-related functional connectivity and the association of fMRI measures with MRS derived GABA levels are significantly different between the two groups. These analyses give support for a disconnection of the fronto-striatal network during interference inhibition in BPD patients that is related to changes in impulsivity ratings, specifically the UPPS sensation seeking score. These analyses give first evidence for the hypothesis that the fronto-striatal network during inhibitory control serves to mediate the association between ACC GABA levels and impulsivity symptomatology in patients with BPD.

References

- Aron, A.R., Durston, S., Eagle, D.M., Logan, G.D., Stinear, C.M., Stuphorn, V., 2007. Converging evidence for a fronto-basal-ganglia network for inhibitory control of action and cognition. *The Journal of neuroscience : the official journal of the Society for Neuroscience* 27, 11860-11864.
- Arrubla, J., Tse, D.H., Amkreutz, C., Neuner, I., Shah, N.J., 2014. GABA concentration in posterior cingulate cortex predicts putamen response during resting state fMRI. *PloS one* 9, e106609.

EMPIRICAL STUDIES

Attwell, D., Iadecola, C., 2002. The neural basis of functional brain imaging signals. *Trends Neurosci* 25, 621-625.

Aufhaus, E., Weber-Fahr, W., Sack, M., Tunc-Skarka, N., Oberthuer, G., Hoerst, M., Meyer-Lindenberg, A., Boettcher, U., Ende, G., 2013. Absence of changes in GABA concentrations with age and gender in the human anterior cingulate cortex: a MEGA-PRESS study with symmetric editing pulse frequencies for macromolecule suppression. *Magnetic resonance in medicine : official journal of the Society of Magnetic Resonance in Medicine / Society of Magnetic Resonance in Medicine* 69, 317-320.

Bari, A., Robbins, T.W., 2013. Inhibition and impulsivity: behavioral and neural basis of response control. *Prog Neurobiol* 108, 44-79.

Behan, B., Stone, A., Garavan, H., 2015. Right prefrontal and ventral striatum interactions underlying impulsive choice and impulsive responding. *Hum Brain Mapp* 36, 187-198.

Bohus, M., Limberger Mf Fau - Frank, U., Frank U Fau - Chapman, A.L., Chapman Al Fau - Kuhler, T., Kuhler T Fau - Stieglitz, R.-D., Stieglitz, R.D., 2007. Psychometric properties of the Borderline Symptom List (BSL).

Botvinick, M.M., Cohen, J.D., Carter, C.S., 2004. Conflict monitoring and anterior cingulate cortex: an update. *Trends Cogn Sci* 8, 539-546.

Braver, T.S., Barch, D.M., Gray, J.R., Molfese, D.L., Snyder, A., 2001. Anterior cingulate cortex and response conflict: effects of frequency, inhibition and errors. *Cereb Cortex* 11, 825-836.

Brown, M.R., Benoit, J.R., Juhas, M., Lebel, R.M., MacKay, M., Dametto, E., Silverstone, P.H., Dolcos, F., Dursun, S.M., Greenshaw, A.J., 2015. Neural correlates of high-risk behavior tendencies and impulsivity in an emotional Go/NoGo fMRI task. *Front Syst Neurosci* 9, 24.

Caputi, A., Melzer, S., Michael, M., Monyer, H., 2013. The long and short of GABAergic neurons. *Curr Opin Neurobiol* 23, 179-186.

Courtney, K.E., Ghahremani, D.G., Ray, L.A., 2013. FRONTO-STRIATAL FUNCTIONAL CONNECTIVITY DURING RESPONSE INHIBITION IN ALCOHOL DEPENDENCE. *Addiction biology* 18, 593-604.

Cubillo, A., Halari, R., Ecker, C., Giampietro, V., Taylor, E., Rubia, K., 2010. Reduced activation and inter-regional functional connectivity of fronto-striatal networks in adults with childhood Attention-Deficit Hyperactivity Disorder (ADHD) and persisting symptoms during tasks of motor inhibition and cognitive switching. *J Psychiatr Res* 44, 629-639.

Dalley, J.W., Mar, A.C., Economidou, D., Robbins, T.W., 2008. Neurobehavioral mechanisms of impulsivity: fronto-striatal systems and functional neurochemistry. *Pharmacol Biochem Behav* 90, 250-260.

Delmonte, S., Gallagher, L., O'Hanlon, E., McGrath, J., Balsters, J.H., 2013. Functional and structural connectivity of frontostriatal circuitry in Autism Spectrum Disorder. *Frontiers in Human Neuroscience* 7, 430.

EMPIRICAL STUDIES

- DeVito, E.E., Meda, S.A., Jiantonio, R., Potenza, M.N., Krystal, J.H., Pearlson, G.D., 2013. Neural correlates of impulsivity in healthy males and females with family histories of alcoholism. *Neuropsychopharmacology* 38, 1854-1863.
- Dharmadhikari, S., Ma, R., Yeh, C.L., Stock, A.K., Snyder, S., Zauber, S.E., Dydak, U., Beste, C., 2015. Striatal and thalamic GABA level concentrations play differential roles for the modulation of response selection processes by proprioceptive information. *NeuroImage* 120, 36-42.
- Ding, W.N., Sun, J.H., Sun, Y.W., Chen, X., Zhou, Y., Zhuang, Z.G., Li, L., Zhang, Y., Xu, J.R., Du, Y.S., 2014. Trait impulsivity and impaired prefrontal impulse inhibition function in adolescents with internet gaming addiction revealed by a Go/No-Go fMRI study. *Behav Brain Funct* 10, 20.
- Donahue, M.J., Near, J., Blicher, J.U., Jezzard, P., 2010. Baseline GABA concentration and fMRI response. *NeuroImage* 53, 392-398.
- Duncan, N.W., Wiebking, C., Northoff, G., 2014. Associations of regional GABA and glutamate with intrinsic and extrinsic neural activity in humans-a review of multimodal imaging studies. *Neurosci Biobehav Rev* 47, 36-52.
- Ende, G., X., A.-O., Cackowski, S., Van Eijk, J., Sack, M., Demirakca, T., Kleindienst, N., Bohus, M., Sobanski, E., Krause-Utz, A., Schmahl, C., 2015. Impulsivity and Aggression in Female BPD and ADHD Patients: Association with ACC Glutamate and GABA Concentrations. *LID* - 10.1038/npp.2015.153 [doi].
- First, M., Spitzer, R., Gibbon, M., Williams, J.B., 1997. Structured Clinical Interview for DSM-IV® Axis I Disorders (SCID-I), Clinician Version, User's Guide. American Psychiatric Press, Washington, DC.
- Grant, J.E., Kim, S.W., 2014. Brain circuitry of compulsivity and impulsivity. *CNS spectrums* 19, 21-27.
- Harden, K.P., Tucker-Drob, E.M., 2011. Individual differences in the development of sensation seeking and impulsivity during adolescence: further evidence for a dual systems model.
- Harrison, B.J., Soriano-Mas, C., Pujol, J., et al., 2009a. ALtered corticostriatal functional connectivity in obsessive-compulsive disorder. *Archives of General Psychiatry* 66, 1189-1200.
- Harrison, B.J., Soriano-Mas, C., Pujol, J., Ortiz, H., Lopez-Sola, M., Hernandez-Ribas, R., Deus, J., Alonso, P., Yucel, M., Pantelis, C., Menchon, J.M., Cardoner, N., 2009b. Altered corticostriatal functional connectivity in obsessive-compulsive disorder. *Arch Gen Psychiatry* 66, 1189-1200.
- Hayes, D.J., Jupp, B., Sawiak, S.J., Merlo, E., Caprioli, D., Dalley, J.W., 2014. Brain gamma-aminobutyric acid: a neglected role in impulsivity. *Eur J Neurosci* 39, 1921-1932.
- Holtmann, J., Herbort, M.C., Wustenberg, T., Soch, J., Richter, S., Walter, H., Roepke, S., Schott, B.H., 2013. Trait anxiety modulates fronto-limbic processing of emotional interference in borderline personality disorder. *Front Hum Neurosci* 7, 54.
- Horn, N.R., Dolan, M., Elliott, R., Deakin, J.F., Woodruff, P.W., 2003. Response inhibition and impulsivity: an fMRI study. *Neuropsychologia* 41, 1959-1966.

EMPIRICAL STUDIES

Hu, Y., Chen, X., Gu, H., Yang, Y., 2013. Resting-state glutamate and GABA concentrations predict task-induced deactivation in the default mode network. *The Journal of neuroscience : the official journal of the Society for Neuroscience* 33, 18566-18573.

Jahfari, S., Waldorp L Fau - van den Wildenberg, W.P.M., van den Wildenberg Wp Fau - Scholte, H.S., Scholte Hs Fau - Ridderinkhof, K.R., Ridderinkhof Kr Fau - Forstmann, B.U., Forstmann, B.U., 2011. Effective connectivity reveals important roles for both the hyperdirect (fronto-subthalamic) and the indirect (fronto-striatal-pallidal) fronto-basal ganglia pathways during response inhibition.

Kaladjian, A., Jeanningros, R., Azorin, J.M., Anton, J.L., Mazzola-Pomietto, P., 2011. Impulsivity and neural correlates of response inhibition in schizophrenia. *Psychological medicine* 41, 291-299.

Kerns, J.G., Cohen, J.D., MacDonald, A.W., 3rd, Cho, R.Y., Stenger, V.A., Carter, C.S., 2004. Anterior cingulate conflict monitoring and adjustments in control. *Science* 303, 1023-1026.

Kuhn, S., Schubert, F., Mекle, R., Wenger, E., Ittermann, B., Lindenberger, U., Gallinat, J., 2015. Neurotransmitter changes during interference task in anterior cingulate cortex: evidence from fMRI-guided functional MRS at 3 T.

L. Birkley, E., T. Smith, G., 2011. Recent Advances in Understanding the Personality Underpinnings of Impulsive Behavior and their Role in Risk for Addictive Behaviors. *Current Drug Abuse Reviewse* 4, 215-227.

Lee, A.T., Vogt, D., Rubenstein, J.L., Sohal, V.S., 2014. A class of GABAergic neurons in the prefrontal cortex sends long-range projections to the nucleus accumbens and elicits acute avoidance behavior. *The Journal of neuroscience : the official journal of the Society for Neuroscience* 34, 11519-11525.

Logothetis, N.K., 2002. The neural basis of the blood-oxygen-level-dependent functional magnetic resonance imaging signal. *Philosophical Transactions of the Royal Society B: Biological Sciences* 357, 1003-1037.

Logothetis, N.K., Pauls, J., Augath, M., Trinath, T., Oeltermann, A., 2001. Neurophysiological investigation of the basis of the fMRI signal. *Nature* 412, 150-157.

Loranger, A.W., 1999. *International Personality Disorder Examination (IPDE): DSMIV and ICD-10 Modules*. Psychological Assessment Resources, Odessa, FL.

Marsh, R., Horga, G., Parashar, N., Wang, Z., Peterson, B.S., Simpson, H.B., 2014. Altered Activation in Fronto-Striatal Circuits During Sequential Processing of Conflict in Unmedicated Adults with Obsessive-Compulsive Disorder. *Biological Psychiatry* 75, 615-622.

McLaren, D.G., Ries, M.L., Xu, G., Johnson, S.C., 2012. A generalized form of context-dependent psychophysiological interactions (gPPI): a comparison to standard approaches. *NeuroImage* 61, 1277-1286.

Minzenberg, M.J., Lesh, T.A., Niendam, T.A., Cheng, Y., Carter, C.S., 2015. Conflict-Related Anterior Cingulate Functional Connectivity Is Associated With Past Suicidal Ideation and Behavior in Recent-Onset Psychotic Major Mood Disorders.

EMPIRICAL STUDIES

- Muthukumaraswamy, S.D., Edden, R.A., Jones, D.K., Swettenham, J.B., Singh, K.D., 2009. Resting GABA concentration predicts peak gamma frequency and fMRI amplitude in response to visual stimulation in humans. *Proc Natl Acad Sci U S A* 106, 8356-8361.
- Norbury, A., Husain, M., 2015. Sensation-seeking: Dopaminergic modulation and risk for psychopathology. *Behavioural Brain Research* 288, 79-93.
- Northoff, G., Walter, M., Schulte, R.F., Beck, J., Dydak, U., Henning, A., Boeker, H., Grimm, S., Boesiger, P., 2007. GABA concentrations in the human anterior cingulate cortex predict negative BOLD responses in fMRI. *Nat Neurosci* 10, 1515-1517.
- Olson, S.L., Bates, J.E., Sandy, J.M., Schilling, E.M., 2002. Early developmental precursors of impulsive and inattentive behavior: from infancy to middle childhood. *J Child Psychol Psychiatry* 43, 435-447.
- Olson, S.L., Schilling, E.M., Bates, J.E., 1999. Measurement of Impulsivity: Construct Coherence, Longitudinal Stability, and Relationship with Externalizing Problems in Middle Childhood and Adolescence. *Journal of Abnormal Child Psychology* 27, 151-165.
- Orr, J.M., Weissman, D.H., 2009. Anterior cingulate cortex makes 2 contributions to minimizing distraction. *Cereb Cortex* 19, 703-711.
- Ortin, A., Lake, A.M., Kleinman, M., Gould, M.S., 2012. Sensation Seeking as Risk Factor for Suicidal Ideation and Suicide Attempts in Adolescence. *Journal of affective disorders* 143, 214-222.
- Paine, T.A., Slipp, L.E., Carlezon, W.A., Jr., 2011. Schizophrenia-like attentional deficits following blockade of prefrontal cortex GABAA receptors. *Neuropsychopharmacology* 36, 1703-1713.
- Peters, J.R., Upton Bt Fau - Baer, R.A., Baer, R.A., 2013. Brief report: relationships between facets of impulsivity and borderline personality features.
- Quetscher, C., Yildiz, A., Dharmadhikari, S., Glaubitz, B., Schmidt-Wilcke, T., Dydak, U., Beste, C., 2015. Striatal GABA-MRS predicts response inhibition performance and its cortical electrophysiological correlates. *Brain structure & function* 220, 3555-3564.
- Quinn, P.D., Harden, K.P., 2013. Differential changes in impulsivity and sensation seeking and the escalation of substance use from adolescence to early adulthood. *Dev Psychopathol.* 25(1), 223-239.
- Sampaio-Baptista, C., Filippini, N., Stagg, C.J., Near, J., Scholz, J., Johansen-Berg, H., 2015. Changes in functional connectivity and GABA levels with long-term motor learning. *NeuroImage* 106, 15-20.
- Schilling, C., Kuhn, S., Romanowski, A., Schubert, F., Kathmann, N., Gallinat, J., 2012. Cortical thickness correlates with impulsiveness in healthy adults. *NeuroImage* 59, 824-830.
- Schmidt, R.E., Gay, P., d'Acremont, M., Van der Linden, M., 2008. A German Adaptation of the UPPS Impulsive Behavior Scale: Psychometric Properties and Factor Structure. *Swiss Journal of Psychology* 67, 107-112.
- Sebastian, A., Jung, P., Krause-Utz, A., Lieb, K., Schmahl, C., Tüscher, O., 2014. Frontal Dysfunctions of Impulse Control – A Systematic Review in Borderline Personality Disorder and Attention-Deficit/Hyperactivity Disorder. *Frontiers in Human Neuroscience* 8, 698.

EMPIRICAL STUDIES

Sebastian, A., Pohl, M.F., Kloppel, S., Feige, B., Lange, T., Stahl, C., Voss, A., Klauer, K.C., Lieb, K., Tuscher, O., 2013. Disentangling common and specific neural subprocesses of response inhibition. *NeuroImage* 64, 601-615.

Silveri, M.M., Sneider, J.T., Crowley, D.J., Covell, M.J., Acharya, D., Rosso, I.M., Jensen, J.E., 2013. Frontal lobe gamma-aminobutyric acid levels during adolescence: associations with impulsivity and response inhibition. *Biol Psychiatry* 74, 296-304.

Sofuoglu, M., Mouratidis, M., Yoo, S., Culligan, K., Kosten, T., 2005. Effects of tiagabine in combination with intravenous nicotine in overnight abstinent smokers. *Psychopharmacology (Berl)* 181, 504-510.

Tekin, S., Cummings, J.L., 2002. Frontal-subcortical neuronal circuits and clinical neuropsychiatry: an update. *Journal of psychosomatic research* 53, 647-654.

van Eijk, J., Sebastian, A., Krause-Utz, A., Cackowski, S., Demirakca, T., Biedermann, S.V., Lieb, K., Bohus, M., Schmahl, C., Ende, G., Tuscher, O., 2015. Women with borderline personality disorder do not show altered BOLD responses during response inhibition. *Psychiatry Res.*

Weber-Fahr, W., Ende, G., Braus, D.F., Bachert, P., Soher, B.J., Henn, F.A., Buchel, C., 2002. A fully automated method for tissue segmentation and CSF-correction of proton MRSI metabolites corroborates abnormal hippocampal NAA in schizophrenia. *NeuroImage* 16, 49-60.

Weerts, E.M., Froestl, W., Kaminski, B.J., Griffiths, R.R., 2007. Attenuation of cocaine-seeking by GABA(B) receptor agonists baclofen and CGP44532 but not the GABA reuptake inhibitor tiagabine in baboons. *Drug and alcohol dependence* 89, 206-213.

Whiteside, S.P., Lynam, D.R., 2001. The Five Factor Model and impulsivity: using a structural model of personality to understand impulsivity. *Personality and Individual Differences* 30, 669-689.

Wilbertz, T., Deserno, L., Horstmann, A., Neumann, J., Villringer, A., Heinze, H.J., Boehler, C.N., Schlagenhaut, F., 2014. Response inhibition and its relation to multidimensional impulsivity. *NeuroImage* 103, 241-248.

Wingenfeld, K., Rullkoetter, N., Mensebach, C., Beblo, T., Mertens, M., Kreisel, S., Toepper, M., Driessen, M., Woermann, F.G., 2009. Neural correlates of the individual emotional Stroop in borderline personality disorder. *Psychoneuroendocrinology* 34, 571-586.

Wittchen, H., Wunderlich, U., Gruschwitz, S., Zaudig, M., 1997. *StrukturiertesKlinisches Interview für DSM-IV Achse I*. Hogrefe, Göttingen (Germany).

Statement of Contribution

In this study, I was responsible for all the data analysis including fMRI data pre-processing (BOLD activation and functional connectivity analysis), voxel-wise correlation analysis for the multimodal imaging data (MRS & fMRI), and the mediation analysis. I did the according

EMPIRICAL STUDIES

literature research and study, and was responsible for the conceptual design and wrote the manuscript.

CHAPTER III.
GENERAL DISCUSSION

8 General discussion

In the following sections, a general discussion is presented, including a brief summary of the main findings and related considerations. Current limitations and possible directions for future research are also included.

8.1 Brain recovery during early alcohol abstinence

8.1.1 Summary of the findings

Alcohol dependence as a prevalent mental disorder causes a widespread and multifocal system alteration in the brain, with a potential to partially recover during abstinence. In this project, we investigated the morphology and brain chemistry changes during the first two weeks of abstinence in ADPs. Moreover, we were the first to report of how the ‘hyperglutamatergic state’ induced by withdrawal impacts on hippocampal GM volume during abstinence. This project consists of two studies (corresponding to the first two empirical studies in the Chapter II) .

In the first study, one aim was to explore the nature of abstinence-induced cortical volume recovery observed in our preliminary VBM investigation (van Eijk et al., 2013). The FreeSurfer results suggest that the cortical volume regains is predominantly driven by an increase in CTh during early abstinence, while no longitudinal changes in SA were observed. Additionally, we found that the CTh reduction was more pronounced in sulci than gyri among the affected regions. A greater thickness recovery was observed in the sulcal part of affected areas than the gyral part, particular evident in frontal regions. Taken together, our findings suggest that sulci are more vulnerable to excessive alcohol consumption and abstinence-induced recovery.

In addition to cortical areas, another aim was to corroborate our previous VBM finding that no subcortical regions (e.g. hippocampus) showed volume regains within the first two weeks of abstinence (van Eijk et al., 2013). In this study, with a more precise subcortical segmentation method (FreeSurfer), the reanalysis results are in line with the VBM findings.

GENERAL DISCUSSION

We found ADPs at day 1 of abstinence had significantly lower subcortical volumes than HCs in most reward system regions, including putamen, nucleus accumbens, amygdala, and hippocampus. But none of them demonstrated volume regains after abstinence. Thereby, one may conclude that the alcohol-induced shrinkage of subcortical structures is likely to be non-reversible by short-term abstinence.

However, important to note, we found inconsistent results of ‘alcohol-induced hippocampus reduction’ generated by VBM (in SPM) and FreeSurfer. Significant lower hippocampal volumes were found in ADPs relative to HCs for both time points with FreeSurfer (Wang et al., 2016), whereas no group differences were observed using VBM (Frischknecht et al.; van Eijk et al., 2013). These disparate results may due to differences in segmentation algorithms and statistical inference methods applied in VBM versus FreeSurfer (Rajagopalan et al., 2014). It seems that FreeSurfer is more sensitive for GM atrophy detection and in good concordance with other studies suggesting lower volumes of hippocampus in ADPs and abstainers with 12 months abstinence (Durazzo et al., 2011; Sullivan et al., 2005b).

In addition to a whole-brain morphological analysis, the hippocampus was of particular interest in this project. This is due to that the hippocampus is not only a region where volume loss is often caused from alcohol itself, but also is rich in glutamatergic innervation and vulnerable to Glu-excitotoxicity. Therefore, MRS and MRI of the hippocampus were performed investigating a human sample and a comparable rat model (the second study).

In the second study, our rat model demonstrated elevated Glu/Gln ratios during acute withdrawal (12h and 60h after stopping alcohol intake) and a trend for an increase in Glu levels at 12h compared to control rats, in support of a ‘hyper glutamatergic state’ induced by withdrawal. However, different from the previous human MRS findings (Hermann et al., 2012a), no group differences in Glu and Glx levels were observed either between ADPs and HCs or between two time points during the first two weeks of abstinence. This inconsistency might due to the unreliability of the separation of hippocampal Glu and Gln peaks in the 3T scanner. The constant Glx value may result from an opposite changes in Glu and Gln levels by a comparable extent. This interpretation is supported by our exploratory analysis of Glx in animals, where no difference during withdrawal could be observed.

GENERAL DISCUSSION

The main novel finding was that in both species a negative association was found between Glu markers (Glx and Glu/Gln ratios) and GM volume in the hippocampus after alcohol withdrawal (but not during withdrawal itself), suggesting that this tissue damage is a consequence of withdrawal rather than of chronic alcohol intoxication, caused by withdrawal-induced hyperglutamatergic neurotoxicity. In support of our interpretation, one clinical finding suggests that hippocampal volume reductions after alcohol withdrawal were associated with alcohol withdrawal severity (Barnes et al., 2010).

Last, we found lower NAA levels in the hippocampus during withdrawal which normalized within two weeks of abstinence in humans and after a few hours in the rat model. Notably, this NAA normalization phenomenon was not observed in ADPs who had severe withdrawal symptoms treated with benzodiazepine, in this subgroup the statistically significant differences still persist after 2 weeks of abstinence. The findings suggest that severe withdrawal may cause a prolonged impairment of neuronal integrity, and also gives a potential explanation for the mixed findings with regard to NAA reduction in abstinent ADPs (Ende et al., 2005; Meyerhoff et al., 2013).

8.1.2 Limitation

Aside from the major strengths of the study, some limitations also should be discussed. The most challenging work of this project is to do the successful MR measurement for the ADPs during acute alcohol withdrawal. During this period, the physical symptoms of CNS hyperexcitability, such as tremor, restlessness, high blood pressure, increased heart rate, makes it difficult for ADPs to cooperate when they are in the scanner. This is reflected by increased movements compromising the quality of the MR spectra.

Moreover, as indicated by the morphometric results using the two different approaches (VBM, FreeSurfer) (van Eijk et al., 2013; Wang et al., 2016), VBM has been found to be not sensitive enough to detect the disease associated subcortical volume changes. This should be taken into consideration in future studies.

8.1.3 Outlook

The present work adds knowledge about biological mechanisms underlying brain recovery during the first two weeks of abstinence. Yet these developments prompt a series of research questions, which are supposed to be addressed in future studies:

1) In addition to the Glu system, GABA has been also shown to play a crucial role in neuroadaptations during alcohol dependence and withdrawal. Are there dynamically changes in ADPs during withdrawal and abstinence? Does GABA also normalize after short term of abstinence? Is it also related to brain volume recovery during abstinence?

2) The learning theory (Grusser et al., 2004) postulates that increased reactivity to alcohol-related cues is a major precipitator of craving and relapse, thereby helping to maintain addictive behaviours. Do brain functions related to cue reactivity also show partial recovery during abstinence? Does the neurochemical adaptations induced by withdrawal also influence on this protracted altered cue-related activity in abstinent ADPs?

8.2 Biological mechanisms underlying impulsivity in BPD

8.2.1 Summary of the findings

This study emphasized the additional value of multimodal imaging analyses to unravel group difference between BPD patients and HCs which could not be detected by the BOLD response and the ACC GABA levels per se (Ende et al., 2015a; van Eijk et al., 2015a). The superior aim was to explore the interrelationship between GABA, neural correlates of interference inhibition, and impulsivity traits in BPD. Moreover, the hierarchical analyses was applied to test the hypothesis that the fronto-striatal network during inhibitory control serves to mediate the association between ACC GABA levels and impulsivity symptomatology in patients with BPD. There are several novel findings in this study.

In our study, ACC GABA levels in BPD are positively correlated with BOLD activation in the ACC and bilateral caudate during interference inhibition, suggesting that GABA levels in the ACC are not only associated with subsequent task-induced activation itself, but also

GENERAL DISCUSSION

related to activation in other functionally connected fronto-striatal regions (e.g. caudate) during interference inhibition.

In order to confirm our assumption that the ACC GABA levels are also related to activation in the caudate due to the functional interaction between those two regions during interference inhibition, we applied the gPPI method to quantify the task-dependent functional connectivity. We found strong functional connectivity between the ACC and caudate during the task. Notably, in contrast to HCs, BPD patients demonstrated weaker ACC-caudate connectivity during interference inhibition. These results are in agreement with previous findings suggesting that a disconnectivity of the fronto-striatal network is an important pathological factor contributing to neuropsychiatric disorders associated with impulsive behavior (Cubillo et al., 2010; Delmonte et al., 2013; Harrison et al., 2009b; Marsh et al., 2014). In support of this view, we found that the weaker the functional connectivity between the ACC and caudate, the higher are the sensation seeking scores reported by BPD patients.

Moreover, in line with the BOLD activation effect, GABA levels in the ACC also showed a positive correlation with the strength of ACC-caudate functional connectivity. Furthermore, compared to HCs, BPD patients demonstrated a stronger correlation of GABA levels with ACC-caudate connectivity strength. Taken together, the ACC GABAergic system seems to play a crucial role in modulating the activity and integrity of the fronto-striatal network during interference inhibition.

However, it is important to mention that in contrast to most previous studies our work found that ACC GABA was positively correlated with the BOLD response and functional connectivity strength. Our findings not only add an important supporting evidence but also extend the idea brought out in previous studies (Lipp et al., 2010), that it is probably oversimplified to conclude that more GABA infers more inhibition and results in less BOLD response as well as weaker connectivity. In line with our results, Lipp et al. (2010) also found positive correlations between GABA and fear-related BOLD response. Moreover, more recently, there are two studies which found no correlation between those two measures (Cousijn et al., 2014; Harris et al., 2015).

GENERAL DISCUSSION

In addition, to extend our prior exploratory MRS observation (Ende et al., 2016) that ACC GABA is important in regulation of impulsivity (evaluated by total scores of Barratt impulsiveness scale (BIS)), in this study we tested which impulsivity facets (evaluated by UPPS subscales) are associated with GABA. We found that among all UPPS scales ACC GABA was only significantly correlated with the UPPS sensation seeking score in BPD patients, suggesting that impulsive sensation seeking may have a different neurochemical basis from other forms of impulsivity, and is greatly associated with the GABAergic system in the ACC.

Finally, our findings suggest that the clusters in the fronto-striatal network associated with sensation seeking largely overlap with the clusters associated with ACC GABA levels. Mediation analysis revealed that the left caudate BOLD and ACC-left caudate connectivity served as mediator, mediating the association between GABA and UPPS sensation seeking. Thus, based on the above findings, we may conclude that GABAergic transmission in the ACC drives the inhibitory-related fronto-striatal brain network, where the disruption of fronto-striatal connectivity is of core relevance to the sensation seeking symptom in BPD patients.

8.2.2 Limitations

Although our findings are novel and robust, there are still several limitations in the present study. One limitation of this study is the unspecificity of GABA MRS signals. Because MRS can only measure the whole GABA pool within a region, it cannot be determined by which neural compartment (e.g. the intracellular or the extra-synaptic GABA pool) our findings were driven. So, it does not necessarily relate to GABA transmission. Additionally, the present work lacked a control region for the GABA measurement which would be important to clarify the region specificity of the effects found in this study. On the other hand, our GABA MRS measurement is acquired before the fMRI measurement, thus, we cannot rule out that the interference inhibition paradigm had an effect on the GABA concentration, potentially also influencing the relationship between GABA levels and BOLD responses or connectivity. Recently, a few studies have suggested that GABA may change by experimental task (Kuhn et al., 2011; Michels et al., 2012). Therefore, in future, it would be better to

GENERAL DISCUSSION

measure the MRS and fMRI at the same functional level, and functional MRS could be considered. Regarding the experimental design, our mediation analysis was not able to establish causal directions between those variables due to the cross-sectional design. Therefore, the use of animal models (translational approach) or administration of GABA related medication might provide further insight here.

8.2.3 Future directions

The current understanding is that the BOLD signal is a measure of a certain region, resulting from the balanced proportional changes in excitation-inhibition activity (Logothetis, 2008). This means whether GABA transmission leads to an increased or decreased BOLD response also depends on the excitatory transmission (e.g. Glu). In particular, glutamatergic signaling in the fronto-striatal network has shown to be closely associated with impulsive and compulsive behavior (Naaijen et al., 2015). Therefore, in future, analysis of GABA and excitatory neurotransmitters (e.g. Glu), might provide a more comprehensive picture of the relationship between brain neurochemistry and BOLD response.

It was previously shown that the resting/baseline neural activity/blood flow levels are the important factors contributing to task-induced BOLD changes (Northoff et al., 2010). For example, when baseline CBF is increased, task-related BOLD responses become slower and weaker, whereas downregulating baseline CBF can give rise to the opposite effect (Cohen et al., 2002). So we assume that the resting state fMRI BOLD signal or the resting state arterial spin labeling (ASL) signal might mediate the association effect between resting GABA levels and task-induced BOLD signal in the current study. This potential mediator for the task-induced BOLD response is missing in this study and should be included in future studies.

9 Summary

The present doctoral thesis focused on the multimodal imaging investigation of brain mechanisms in neuropsychiatric disorders, emphasizing on the research questions of whether and how neurochemistry is associated with brain anatomical structures and brain functions. The aim of the thesis is to provide a biochemical insight underlying the altered brain morphology and functions in the two disorders studied, which might ultimately offer evidence for novel therapeutic implications. There are two brain imaging projects included in this thesis.

In project I, the first aim was to explore the mechanism of partial volume recovery during the first two weeks of abstinence from alcohol at a whole-brain level. The hippocampus was then chosen as a seed region, to investigate the abstinence-induced neurochemical changes and whether the hyperglutamatergic state induced by alcohol withdrawal may affect GM volume recovery in the hippocampus. We found cortical thickness alteration corresponds to the partial cortical volumetric recovery. Moreover, alcohol differentially impacts on sulci and gyri of the neocortex. Sulci are more susceptible to excessive alcohol consumption and abstinence-induced recovery. Lower subcortical volume was found in alcohol dependent patients at withdrawal, and no subcortical volume regain was observed during the initial two weeks of abstinence. In support of a ‘hyperglutamatergic state’ induced by withdrawal, our rat model demonstrated elevated Glu/Gln ratios during acute withdrawal (12h and 60h after stopping alcohol intake) and a trend towards an increase in Glu levels at 12h compared to control rats. The main novel finding of this study was that in both species a negative association was found between Glu markers and GM volume in the hippocampus after alcohol withdrawal (but not during withdrawal), suggesting that this tissue damage is a consequence of withdrawal and results from withdrawal-induced hyperglutamatergic neurotoxicity.

In project II, the study emphasized the additional value of multimodal imaging analyses to unravel group differences between BPD patients and HCs which could not be detected by BOLD response and ACC GABA levels per se. The superior aim was to explore the interrelationship between GABA, neural correlates of interference inhibition, and impulsivity traits in BPD. We found task-related functional connectivity and the association of fMRI

measures with MRS derived GABA levels are significantly different between the two groups. These analyses give support for a disconnection of the fronto-striatal network during interference inhibition in BPD patients that is related to elevated impulsivity ratings, specifically the UPPS sensation seeking score. Our hierarchical analyses also give first evidence for the hypothesis that the fronto-striatal network during inhibitory control serves to mediate the association between ACC GABA levels and impulsivity symptomatology in patients with BPD. In other words, GABAergic transmission in the ACC drives the inhibitory-related fronto-striatal brain network, whereas the disruption of fronto-striatal connectivity is of core relevance to the sensation seeking symptom in BPD patients.

Taken together, multimodal imaging fusion analysis of neurobiochemistry - structure/function relationship can offer opportunities to deepen our understanding of neurobiological mechanism of brain disorders.

10 Reference

- Aoki, Y., Abe, O., Yahata, N., Kuwabara, H., Natsubori, T., Iwashiro, N., . . . Yamasue, H. (2012). Absence of age-related prefrontal NAA change in adults with autism spectrum disorders. *Transl Psychiatry*, 2, e178. doi:10.1038/tp.2012.108
- Aron, A. R., Durston, S., Eagle, D. M., Logan, G. D., Stinear, C. M., & Stuphorn, V. (2007). Converging evidence for a fronto-basal-ganglia network for inhibitory control of action and cognition. *J Neurosci*, 27(44), 11860-11864. doi:10.1523/JNEUROSCI.3644-07.2007
- Ashburner, J. (2009). Computational anatomy with the SPM software. *Magn Reson Imaging*, 27(8), 1163-1174. doi:<http://doi.org/10.1016/j.mri.2009.01.006>
- Ashburner, J., & Friston, K. J. (2000). Voxel-Based Morphometry—The Methods. *Neuroimage*, 11(6), 805-821. doi:<http://doi.org/10.1006/nimg.2000.0582>
- Ashburner, J., & Friston, K. J. (2001). Why Voxel-Based Morphometry Should Be Used. *Neuroimage*, 14(6), 1238-1243. doi:<http://doi.org/10.1006/nimg.2001.0961>
- Attwell, D., & Iadecola, C. (2002). The neural basis of functional brain imaging signals. *Trends Neurosci*, 25(12), 621-625. doi:10.1016/S0166-2236(02)02264-6
- Bari, A., & Robbins, T. W. (2013). Inhibition and impulsivity: behavioral and neural basis of response control. *Prog Neurobiol*, 108(1873-5118 (Electronic)), 44-79. doi:10.1016/j.pneurobio.2013.06.005
- Barnes, J., Ridgway, G. R., Bartlett, J., Henley, S. M., Lehmann, M., Hobbs, N., . . . Fox, N. C. (2010). Head size, age and gender adjustment in MRI studies: a necessary nuisance? *Neuroimage*, 53(4), 1244-1255. doi:S1053-8119(10)00869-4
- Bauer, J., Pedersen, A., Scherbaum, N., Bening, J., Patschke, J., Kugel, H., . . . Ohrmann, P. (2013). Craving in alcohol-dependent patients after detoxification is related to glutamatergic dysfunction in the nucleus accumbens and the anterior cingulate cortex. *Neuropsychopharmacology*, 38(8), 1401-1408. doi:10.1038/npp.2013.45
- Becker, H. (1998). Kindling in alcohol withdrawal. *Alcohol Health Res World.*, 22(1)(0090-838X (Print)), 25-33.
- Bergouignan, L., Chupin, M., Czechowska, Y., Kinkingnehun, S., Lemogne, C., Le Bastard, G., . . . Fossati, P. (2009). Can voxel based morphometry, manual segmentation and automated segmentation equally detect hippocampal volume differences in acute depression? *Neuroimage*, 45(1), 29-37. doi:10.1016/j.neuroimage.2008.11.006
- Bergouignan, L., Chupin, M., Czechowska, Y., Kinkingnehun, S., Lemogne, C., Le Bastard, G., . . . Fossati, P. (2009). Can voxel based morphometry, manual segmentation and automated segmentation equally detect hippocampal volume differences in acute depression? *Neuroimage*, 45(1), 29-37. doi:<https://doi.org/10.1016/j.neuroimage.2008.11.006>
- Botvinick, M. M., Cohen, J. D., & Carter, C. S. (2004). Conflict monitoring and anterior cingulate cortex: an update. *Trends Cogn Sci*, 8(12), 539-546. doi:10.1016/j.tics.2004.10.003

-
- Brousse, G., Arnaud, B., Vorspan, F., Richard, D., Dissard, A., Dubois, M., . . . Schmidt, J. (2012). Alteration of glutamate/GABA balance during acute alcohol withdrawal in emergency department: a prospective analysis. *Alcohol Alcohol*, 47(5), 501-508. doi:10.1093/alcalc/ags078
- Brown, M. R., Benoit, J. R., Juhas, M., Lebel, R. M., MacKay, M., Dametto, E., . . . Greenshaw, A. J. (2015). Neural correlates of high-risk behavior tendencies and impulsivity in an emotional Go/NoGo fMRI task. *Front Syst Neurosci*, 9, 24. doi:10.3389/fnsys.2015.00024
- Bullmore, E. T., & Bassett, D. S. (2011). Brain graphs: graphical models of the human brain connectome. *Annu Rev Clin Psychol*, 7, 113-140. doi:10.1146/annurev-clinpsy-040510-143934
- Buxton, R. B. (2013). The physics of functional magnetic resonance imaging (fMRI). *Reports on progress in physics. Physical Society (Great Britain)*, 76(9), 096601-096601. doi:10.1088/0034-4885/76/9/096601
- Calhoun, V. D., & Sui, J. (2016). Multimodal fusion of brain imaging data: A key to finding the missing link(s) in complex mental illness. *Biol Psychiatry Cogn Neurosci Neuroimaging*, 1(3), 230-244. doi:10.1016/j.bpsc.2015.12.005
- Cippitelli, A., Damadzic, R., Frankola, K., Goldstein, A., Thorsell, A., Singley, E., . . . Heilig, M. (2010). Alcohol-Induced Neurodegeneration, Suppression of Transforming Growth Factor-beta, and Cognitive Impairment in Rats: Prevention by Group II Metabotropic Glutamate Receptor Activation. *Biol Psychiatry*, 67(9), 823-830. doi:S0006-3223(09)01479-6
- Cohen, E. R., Ugurbil, K., & Kim, S. G. (2002). Effect of basal conditions on the magnitude and dynamics of the blood oxygenation level-dependent fMRI response. *J Cereb Blood Flow Metab*, 22(9), 1042-1053. doi:10.1097/00004647-200209000-00002
- Collins, D. L., Neelin, P., Peters, T. M., & Evans, A. C. (1994). Automatic 3D intersubject registration of MR volumetric data in standardized Talairach space. *J Comput Assist Tomogr*, 18(2), 192-205.
- Cousijn, H., Haegens, S., Wallis, G., Near, J., Stokes, M. G., Harrison, P. J., & Nobre, A. C. (2014). Resting GABA and glutamate concentrations do not predict visual gamma frequency or amplitude. *Proceedings of the National Academy of Sciences of the United States of America*, 111(25), 9301-9306. doi:10.1073/pnas.1321072111
- Crews, F. T., Buckley, T., Dodd, P. R., Ende, G., Foley, N., Harper, C., . . . Sullivan, E. V. (2005). Alcoholic Neurobiology: Changes In Dependence and Recovery. *Alcoholism: Clinical and Experimental Research*, 29(8), 1504-1513. doi:10.1097/01.alc.0000175013.50644.61
- Cubillo, A., Halari, R., Ecker, C., Giampietro, V., Taylor, E., & Rubia, K. (2010). Reduced activation and inter-regional functional connectivity of fronto-striatal networks in adults with childhood Attention-Deficit Hyperactivity Disorder (ADHD) and persisting symptoms during tasks of motor inhibition and cognitive switching. *J Psychiatr Res*, 44(10), 629-639. doi:10.1016/j.jpsychires.2009.11.016
- Cui, C., Noronha, A., Warren, K. R., Koob, G. F., Sinha, R., Thakkar, M., . . . Sullivan, E. V. (2015). Brain pathways to recovery from alcohol dependence. *Alcohol*, 49(5), 435-452. doi:10.1016/j.alcohol.2015.04.006

-
- Dale, A. M., Fischl, B., & Sereno, M. I. (1999). Cortical surface-based analysis. I. Segmentation and surface reconstruction. *Neuroimage*, *9*(2), 179-194. doi:10.1006/nimg.1998.0395
- Dalley, J. W., Everitt B J Fau - Robbins, T. W., & Robbins, T. W. Impulsivity, compulsivity, and top-down cognitive control. (1097-4199 (Electronic)).
- Dalley, J. W., Everitt, B. J., & Robbins, T. W. (2011). Impulsivity, compulsivity, and top-down cognitive control. *Neuron*, *69*(4), 680-694. doi:10.1016/j.neuron.2011.01.020
- Dalley, J. W., Mar, A. C., Economidou, D., & Robbins, T. W. (2008). Neurobehavioral mechanisms of impulsivity: fronto-striatal systems and functional neurochemistry. *Pharmacol Biochem Behav*, *90*(2), 250-260. doi:10.1016/j.pbb.2007.12.021
- Dalley, J. W., Mar, A. C., Economidou, D., & Robbins, T. W. (2008). Neurobehavioral mechanisms of impulsivity: Fronto-striatal systems and functional neurochemistry. *Pharmacology Biochemistry and Behavior*, *90*(2), 250-260. doi:<https://doi.org/10.1016/j.pbb.2007.12.021>
- Delmonte, S., Gallagher, L., O'Hanlon, E., McGrath, J., & Balsters, J. H. (2013). Functional and structural connectivity of frontostriatal circuitry in Autism Spectrum Disorder. *Frontiers in Human Neuroscience*, *7*, 430. doi:10.3389/fnhum.2013.00430
- Demirakca, T., Ende, G., Kammerer, N., Welzel-Marquez, H., Hermann, D., Heinz, A., & Mann, K. (2011a). Effects of alcoholism and continued abstinence on brain volumes in both genders. *Alcoholism Clinical and Experimental Research*, *35* SRC - GoogleScholar, 1678-1685.
- Demirakca, T., Ende, G., Kammerer, N., Welzel-Marquez, H., Hermann, D., Heinz, A., & Mann, K. (2011b). Effects of alcoholism and continued abstinence on brain volumes in both genders. *Alcohol Clin Exp Res*, *35*(9), 1678-1685. doi:10.1111/j.1530-0277.2011.01514.x
- Desikan, R. S., Segonne, F., Fischl, B., Quinn, B. T., Dickerson, B. C., Blacker, D., . . . Killiany, R. J. (2006). An automated labeling system for subdividing the human cerebral cortex on MRI scans into gyral based regions of interest. *Neuroimage*, *31*(3), 968-980. doi:10.1016/j.neuroimage.2006.01.021
- Destrieux, C., Fischl, B., Dale, A., & Halgren, E. (2010). Automatic parcellation of human cortical gyri and sulci using standard anatomical nomenclature. *Neuroimage*, *53*(1), 1-15. doi:10.1016/j.neuroimage.2010.06.010
- DeVito, E. E., Meda, S. A., Jiantonio, R., Potenza, M. N., Krystal, J. H., & Pearlson, G. D. (2013). Neural correlates of impulsivity in healthy males and females with family histories of alcoholism. *Neuropsychopharmacology*, *38*(10), 1854-1863. doi:10.1038/npp.2013.92
- Ding, W. N., Sun, J. H., Sun, Y. W., Chen, X., Zhou, Y., Zhuang, Z. G., . . . Du, Y. S. (2014). Trait impulsivity and impaired prefrontal impulse inhibition function in adolescents with internet gaming addiction revealed by a Go/No-Go fMRI study. *Behav Brain Funct*, *10*(1), 20. doi:10.1186/1744-9081-10-20
- Du, A. T., Schuff, N., Kramer, J. H., Rosen, H. J., Gorno-Tempini, M. L., Rankin, K., . . . Weiner, M. W. (2007). Different regional patterns of cortical thinning in Alzheimer's disease and frontotemporal dementia. *Brain*, *130*(Pt 4), 1159-1166. doi:10.1093/brain/awm016

-
- Durazzo, T. C., Gazdzinski, S., Banys, P., & Meyerhoff, D. J. (2004). Cigarette smoking exacerbates chronic alcohol-induced brain damage: a preliminary metabolite imaging study. *Alcohol Clin Exp Res*, 28(12), 1849-1860.
- Durazzo, T. C., Gazdzinski, S., Mon, A., & Meyerhoff, D. J. (2010). Cortical perfusion in alcohol-dependent individuals during short-term abstinence: relationships to resumption of hazardous drinking after treatment. *Alcohol*, 44(3), 201-210. doi:10.1016/j.alcohol.2010.03.003
- Durazzo, T. C., Tosun, D., Buckley, S., Gazdzinski, S., Mon, A., Fryer, S. L., & Meyerhoff, D. J. (2011). Cortical thickness, surface area, and volume of the brain reward system in alcohol dependence: relationships to relapse and extended abstinence. *Alcohol Clin Exp Res*, 35(6), 1187-1200. doi:10.1111/j.1530-0277.2011.01452.x
- Ende, G., Cackowski, S., Van Eijk, J., Sack, M., Demirakca, T., Kleindienst, N., . . . Schmahl, C. (2016). Impulsivity and Aggression in Female BPD and ADHD Patients: Association with ACC Glutamate and GABA Concentrations. *Neuropsychopharmacology*, 41(2), 410-418. doi:10.1038/npp.2015.153
- Ende, G., Cackowski, S., VanEijk, J., Sack, M., Demirakca, T., Kleindienst, N., . . . Schmahl, C. (2015). Impulsivity and Aggression in Female BPD and ADHD Patients: Association With ACC Glutamate and GABA Concentrations. *Neuropsychopharmacology*. doi:10.1038/npp.2015.153
- Ende, G., Welzel, H., Walter, S., Weber-Fahr, W., Diehl, A., Hermann, D., . . . Mann, K. (2005). Monitoring the effects of chronic alcohol consumption and abstinence on brain metabolism: a longitudinal proton magnetic resonance spectroscopy study. *Biol Psychiatry*, 58(12), 974-980. doi:10.1016/j.biopsych.2005.05.038
- Fein, G., Landman, B., Tran, H., McGillivray, S., Finn, P., Barakos, J., & Moon, K. (2006). Brain atrophy in long-term abstinent alcoholics who demonstrate impairment on a simulated gambling task. *Neuroimage*, 32(3), 1465-1471. doi:10.1016/j.neuroimage.2006.06.013
- Fergus, A., & Lee, K. S. (1997). GABAergic regulation of cerebral microvascular tone in the rat. *J Cereb Blood Flow Metab*, 17(9), 992-1003. doi:10.1097/00004647-199709000-00009
- Fergus, A., & Lee, K. S. (1997). Regulation of cerebral microvessels by glutamatergic mechanisms. *Brain Res*, 754(1-2), 35-45. doi:[https://doi.org/10.1016/S0006-8993\(97\)00040-1](https://doi.org/10.1016/S0006-8993(97)00040-1)
- Fischl, B., & Dale, A. M. (2000). Measuring the thickness of the human cerebral cortex from magnetic resonance images. *Proc Natl Acad Sci U S A*, 97(20), 11050-11055. doi:10.1073/pnas.200033797
- Fischl, B., Salat, D. H., Busa, E., Albert, M., Dieterich, M., Haselgrove, C., . . . Dale, A. M. (2002). Whole brain segmentation: automated labeling of neuroanatomical structures in the human brain. *Neuron*, 33(3), 341-355.
- Fischl, B., Salat, D. H., van der Kouwe, A. J., Makris, N., Segonne, F., Quinn, B. T., & Dale, A. M. (2004). Sequence-independent segmentation of magnetic resonance images. *Neuroimage*, 23 Suppl 1, S69-84. doi:10.1016/j.neuroimage.2004.07.016
- Frischknecht, U., Hermann, D., Tunc-Skarka, N., Wang, G.-Y., Sack, M., van Eijk, J., . . . Weber-Fahr, W. (2017). Negative Association Between MR-Spectroscopic Glutamate Markers and

Gray Matter Volume After Alcohol Withdrawal in the Hippocampus: A Translational Study in Humans and Rats. *Alcoholism: Clinical and Experimental Research*, 41(2), 323-333. doi:10.1111/acer.13308

- Frischknecht, U., Hermann, D., Tunc-Skarka, N., Wang, G. Y., Sack, M., van Eijk, J., . . . Weber-Fahr, W. Negative Association Between MR-Spectroscopic Glutamate Markers and Gray Matter Volume After Alcohol Withdrawal in the Hippocampus: A Translational Study in Humans and Rats. (1530-0277 (Electronic)).
- Fyer, M. R., Frances, A. J., Sullivan, T., Hurt, S. W., & Clarkin, J. (1988). Comorbidity of borderline personality disorder. *Arch Gen Psychiatry*, 45(4), 348-352.
- Gazdzinski, S., Durazzo Tc Fau - Yeh, P.-H., Yeh Ph Fau - Hardin, D., Hardin D Fau - Banys, P., Banys P Fau - Meyerhoff, D. J., & Meyerhoff, D. J. Chronic cigarette smoking modulates injury and short-term recovery of the medial temporal lobe in alcoholics. (0165-1781 (Print)). doi:D - NLM: NIHMS40918
- Gore, J. C. (2003). Principles and practice of functional MRI of the human brain. *Journal of Clinical Investigation*, 112(1), 4-9. doi:10.1172/JCI200319010
- Grace, A. A., Floresco, S. B., Goto, Y., & Lodge, D. J. (2007). Regulation of firing of dopaminergic neurons and control of goal-directed behaviors. *Trends Neurosci*, 30(5), 220-227. doi:10.1016/j.tins.2007.03.003
- Grusser, S. M., Wrase, J., Klein, S., Hermann, D., Smolka, M. N., Ruf, M., . . . Heinz, A. (2004). Cue-induced activation of the striatum and medial prefrontal cortex is associated with subsequent relapse in abstinent alcoholics. *Psychopharmacology (Berl)*, 175(3), 296-302. doi:10.1007/s00213-004-1828-4
- Gunderson, J. G., Stout, R. L., McGlashan, T. H., Shea, M. T., Morey, L. C., Grilo, C. M., . . . Skodol, A. E. (2011). Ten-year course of borderline personality disorder: psychopathology and function from the Collaborative Longitudinal Personality Disorders study. *Arch Gen Psychiatry*, 68(8), 827-837. doi:10.1001/archgenpsychiatry.2011.37
- Harris, A. D., Puts, N. A., Anderson, B. A., Yantis, S., Pekar, J. J., Barker, P. B., & Edden, R. A. (2015). Multi-regional investigation of the relationship between functional MRI blood oxygenation level dependent (BOLD) activation and GABA concentration. *PLoS One*, 10(2), e0117531. doi:10.1371/journal.pone.0117531
- Harrison, B. J., Soriano-Mas, C., Pujol, J., Ortiz, H., Lopez-Sola, M., Hernandez-Ribas, R., . . . Cardoner, N. (2009). Altered corticostriatal functional connectivity in obsessive-compulsive disorder. *Arch Gen Psychiatry*, 66(11), 1189-1200. doi:10.1001/archgenpsychiatry.2009.152
- Hayes, D. J., Jupp, B., Sawiak, S. J., Merlo, E., Caprioli, D., & Dalley, J. W. (2014). Brain gamma-aminobutyric acid: a neglected role in impulsivity. *Eur J Neurosci*, 39(11), 1921-1932. doi:10.1111/ejn.12485
- Heilig, M., Egli, M., Crabbe, J. C., & Becker, H. C. (2010). Acute withdrawal, protracted abstinence and negative affect in alcoholism: Are they linked? *Addiction biology*, 15(2), 169-184. doi:10.1111/j.1369-1600.2009.00194.x

-
- Hermann, D., Weber-Fahr, W., Sartorius, A., Hoerst, M., Frischknecht, U., Tunc-Skarka, N., . . . H., W. (2012). Translational magnetic resonance spectroscopy reveals excessive central glutamate levels during alcohol withdrawal in humans and rats. *Biological Psychiatry, 71* SRC - GoogleScholar, 1015-1021.
- Hermann, D., Weber-Fahr, W., Sartorius, A., Hoerst, M., Frischknecht, U., Tunc-Skarka, N., . . . Sommer, W. H. (2012). Translational magnetic resonance spectroscopy reveals excessive central glutamate levels during alcohol withdrawal in humans and rats. *Biol Psychiatry, 71*(11), 1015-1021. doi:10.1016/j.biopsych.2011.07.034
- Hoerst, M., Weber-Fahr W Fau - Tunc-Skarka, N., Tunc-Skarka N Fau - Ruf, M., Ruf M Fau - Bohus, M., Bohus M Fau - Schmahl, C., Schmahl C Fau - Ende, G., & Ende, G. Correlation of glutamate levels in the anterior cingulate cortex with self-reported impulsivity in patients with borderline personality disorder and healthy controls. (1538-3636 (Electronic)).
- Hoffman, P. L. (1995). Glutamate receptors in alcohol withdrawal-induced neurotoxicity. *Metab Brain Dis, 10*(1), 73-79.
- Horn, N. R., Dolan, M., Elliott, R., Deakin, J. F., & Woodruff, P. W. (2003). Response inhibition and impulsivity: an fMRI study. *Neuropsychologia, 41*(14), 1959-1966.
- Jacob, G. A., Gutz, L., Bader, K., Lieb, K., Tüscher, O., & Stahl, C. (2010). Impulsivity in Borderline Personality Disorder: Impairment in Self-Report Measures, but Not Behavioral Inhibition. *Psychopathology, 43*(3), 180-188.
- Kaladjian, A., Jeanningros, R., Azorin, J. M., Anton, J. L., & Mazzola-Pomietto, P. (2011). Impulsivity and neural correlates of response inhibition in schizophrenia. *Psychol Med, 41*(2), 291-299. doi:10.1017/s0033291710000796
- Kerns, J. G., Cohen, J. D., MacDonald, A. W., 3rd, Cho, R. Y., Stenger, V. A., & Carter, C. S. (2004). Anterior cingulate conflict monitoring and adjustments in control. *Science, 303*(5660), 1023-1026. doi:10.1126/science.1089910
- King, K. G., Glodzik, L., Liu, S., Babb, J. S., de Leon, M. J., & Gonen, O. (2008). Anteroposterior hippocampal metabolic heterogeneity: three-dimensional multivoxel proton 1H MR spectroscopic imaging--initial findings. *Radiology, 249*(1), 242-250. doi:10.1148/radiol.2491071500
- Kuceyeski, A., Meyerhoff, D. J., Durazzo, T. C., & Raj, A. (2013). Loss in connectivity among regions of the brain reward system in alcohol dependence. *Hum Brain Mapp, 34*(12), 3129-3142. doi:10.1002/hbm.22132
- Kühn, S., Charlet, K., Schubert, F., & et al. (2014). Plasticity of hippocampal subfield volume cornu ammonis 2+3 over the course of withdrawal in patients with alcohol dependence. *JAMA Psychiatry, 71*(7), 806-811. doi:10.1001/jamapsychiatry.2014.352
- Kuhn, S., Schubert, F., Mекle, R., Wenger, E., Ittermann, B., Lindenberger, U., . . . Smith, G. (2011). Neurotransmitter changes during interference task in anterior cingulate cortex: evidence from fMRI-guided functional MRS at 3 T. *L T Recent Advances in Understanding the Personality Underpinnings of Impulsive Behavior and their Role in Risk for Addictive Behaviors Current Drug Abuse Reviewse, 4* SRC - GoogleScholar, 215-227.

-
- Laramée, P., Kusel, J., Leonard, S., Aubin, H.-J., François, C., & Daeppen, J.-B. (2013). The Economic Burden of Alcohol Dependence in Europe. *Alcohol and Alcoholism*, 48(3), 259-269. doi:10.1093/alcalc/agt004
- Lipp, I., Evans, C. J., Lewis, C., Murphy, K., Wise, R. G., & Caseras, X. (2010). The relationship between fearfulness, GABA+, and fear-related BOLD responses in the insula. *PLoS one e011*, 10 SRC - GoogleScholar.
- Logothetis, N. K. (2008). What we can do and what we cannot do with fMRI. *Nature*, 453(7197), 869-878. doi:10.1038/nature06976
- Logothetis, N. K., & Pfeuffer, J. (2004). On the nature of the BOLD fMRI contrast mechanism. *Magn Reson Imaging*, 22(10), 1517-1531. doi:10.1016/j.mri.2004.10.018
- Lovick, T. A., Brown La Fau - Key, B. J., & Key, B. J. Neurovascular relationships in hippocampal slices: physiological and anatomical studies of mechanisms underlying flow-metabolism coupling in intraparenchymal microvessels. (0306-4522 (Print)).
- Lynch, J., Peeling, J., Auty, A., & Sutherland, G. R. (1993). Nuclear magnetic resonance study of cerebrospinal fluid from patients with multiple sclerosis. *Can J Neurol Sci*, 20(3), 194-198.
- Makris, N., Oscar-Berman, M., Jaffin, S. K., Hodge, S. M., Kennedy, D. N., Caviness, V. S., . . . Harris, G. J. (2008). Decreased volume of the brain reward system in alcoholism. *Biol Psychiatry*, 64(3), 192-202. doi:10.1016/j.biopsych.2008.01.018
- Marsh, R., Horga, G., Parashar, N., Wang, Z., Peterson, B. S., & Simpson, H. B. (2014). Altered Activation in Fronto-Striatal Circuits During Sequential Processing of Conflict in Unmedicated Adults with Obsessive-Compulsive Disorder. *Biological Psychiatry*, 75(8), 615-622. doi:<http://dx.doi.org/10.1016/j.biopsych.2013.02.004>
- Martinotti, G., Di Nicola, M., Reina, D., Andreoli, S., Focà, F., Cunniff, A., . . . Janiri, L. (2008). Alcohol Protracted Withdrawal Syndrome: The Role of Anhedonia. *Substance Use & Misuse*, 43(3-4), 271-284. doi:10.1080/10826080701202429
- Mauchnik, J., & Schmahl, C. (2010). The latest neuroimaging findings in borderline personality disorder. *Curr Psychiatry Rep*, 12(1), 46-55. doi:10.1007/s11920-009-0089-7
- McLaren, D. G., Ries, M. L., Xu, G., & Johnson, S. C. (2012). A generalized form of context-dependent psychophysiological interactions (gPPI): a comparison to standard approaches. *Neuroimage*, 61(4), 1277-1286. doi:10.1016/j.neuroimage.2012.03.068
- Meyerhoff, D. J., Durazzo, T. C., & Ende, G. (2013). Chronic alcohol consumption, abstinence and relapse: brain proton magnetic resonance spectroscopy studies in animals and humans. *Curr Top Behav Neurosci*, 13, 511-540. doi:10.1007/7854_2011_131
- Michels, L., Martin, E., Klaver, P., Edden, R., Zelaya, F., Lythgoe, D. J., . . . O'Gorman, R. L. (2012). Frontal GABA levels change during working memory. *PLoS One*, 7(4), e31933. doi:10.1371/journal.pone.0031933
- Mon, A., Durazzo, T. C., & Meyerhoff, D. J. (2012). Glutamate, GABA, and other cortical metabolite concentrations during early abstinence from alcohol and their associations with neurocognitive changes. *Drug Alcohol Depend*, 125(1-2), 27-36. doi:10.1016/j.drugalcdep.2012.03.012

-
- Mullins, P. G., McGonigle, D. J., O'Gorman, R. L., Puts, N. A. J., Vidyasagar, R., Evans, C. J., & Edden, R. A. E. (2014). Current practice in the use of MEGA-PRESS spectroscopy for the detection of GABA. *Neuroimage*, 86, 43-52. doi:<http://doi.org/10.1016/j.neuroimage.2012.12.004>
- Naaijen, J., Lythgoe, D. J., Amiri, H., Buitelaar, J. K., & Glennon, J. C. (2015). Fronto-striatal glutamatergic compounds in compulsive and impulsive syndromes: A review of magnetic resonance spectroscopy studies. *Neuroscience & Biobehavioral Reviews*, 52(0), 74-88. doi:<http://dx.doi.org/10.1016/j.neubiorev.2015.02.009>
- Northoff, G., Qin, P., & Nakao, T. (2010). Rest-stimulus interaction in the brain: a review. *Trends Neurosci*, 33(6), 277-284. doi:10.1016/j.tins.2010.02.006
- O'Neill, J., Cardenas, V. A., & Meyerhoff, D. J. (2001). Effects of abstinence on the brain: quantitative magnetic resonance imaging and magnetic resonance spectroscopic imaging in chronic alcohol abuse. *Alcohol Clin Exp Res*, 25(11), 1673-1682.
- Olson, S. L., Bates, J. E., Sandy, J. M., & Schilling, E. M. (2002). Early developmental precursors of impulsive and inattentive behavior: from infancy to middle childhood. *J Child Psychol Psychiatry*, 43(4), 435-447.
- Olson, S. L., Schilling, E. M., & Bates, J. E. (1999). Measurement of Impulsivity: Construct Coherence, Longitudinal Stability, and Relationship with Externalizing Problems in Middle Childhood and Adolescence. *Journal of Abnormal Child Psychology*, 27(2), 151-165. doi:10.1023/A:1021915615677
- Peters, J. R., Upton, B. T., & Baer, R. A. (2013). Brief report: relationships between facets of impulsivity and borderline personality features. *J Pers Disord*, 27(4), 547-552. doi:10.1521/pedi_2012_26_044
- Pfefferbaum, A., Sullivan, E. V., Mathalon, D. H., Shear, P. K., Rosenbloom, M. J., & Lim, K. O. (1995). Longitudinal changes in magnetic resonance imaging brain volumes in abstinent and relapsed alcoholics. *Alcohol Clin Exp Res*, 19(5), 1177-1191.
- Prendergast, M. A., Harris, B. R., Mullholland, P. J., Blanchard, J. A., 2nd, Gibson, D. A., Holley, R. C., & Littleton, J. M. (2004). Hippocampal CA1 region neurodegeneration produced by ethanol withdrawal requires activation of intrinsic polysynaptic hippocampal pathways and function of N-methyl-D-aspartate receptors. *Neuroscience*, 124(4), 869-877. doi:10.1016/j.neuroscience.2003.12.013
- Puts, N. A. J., & Edden, R. A. E. (2012). In vivo magnetic resonance spectroscopy of GABA: A methodological review. *Prog Nucl Magn Reson Spectrosc*, 60, 29-41. doi:<http://doi.org/10.1016/j.pnmrs.2011.06.001>
- Quetscher, C., Yildiz, A., Dharmadhikari, S., Glaubit, B., Schmidt-Wilcke, T., Dydak, U., & Beste, C. (2015). Striatal GABA-MRS predicts response inhibition performance and its cortical electrophysiological correlates. *Brain Struct Funct*, 220(6), 3555-3564. doi:10.1007/s00429-014-0873-y
- RA., d. G. (2007). *In Vivo NMR Spectroscopy: Principles and Techniques*. 2nd.

-
- Rajagopalan, V., Yue, G. H., & Pioro, E. P. (2014). Do preprocessing algorithms and statistical models influence voxel-based morphometry (VBM) results in amyotrophic lateral sclerosis patients? A systematic comparison of popular VBM analytical methods. *Journal of Magnetic Resonance Imaging*, *40*(3), 662-667. doi:10.1002/jmri.24415
- Rehm, J., Mathers, C., Popova, S., Thavorncharoensap, M., Teerawattananon, Y., & Patra, J. (2009). Global burden of disease and injury and economic cost attributable to alcohol use and alcohol-use disorders. *The Lancet*, *373*(9682), 2223-2233. doi:10.1016/S0140-6736(09)60746-7
- Rissman, J., Gazzaley, A., & D'Esposito, M. (2004). Measuring functional connectivity during distinct stages of a cognitive task. *Neuroimage*, *23*(2), 752-763. doi:10.1016/j.neuroimage.2004.06.035
- Rossetti, Z. L., & Carboni, S. (1999). Ethanol withdrawal is associated with increased extracellular glutamate in the rat striatum. *Eur J Pharmacol*, *283*(1-3)(0014-2999 (Print)), 177-183.
- Sameti, M., Smith, S., Patenaude, B., & Fein, G. (2011). Subcortical volumes in long-term abstinent alcoholics: associations with psychiatric comorbidity. *Alcohol Clin Exp Res*, *35*(6), 1067-1080. doi:10.1111/j.1530-0277.2011.01440.x
- Schulte, T., Oberlin, B. G., Kareken, D. A., Marinkovic, K., Muller-Oehring, E. M., Meyerhoff, D. J., & Tapert, S. (2012). How acute and chronic alcohol consumption affects brain networks: insights from multimodal neuroimaging. *Alcohol Clin Exp Res*, *36*(12), 2017-2027. doi:10.1111/j.1530-0277.2012.01831.x
- Sebastian, A., Jung, P., Krause-Utz, A., Lieb, K., Schmahl, C., & Tuscher, O. (2014). Frontal dysfunctions of impulse control - a systematic review in borderline personality disorder and attention-deficit/hyperactivity disorder. *Front Hum Neurosci*, *8*(1662-5161 (Electronic)), 698. doi:10.3389/fnhum.2014.00698
- Sebastian, A., Jung, P., Krause-Utz, A., Lieb, K., Schmahl, C., & Tüscher, O. (2014). Frontal Dysfunctions of Impulse Control – A Systematic Review in Borderline Personality Disorder and Attention-Deficit/Hyperactivity Disorder. *Front Hum Neurosci*, *8*, 698. doi:10.3389/fnhum.2014.00698
- Segobin, S. H., Chetelat, G., Le Berre, A. P., Lannuzel, C., Boudehent, C., Vabret, F., . . . Pitel, A. L. (2014). Relationship between brain volumetric changes and interim drinking at six months in alcohol-dependent patients. *Alcohol Clin Exp Res*, *38*(3), 739-748. doi:10.1111/acer.12300
- Segonne, F., Dale, A. M., Busa, E., Glessner, M., Salat, D., Hahn, H. K., & Fischl, B. (2004). A hybrid approach to the skull stripping problem in MRI. *Neuroimage*, *22*(3), 1060-1075. doi:10.1016/j.neuroimage.2004.03.032
- Segonne, F., Pacheco, J., & Fischl, B. (2007). Geometrically accurate topology-correction of cortical surfaces using nonseparating loops. *IEEE Trans Med Imaging*, *26*(4), 518-529. doi:10.1109/TMI.2006.887364
- Shear, P. K., Jernigan, T. L., & Butters, N. (1994). Volumetric magnetic resonance imaging quantification of longitudinal brain changes in abstinent alcoholics. *Alcohol Clin Exp Res*, *18*(1), 172-176.

-
- Simpson, S. A., Wilson, M. P., & Nordstrom, K. (2016). Psychiatric Emergencies for Clinicians: Emergency Department Management of Alcohol Withdrawal. *J Emerg Med, 51*(3), 269-273. doi:10.1016/j.jemermed.2016.03.027
- Spanagel, R. (2009). Alcoholism: a systems approach from molecular physiology to addictive behavior. *Physiol Rev, 89*(2), 649-705. doi:89/2/649 [pii]10.1152/physrev.00013.2008
- Sullivan, E. V., Deshmukh, A., De Rosa, E., Rosenbloom, M. J., & Pfefferbaum, A. (2005). Striatal and forebrain nuclei volumes: contribution to motor function and working memory deficits in alcoholism. *Biol Psychiatry, 57*(7), 768-776. doi:10.1016/j.biopsych.2004.12.012
- Sullivan, E. V., Deshmukh, A., Rosa, E., Rosenbloom, M. J., & Pfefferbaum, A. (2005). De . Striatal and forebrain nuclei volumes: contribution to motor function and working memory deficits in alcoholism. *Biological Psychiatry, 57 SRC - GoogleScholar, 768-776*.
- Tsai, G. E., Ragan, P., Chang, R., Chen, S., Linnoila, V. M., & Coyle, J. T. (1998). Increased glutamatergic neurotransmission and oxidative stress after alcohol withdrawal. *Am J Psychiatry, 155*(6), 726-732.
- van Eijk, J., Demirakca, T., Frischknecht, U., Hermann, D., Mann, K., & Ende, G. (2013). Rapid partial regeneration of brain volume during the first 14 days of abstinence from alcohol. *Alcohol Clin Exp Res, 37*(1), 67-74. doi:10.1111/j.1530-0277.2012.01853.x
- van Eijk, J., Sebastian, A., Krause-Utz, A., Cackowski, S., Demirakca, T., Biedermann, S. V., . . . Tuscher, O. (2015a). Women with borderline personality disorder do not show altered BOLD responses during response inhibition. *Psychiatry Res*. doi:10.1016/j.psychresns.2015.09.017
- van Eijk, J., Sebastian, A., Krause-Utz, A., Cackowski, S., Demirakca, T., Biedermann, S. V., . . . Tuscher, O. (2015b). Women with borderline personality disorder do not show altered BOLD responses during response inhibition. *Psychiatry Res, 234*(3), 378-389. doi:10.1016/j.psychresns.2015.09.017
- Wang, G. Y., Demirakca, T., van Eijk, J., Frischknecht, U., Ruf, M., Ucar, S., . . . Ende, G. (2016). Longitudinal Mapping of Gyral and Sulcal Patterns of Cortical Thickness and Brain Volume Regain during Early Alcohol Abstinence. *Eur Addict Res, 22*(2), 80-89. doi:10.1159/000438456
- Wang, H., Tan, L., Wang, H. F., Liu, Y., Yin, R. H., Wang, W. Y., . . . Yu, J. T. (2015). Magnetic Resonance Spectroscopy in Alzheimer's Disease: Systematic Review and Meta-Analysis. *J Alzheimers Dis, 46*(4), 1049-1070. doi:10.3233/JAD-143225
- Wingenfeld, K., Rullkoetter, N., Mensebach, C., Beblo, T., Mertens, M., Kreisel, S., . . . Woermann, F. G. (2009). Neural correlates of the individual emotional Stroop in borderline personality disorder. *Psychoneuroendocrinology, 34*(4), 571-586. doi:10.1016/j.psyneuen.2008.10.024
- Wrase, J., Makris, N., Braus, D. F., Mann, K., Smolka, M. N., Kennedy, D. N., . . . Heinz, A. (2008). Amygdala volume associated with alcohol abuse relapse and craving. *Am J Psychiatry, 165*(9), 1179-1184. doi:10.1176/appi.ajp.2008.07121877

Curriculum Vitae

BIOGRAPHY

Name : Guo-Ying Wang
Date of birth: 31.12.1984
Place of birth: Shanxi
Nationality: China
Marital status: Single
Father: Fu-Kuan Wang
Mother: Wen-Lian Zhu

EDUCATION AND ACADEMIC CAREER

| | | |
|-----------|-----------------|---|
| 2013-2017 | Ph.D. Candidate | Medical Faculty Mannheim/Heidelberg University, Germany |
| 2011-2012 | M.Sc. | Translational Medical Research, Medical Faculty Mannheim/Heidelberg University, Germany Awarded: 21.09.2012; Grade 1.7 |
| 2009-2011 | M.Sc. | Department of Neurology, Anhui Medical University & the First Affiliated Hospital of Anhui Medical University, China Awarded: 01.07.2011 |
| 2004-2009 | Bachelor | Anhui Medical University, China Awarded: 01.07.2009 |

Publications

Wang, G.Y., Demirakca, T., van Eijk, J., Frischknecht, U., Ruf, M., Ucar, S., Hermann, D., Mann, K., Kiefer, F., Ende, G., 2016. Longitudinal Mapping of Gyral and Sulcal Patterns of Cortical Thickness and Brain Volume Regain during Early Alcohol Abstinence. *European addiction research* 22, 80-89.

Wang, G.Y., van Eijk, J., Demirakca, T., Sack, M., Krause-Utz, A., Cackowski, S., Schmahl, C., Ende, G., 2017. ACC GABA levels are associated with functional activation and connectivity in the fronto-striatal network during interference inhibition in patients with borderline personality disorder. *NeuroImage* 147, 164-174.

Frischknecht, U., Hermann, D., Tunc-Skarka, N., **Wang, G.-Y.**, Sack, M., van Eijk, J., Demirakca, T., Falfan-Melgoza, C., Krumm, B., Dieter, S., Spanagel, R., Kiefer, F., Mann, K.F., Sommer, W.H., Ende, G., Weber-Fahr, W., 2017. Negative Association Between MR-Spectroscopic Glutamate Markers and Gray Matter Volume After Alcohol Withdrawal in the Hippocampus: A Translational Study in Humans and Rats. *Alcoholism: Clinical and Experimental Research* 41, 323-333.

Acknowledgement

Firstly, I would like to express my sincere gratitude to my advisor Prof. Gabriele Ende for the continuous support of my Ph.D. study and related research, for her patience, motivation, and immense knowledge. Her guidance helped me in all the time of research and writing of this thesis. I could not have imagined having a better advisor and mentor for my Ph.D. study.

Besides my advisor, I would like to thank the rest of my thesis committee: Prof. Christian Schmahl, Prof. Derik Hermann for their insightful comments, but also for the hard questions which incited me to widen my research from various perspectives.

My sincere thanks also go to Dr. Traute Demirakca, Matthias Ruf, Dr. Wolfgang Weber-Fahr, Dr. Markus Sack, Dr. Ulrich Frischknecht and Dr. Natalia Gass who offer me a lot of help for the data analysis, facility setting, data acquirement, idea contribution and thesis correction. Without their precious support it would not be possible to conduct this research.

I also thank my fellow labmates: Dr. Isabella Wolf, Vita Cardinale, and Gunilla Oberthuer for the stimulating discussions and for all the fun we have had in the last four years. Also I thank my friends: Zen-Xiang Zang. In particular, I am grateful to Dr. Heng-Yi Cao for enlightening me the first glance of research.

Last but not least, I would like to thank my family for supporting me spiritually throughout writing this thesis and my life in general.